

DEVELOPMENTS OF ROOM TEMPERATURE PHOSPHORIMETRY
AND A SPIKED MOBILE PHASE FLUORESCENCE DETECTOR-HIGH
PERFORMANCE LIQUID CHROMATOGRAPHY SYSTEM

BY

SYANG YANG SU

A DISSERTATION PRESENTED TO THE GRADUATE COUNCIL
OF THE UNIVERSITY OF FLORIDA IN
PARTIAL FULFILLMENT OF THE REQUIREMENTS
FOR THE DEGREE OF DOCTOR OF PHILOSOPHY

UNIVERSITY OF FLORIDA
1982

ACKNOWLEDGEMENTS

I wish to express my hearty gratitude to my research director, Dr. James D. Winefordner, for his advice and guidance, and especially for his encouraging me whenever I desperately needed it. I give special thanks to Dr. J.G. Dorsey, Dr. E. Voigtman, Dr. Strong Huang, and Dr. J.L. Ward for their critical advice and help on the HPLC and RTP research work, and Dr. W.B. Person for being a committee member for my oral examination. I also wish to thank Mr. R.P. Bateh, Mr. E.P.C. Lai, and Ms. L. Hirschy and the other people in the group for their friendship and help, and the coworkers for helping me on the research works.

My gratitude is also extended to my wife, Miau Yen, without whom this dissertation might never have existed, to my great parents for their spiritual and material support, and finally to my two little boys, Phil W.S. and Joe W.K., for their smiling, crying, and lovely behavior which support me and remind me to work hard with a cheerful and hopeful mind.

TABLE OF CONTENTS

	PAGE
ACKNOWLEDGEMENTS	ii
LIST OF TABLES	vi
LIST OF FIGURES	viii
ABSTRACT	xii
CHAPTER	
1 GENERAL INTRODUCTION	1
2 BACKGROUND INFORMATION ON ROOM TEMPERATURE PHOSPHORIMETRY	4
Historical Background of Solid Substrate Room Temperature Phosphorimetry (RTP) ...	4
Phosphorescence vs. Fluorescence	7
Theoretical Phosphorimetric Intensity Expressions	11
Room Temperature Phosphorescence (RTP) vs. Low Temperature Phosphorescence (LTP) ...	14
Solid Substrate RTP vs. Micellar RTP and Liquid RTP	15
Theories of Solid Substrate RTP	17
Solid Substrates	18
Instrumentation	20
3 DEVELOPMENT OF NEW SOLID SUBSTRATES FOR RTP	21
Introduction	21
Experimental	23
Instrumentation	23
Chemicals	27
Procedure	27
Inorganic compound plates	27
Ion exchange filter paper	29
Results and Discussion	30
Inorganic Compound Plates	30
Ion Exchange Filter Papers	34
Background luminescence and the presence of heavy atoms	34
Analytical figures of merit	34

CHAPTER	PAGE
Special characteristics of some PAHs..	36
Conclusions and Future Work	44
4 ROOM TEMPERATURE PHOSPHORESCENCE BACKGROUND CORRECTION BY USE OF COMPUTER APPROACH ...	48
Introduction	48
Experimental	49
Instrumentation	49
Chemicals	50
Procedure	50
Sample preparation	50
Instrument/computer operation	50
Calculation of LOD, slope from conventionally recorded spectra	52
Calculation of LOD by peak-to-peak noise method and the computer stored data	52
Results and Discussion	53
Blank Corrected Spectra	56
Calibrations Curves	56
Conclusions and Future Work	56
5 STUDIES OF HEAVY ATOM EFFECT AND SAMPLE DRYING PROCEDURE FOR RTP	65
Introduction	65
Experimental	67
Instrumentation	67
Chemicals	67
Procedure	67
Results and Discussion	68
Sample Drying Procedure	68
Effect of Heavy Atom Effect on Response and Calibration Curves	75
Conclusions and Future Work	88
6 SPIKED MOBILE PHASE FLUORESCENCE DETECTOR FOR HPLC	89
Introduction	89
Theoretical Background	89
Experimental I	98
Instrumentation	98
Chemical	98
Procedure	100
Results and Discussion I	100
Experimental II	104
Instrumentation	104
Chemicals	105

CHAPTER	PAGE
Results and Discussion II	105
Negative Peaks	105
Solvent Effect	107
Positive Peaks	108
Quartz Sample Cell	109
Synthetic Mixtures	110
Calibration Curve	115
Solvent Programming	115
Instrumentation	121
Conclusions and Future Work	121
7 SUMMARY AND FUTURE WORK	123
REFERENCES	125
APPENDICES	
A ROOM TEMPERATURE PHOSPHORESCENCE SPECTRA OF COMPOUNDS NOT SHOWN IN TEXT	132
B BASIC PROGRAM AND CIRCUITRY OF LOW PASS FILTER USED IN THE STUDY OF RTP BACKGROUND LUMINESCENCE CORRECTION BY COMPUTER APPROACH	138
C MECHANICAL DRAWINGS OF VERSATILE LUMINESCENCE SAMPLING DEVICE	153
D HISTOGRAMS OF SEVERAL MODEL COMPOUNDS	157
E RESPONSE AND CALIBRATION CURVES OF COMPOUNDS NOT SHOWN IN TEXT	167
BIOGRAPHICAL SKETCH	174

LIST OF TABLES

TABLE	PAGE
1 A Concise Comparison Between Varieties of Luminescence Techniques	9
2 A Table of Components of Instrument for RTP Study	26
3 Compounds Studied by RTP and Their Sources ...	28
4 Excitation and Emission Room Temperature Phosphorescence Wavelengths and Corresponding Limits of Detection for Several PAHs in the Presence of Various Heavy Atoms and with Several Inorganic Compound Plate Substrates.	31
5 Background Luminescence of Substrate DE-81, S & S 903, and DTPA Treated S & S 903 Filter Papers	35
6 Analytical Figures of Merit of Several Model Compounds Evaluated Using DE-81, S & S 903, and DTPA Treated S & S 903 Filter Papers ...	37
7 RTP Net Analyte Intensities of Coronene	42
8 Analytical Figures of Merit for Several Model Compounds Using the Conventional and Computer Approaches	54
9 Characteristics of Sample Drying Study for Several Model Compounds	70
10 Intensity Comparison With and Without Infrared Lamp Heating	74
11 Characteristics of an Ideal HPLC Detector	90
12 Characteristics of the Four Currently Most Popular HPLC Detectors	93
13 Some Possible Candidates of the Spiking Fluorophor with Their Characteristic Wave-lengths and Solvents	97

TABLE	PAGE
14 Detection Characteristics of New Fluorescence Cell for HPLC	101
15 Detection Characteristics of New Fluorescence Cell for HPLC Separations of Ethanol and Methanol	102
16 Detection Characteristics of Several PAHs by the Spiked Mobile Phase Fluorescence Detector	106
17 Comparison of Detection Characteristics of 1 mm and 3 mm i.d. Quartz Tubes Used as Flow Cells in Spiked Mobile Phase Fluorescence Detector	110

LIST OF FIGURES

FIGURE	PAGE
1 A simplified energy diagram for luminescence.	8
2 Structure of anion (top) and cation (bottom) exchange filter papers	24
3 A block diagram of instrument for RTP study .	25
4 RTP spectrum of coronene in 1 M AgNO_3 and on boric acid inorganic compound plate ($\lambda_{\text{ex}} = 310 \text{ nm}$)	33
5 RTP spectrum of coronene in 0.0035 M AgNO_3 and on DE-81 filter paper ($\lambda_{\text{ex}} = 310 \text{ nm}$) ..	41
6 RTP spectra of coronene (5.5 $\mu\text{g/ml}$) without heavy atom on DE-81 (top) and S & S 903 (bottom) filter papers ($\lambda_{\text{ex}} = 310 \text{ nm}$)	43
7 RTP spectra of coronene (10.9 $\mu\text{g/ml}$) in 0.0035 M (left) and 0.7 M (right) AgNO_3 and on DE-81 filter paper ($\lambda_{\text{ex}} = 310 \text{ nm}$) ..	45
8 RTP spectra of phenanthrene (63 $\mu\text{g/ml}$) in 0.1 M TlNO_3 (top) and 0.0035 M AgNO_3 (bottom) and on DE-81 filter paper ($\lambda_{\text{ex}} = 260 \text{ nm}$) ..	46
9 Block diagram of computer and fluorimeter ...	51
10 Analyte (A), blank (B), and blank corrected analyte (C) spectra of privine HCl	57
11 RTP spectra of privine HCl (28 $\mu\text{g/ml}$) obtained from computer-plotter (top) and X-Y recorder (bottom)	58
12 RTP spectra of biphenyl (72 $\mu\text{g/ml}$) obtained from computer-plotter (top) and X-Y recorder (bottom)	59
13 RTP spectra of benomyl (36 $\mu\text{g/ml}$) obtained from computer-plotter (top) and X-Y recorder (bottom)	60

14	RTP spectra of PABA (0.8 μ g/ml) obtained from computer-plotter (top) and X-Y recorder (bottom)	61
15	Calibration curves of four model compounds by (a) computer and (b) conventional outputs	62
16	Typical histogram of RTP sample drying procedure	69
17	RTP response (left) and calibration (right) curves of procaine HCl on DE-81	77
18	RTP response (left) and calibration (right) curves of procaine HCl on S & S 903	79
19	RTP response (left) and calibration (right) curves of carbazole on DE-81	81
20	RTP response (left) and calibration (right) curves of carbazole on S & S 903	83
21	RTP response (left) and calibration (right) curves of phenanthrene on DE-81	85
22	RTP response (left) and calibration (right) curves of phenanthrene on S & S 903	87
23	A postulated chromatogram with positive and negative peaks detected by the spiked mobile phase fluorescence detector	95
24	Diagram of flow cell	99
25	HPLC chromatogram of a 3 component mixture ..	103
26	HPLC chromatogram of a 5 component mixture ..	112
27	HPLC chromatogram of a 6 component mixture ..	114
28	HPLC chromatogram of a 6 component mixture monitored at $\lambda_{ex} = 248$ nm and $\lambda_{em} = 396$ nm	117
29	Calibration curves for several PAHs measured by HPLC-spiked mobile phase fluorescence detector	118
30	HPLC chromatogram of 6 component mixture with solvent programming	119

31	HPLC chromatogram of 6 component mixture with solvent programming monitored at $\lambda_{ex} = 248$ nm and $\lambda_{em} = 396$ nm (details same as Figure 28)	120
32	Oxythioquinox (113 $\mu\text{g}/\text{ml}$) in 1 M NaI and on DE-81 (top) and S & S 903 (bottom) filter papers ($\lambda_{ex} = 396$ nm)	132
33	Biphenyl (72 $\mu\text{g}/\text{ml}$) in 1 M AgNO_3 and on S & S 903 filter paper ($\lambda_{ex} = 266$ nm)	133
34	Naphthalene acetic acid (27 $\mu\text{g}/\text{ml}$) in 1 M NaI and on S & S 903 filter paper ($\lambda_{ex} = 290$ nm)	134
35	2-Aminobenzimidazole (55 $\mu\text{g}/\text{ml}$) in NaI and on DE-81 filter paper ($\lambda_{ex} = 280$ nm)	135
36	Benomyl (144 $\mu\text{g}/\text{ml}$) in 1 M NaI and on S & S 903 filter paper ($\lambda_{ex} = 280$ nm)	136
37	Circuitry of low pass Sallen-Key active filter used in RTP study	138
38	Diagram of 20-spot circular versatile luminescence sampling device	153
39	Diagram of stand of versatile luminescence sampling device for use on Aminco-Bowman spectrophotofluorimeter system	154
40	The top view of the versatile luminescence sampling device with the stand	155
41	Histogram of carbazole without IR lamp heating	157
42	Histogram of carbazole with IR lamp heating..	158
43	Histogram of phenanthrene without IR lamp heating	159
44	Histogram of phenanthrene with IR lamp heating	160
45	Histogram of privine HCl without IR lamp heating	161
46	Histogram of privine HCl with IR lamp heating	162

FIGURE	PAGE
47 Histogram of 2-aminobenzimidazole without IR lamp heating	163
48 Histogram of 2-aminobenzimidazole with IR lamp heating	164
49 RTP response (left) and calibration (right) curves of PABA on DE-81	167
50 RTP response (left) and calibration (right) curves of PABA on S & S 903	169
51 RTP response (left) and calibration (right) curves of NAA on DE-81	171
52 RTP response (left) and calibration (right) curves of NAA on S & S 903	173

Abstract of Dissertation Presented to the Graduate
Council of the University of Florida in Partial
Fulfillment of the Requirements for the Degree
of Doctor of Philosophy

DEVELOPMENTS OF ROOM TEMPERATURE PHOSPHORIMETRY AND A
SPIKED MOBILE PHASE FLUORESCENCE DETECTOR-HIGH
PERFORMANCE LIQUID CHROMATOGRAPHY SYSTEM

By

Syang Yang Su

August, 1982

Chairman: James D. Winefordner
Major Department: Chemistry

Two new solid substrates are developed and evaluated for room temperature phosphorescence (RTP) observation. Inorganic compound plates as well as the ion exchange filter paper substrates open two new directions of exploring the development of solid substrates for RTP. Ion exchange filter papers are better substrates than previously used ones and inorganic compound plates show promise to become good substrates if many parameters are optimized.

Background luminescence corrected analyte phosphorescence spectra achieved by use of a computer interfaced to the Aminco-Bowman spectrophotofluorimeter presents the best means of using the system to carry out automated, precise,

fast, reliable routine analyses. It is also critical for routine analysis to optimize the choice of heavy atom species and concentration and the optimal sample drying procedure and sampling time for each analyte.

In order to approach the ideal universal detection system for high performance liquid chromatography (HPLC), the spiked mobile phase fluorescence (SMPF) detector was developed and resulted in showing rather successful measurement of several non- or weak fluorescent species by giving negative peaks. There are several advantages inherent in the SMPF-HPLC system, including all the advantages of normal fluorescence detection system and some additional ones such as universal sensing ability, a simple instrumental system, and no derivatization of analyte. The limits of detection (LODs) for compounds giving positive peaks lie in the vicinity of ng/ml or lower level and for compounds with negative peaks in the $\mu\text{g}/\text{ml}$ level.

CHAPTER 1 GENERAL INTRODUCTION

There are numerous well developed as well as newly found analytical methodologies and instruments which are used in academic, industrial, and governmental areas for pure research, routine analysis, and regulatory studies. All kinds of analytical techniques may be classified by either one or a combination of the following analytical merits: selectivity and universality; qualitative and quantitative ability; sensitivity; micro or macro samples, etc. At the present time, most analytical chemists are working towards better selectivity of the technique. Compared to others, luminescence, which includes fluorescence and phosphorescence techniques, is a very selective and sensitive analytical means for those compounds which either fluoresce or phosphoresce. However, most chemicals are not able to luminesce, although this fact does increase the degree of selectivity of the luminescence technique but yet limits the range of application of it for chemical analysis. The merit of selectivity of technique certainly simplifies the sample preparation and measurement procedure and minimizes matrix interference during the course of sample analysis.

Room temperature phosphorescence (RTP) is currently one of the most selective analytical techniques and is obtained by observing phosphorescence emission of an excited analyte at room temperature. RTP is more selective yet less sensitive than low temperature phosphorimetry (LTP) which is observed at 77°K. Taking advantage of the excellent selectivity of RTP, several real sample analyses were done by use of RTP without separation, such as para-amino benzoic acid (PABA) content in a vitamin tablet (1); theophylline drug analysis of tablets, capsules, syrups and elixir samples from different manufacturers (2); mebendazole and flurendazole drug analysis (3); and polynuclear aromatic hydrocarbon (PAH) identification and quantification in synthoil (4). However, as stated before, most compounds do not luminesce or optically interfere with each other. In this case, separation of the sample mixture into several discrete pure components by use of a chromatographic technique, e.g., gas chromatography (GC), high performance liquid chromatography (HPLC), or thin layer chromatography (TLC), is necessary before the analytes are detected by use of one or more techniques, such as amperometry, ultraviolet (UV) absorption, refractive index, mass spectrometry, Fourier transformation infrared (FTIR), fluorimetry, flame ionization, electron capture, etc. HPLC is an important, widely used separation technique for routine analysis of drugs, pesticides, polynuclear aromatic hydrocarbons (PAHs), amino acids, sugars, proteins, and so forth.

However, the lack of a universal and sensitive detector is a critical problem for HPLC development. The so called "hyphenated" techniques, which couple two or more analytical techniques together for sample analysis, discussed by Hirschfeld (5) can be used to increase both selectivity and universality of chromatographic methods, such as GC-IR-MS, HPLC-IR-MS, HPLC-NMR, or HPLC-fluorescence-photoacoustic-photoionization, where MS stands for mass spectrometry, NMR for nuclear magnetic resonance, and IR for infrared. However, these hyphenated techniques suffer from the drawbacks of high cost, complicated systems, and interfacing problems. Development of a much simpler, less expensive method for universal HPLC detection is thus a necessity. To approach this project, the "spiked mobile phase fluorescence detector for HPLC system" was introduced by Su et al. (6,7) to detect several non- or weak fluorescent compounds successfully.

CHAPTER 2
BACKGROUND INFORMATION ON ROOM
TEMPERATURE PHOSPHORIMETRY

Historical Background of Solid Substrate
Room Temperature Phosphorimetry (RTP)

The first observation of RTP for organic compounds was made by Millson (8) in 1944, according to Lloyd and Miller (9), but apparently was not widely publicized before 1954 (10). He observed that along with a variety of other fibers various cottons phosphoresced at room temperature, especially when "bone dry."

The second observation was made by Brown in 1958 (11). He wrote, "when viewed on a paper chromatogram in UV light, 2-mercaptoponaphth[2,3]imidazole shows a brilliant yellow phosphorescence for several seconds after withdrawal of the light source. 2-Mercaptobenzimidazole does not do this" (p. 1976). The above two observations have been reported and confirmed by Lloyd and Miller (9).

In 1967, Roth (12) reported a study of the RTP of no fewer than 29 compounds on several supporting media. Of these compounds, 17 were found to phosphoresce sufficiently at microgram or submicrogram levels on cellulose surfaces. Two weakly phosphoresced and the others, including folic acid, chrysene, fluorescein, 8-hydroxyquinoline were

nonphosphorescent. Roth emphasized the value of the RTP technique as a simple selective and non-destructive method for studying chromatograms and electropherograms. Roth's paper (12) has also been mentioned in Chemical Abstracts (13).

All the works by Millson, Brown, and Roth had been entirely overlooked. It is the report of Schulman and Walling (14) that aroused the current interest in analytical applications of the RTP of adsorbed molecules on paper and on the TLC matrices. The work of Schulman and Walling also suggested that the RTP of adsorbed molecules is not greatly affected by oxygen quenching but that a complete absence of water vapor is essential. This view was modified somewhat by the subsequent studies of Wandruszka and Hurtubise (1,15) for few special cases.

After the second paper of Schulman and Walling (16), Paynter, Wellons, and Winefordner (17) reported the first RTP work from the Winefordner group on the study of phosphorescence characteristics of a variety of commercial filter papers and RTP characteristics of several ionic organic molecules adsorbed on filter paper. Since then, there have been many other publications from Winefordner's research group devoted to the development of solid substrates for RTP, including the minimization of paper background luminescence (18), the use of inorganic compound plate (19), the use of DTPA (diethylene triamine pentaacetic acid) treated S & S 903 filter paper (20), and the use of

ion exchange filter papers (21); studies of heavy atom perturbers (21,22); investigations of RTP characteristics of pharmaceutical (23) and biological (24) compounds, pesticides (25,26), and PAHs (27,28); the design of automated sampling system/instrumentation (29,30,31,32) or solid substrate sample holder (33); the analysis of pharmaceutical preparations (2,34); and general reviews (35,36,37).

Seybold and White started their RTP work with two interesting external heavy atom effect studies (38,39). After this, Meyers and Seybold studied the effect of external heavy atom and other factors on RTP and room temperature fluorescence (RTF) of tryptophan and tyrosine (40). Meanwhile, the matrix effect on the lifetime of RTP was studied and reported by Niday and Seybold (41).

It was not until 1976 that the Hurtubise group began development of the RTP technique. The contributions from this group in the field of RTP have been use of sodium acetate (15), silica gel (42,43), and polymer-salt mixture solid substrate studies (44); phosphoroscope design (45); analysis of PABA in a vitamin tablet (1) and related work (46); identification of some nitrogen heterocycles from a shale oil sample (47); a general review (48); and a book (49).

The first RTP experiment designed for an undergraduate educational purpose was reported by Schulman (50). He then published with other coworkers studies on the effect of moisture, oxygen, and nature of the support-phosphor

interaction (51); and the analysis of pteridines (52,53). Parker, Freedlander, and Dunlap also reviewed the theory, instrumentation, substrates, and compounds studied up to 1979 (54,55).

After leaving Winefordner's group, vo-Dinh and coworkers did several excellent studies: the development of an RTP synchronous technique (56); PAH analysis by use of RTP (4,57,58,59); the use of a second-derivative technique in RTP (60); and the use of selective external heavy atom perturbation (SEHAP) RTP technique (61).

There are several other groups working in the RTP area: Jakovljevic studied lead and thallium salts as external heavy atoms in RTP (62); Lloyd developed a packed flow-through cell for RTP measurement (63); Lloyd and Miller reported on the historical background of RTP (9); Miller reviewed the RTP technique (64); and de Lima and de M. Nicola determined 1,8-naphthyridine derivatives under different optimal pH by use of RTP (65).

Phosphorescence vs. Fluorescence

A simplified energy diagram for a typical organic molecule is shown in Figure 1 and a concise comparison between varieties of luminescence techniques is shown in Table 1.

Fluorescence is the emission of electromagnetic radiation of molecules from the lowest excited singlet state (S_1) to the ground singlet state (S_0). However,

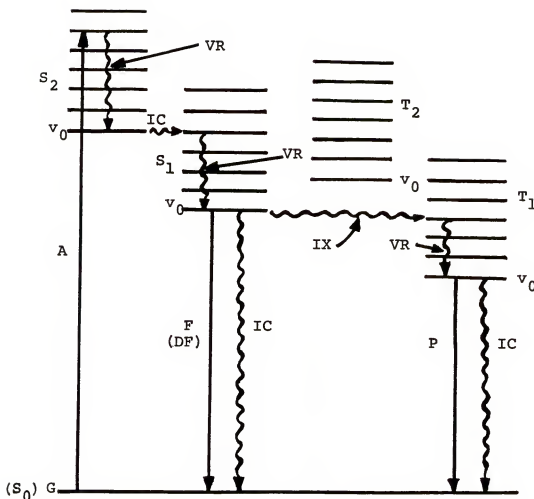


Figure 1. A simplified energy diagram for luminescence

A = absorption
 G = ground electronic state (S_0)
 v_0 = the lowest excited vibrational state
 S_2 = the higher excited singlet state
 S_1 = the lowest excited singlet state
 VR = vibrational relaxation
 IC = internal conversion
 IX = intersystem crossing
 F = fluorescence
 DF = delayed fluorescence
 P = phosphorescence
 T_2 = the higher excited triplet state
 T_1 = the lowest excited triplet state

Table 1. A Concise Comparison Between Varieties of Luminescence Techniques

	Fluorescence		Phosphorescence	
			LTP	RTP
Energy Transition	$S_1 \longrightarrow S_0$		$T_1 \longrightarrow S_0$	
Emission Wavelength	Shorter		Longer	
Lifetime	$\leq 1 \text{ ms}$		$\geq 1 \text{ ms}$	
Sample Preparation	In Solution or Solids		In Glass Matrices	On Solid Substrates ^a
Instrumentation				
a. Time Discrimination	None (usually)		Phosphoroscope ^b	
b. Sampling System	Cuvette		Cryogenic System	Solid Substrate Holder ^c
c. Deoxygenation	None		None	None ^d

For Micellar RTP:

- a. in solution
- b. no phosphoroscope is used by Cline Love et al. (78)
- c. cuvette
- d. deoxygenation is needed

For Liquid RTP:

- a. in solution and pure solvent needed
- b. phosphoroscope
- c. cuvette
- d. deoxygenation is needed

phosphorescence is the emission from the lowest excited triplet state (T_1) to the S_0 state and occurs only when intersystem crossing transition occurs for the excited S_1 molecule. There are several other transitions competing with phosphorescence emission once the molecules are in T_1 state, namely, internal conversion (IC) which releases heat instead of radiation, and delayed fluorescence (66-68) which consists of E-type and P-type delayed fluorescence named after eosin (68) and pyrene (68) individually. E-type delayed fluorescence is produced due to the molecule in T_1 may be reactivated by thermal energy back to S_1 if the molecules have closely spaced S_1 - T_1 energy levels. The P-type delayed fluorescence is observed when triplet-triplet annihilation occurs. The emission of phosphorescence from T_1 to S_0 is a spin-forbidden transition and therefore the relatively long lifetime of phosphorescence (1-100 ms) compared to that of fluorescence (1-100 ns). Phosphorescence emission from a wide variety of conjugated organic compounds is discriminated from fluorescence and scattering light by use of a phosphoroscope operated based on the lifetime difference of these radiations. There are two different kinds of phosphoroscope generally used, the rotating can and the Becquerel (69) disk phosphoroscopes. Unfortunately, the long life times are also the principal disadvantages of phosphorimetry because the excited molecules are normally deactivated by collisions with solvent molecules, molecular oxygen, impurities, and other sample

components. Consequently, phosphorescence is observed generally with the sample in a rigid media such as glass matrices at 77°K (cryogenic conditions) or adsorbed to solid substrate, etc., which prevents the excited molecules from being quenched. On the other hand, the quenching effect for fluorimetry is not as severe for phosphorimetry, and it is usually observed in solution by use of a cuvette as the container.

Theoretical Phosphorimetric Intensity Expressions

For quantitative phosphorimetry, linear relationship between the intensity of phosphorescence and the concentration of the transparent solution is necessary. From the Lambert-Beer Law, the following equation was derived by Keirs, Britt, and Wentworth (70) for phosphorescence of transparent and sufficiently dilute solutions, under the assumptions of no self-absorption, no prefilter, no postfilter phenomena, monochromatic excitation light source, and integrated phosphorescence emission is observed:

$$I_p = 2.3Y_p I_o \epsilon cl$$

where Y_p is the phosphorescence quantum yield, dimensionless;

I_o is the incident light intensity (same units as I_p);

ϵ is the molar extinction coefficient in liter/cm \cdot mole;

c is the concentration, in mole/liter, (M); and

l is the thickness of the solution, in cm.

However, the substrate of RTP is not transparent and not a solution either. Zweidinger and Winefordner (71) used the Kubelka and Munk (72,73) differential equations for diffuse reflectance in optically inhomogeneous and non-transparent media to develop equations which should be valid for RTP measurements. The intensity of the phosphorescence expression for both homogeneous and inhomogeneous matrices is given as the following:

$$I_p = 2Y_p \beta I_o \left[\frac{(1+\beta) \exp(K\bar{b}) + (1-\beta) \exp(-K\bar{b}) - 2}{(1+\beta)^2 \exp(K\bar{b}) - (1-\beta)^2 \exp(-K\bar{b})} \right] \quad (2)$$

where $\beta = \sqrt{k/(k+2s)}$.

k = fraction of radiation absorbed per average path length ($k=2.303\epsilon c$), in cm^{-1} ;

s = fraction of exciting radiation scattered per average path length, in cm^{-1} , s \neq function of analyte concentration;

\bar{b} = average cell path length for diffuse reflectance, in cm; and

$K = \sqrt{k(k+2s)}$, in cm^{-1} .

The following limiting cases are of special interest for RTP studies:

At low concentration of analyte where $kb \ll 1$,

Equation (2) reduces to

$$I_p = 2Y_p I_o \frac{kb}{1 + 2sb} \quad (3)$$

and if $2sb \ll 1$,

$$I_p = 2Y_p I_o kb \quad (4)$$

At high concentration of analyte where $kb \gg 1$, Equation (2) becomes:

$$I_p = 2Y_p I_o \left[\frac{\sqrt{k}}{\sqrt{k+2s} + \sqrt{k}} \right] \quad (5)$$

if $s \gg k$, (intermediate analyte concentration)

$$I_p = 2Y_p I_o \sqrt{\frac{k}{s}} \quad (6)$$

and if $k \gg s$, (high analyte concentration)

$$I_p = Y_p I_o \quad (7)$$

From Equations (4), (6), and (7), RTP quantification is possible due to the simple relationship between the phosphorescence intensity and the concentration of analyte. Besides, the analytical curves of RTP ($\log I_p$ vs $\log C$ or $\log k$) should have a slope of unity at low analyte concentrations, a slope of 0.5 at intermediate analyte concentrations, and a slope of zero at high analyte concentrations.

Room Temperature Phosphorescence (RTP) vs. Low Temperature Phosphorescence (LTP)

The phosphorescence phenomenon was first identified by Lewis and Kasha (74) in 1944 and was evaluated for analytical uses by Kiers, Britt, and Wentworth (70) in 1957. Then up to 1963, several research groups devoted their effort to develop phosphorimetry, i.e., particularly, Freed and Salmre (75), Parker and Hatchard (76), and Latz and Winefordner (77). Since 1963, most of the work in the field of phosphorimetry has been carried out by Winefordner's research group including both low and room temperature phosphorimetry.

However, since the 1975 reviews of phosphorimetry (LTP especially), as reported by Ward, Walden, and Winefordner (37), very little has been done in the field of LTP. In spite of the excellent sensitivity, selectivity of LTP for many biologically and environmentally important molecules, LTP has failed to be a popular method for routine analysis. The reasons are all related to the necessity of low temperature (77°K) for LTP; to achieve the liquid nitrogen low temperature, expensive high-grade optical quartz and other cryogenic equipment are necessary and are very expensive and fragile. Besides, while the sample is introduced into liquid nitrogen, the cooled matrix can be a clear glass, a cracked glass, or a snow, the latter two often causing poor precision of LTP. In attempting to obtain a clear glass which gives reproducible LTP

measurements, the sampling procedure becomes very tedious and time consuming. All of these disadvantages of LTP do not exist when RTP is used for analyses. However, fewer compounds are able to phosphoresce at room temperature on solid substrates and the linear dynamic range (LDR) as well as sensitivity are worse than those of LTP. All in all, RTP has better hope to be popular than LTP if the LDR and sensitivity of RTP can be improved and the generality of use can be extended in RTP.

Solid Substrate RTP vs. Micellar RTP and Liquid RTP

In 1980, Cline-Love, Skrilec, and Habarta (78) reported the first analytically useful micelle-stabilized room temperature phosphorescence work on the analysis of naphthalene, pyrene, and biphenyl. In the same year, the study of nine substituted arenes was published by the same authors (79). Since then, their research studies on micellar RTP have been devoted to lifetime and spectral studies (80); background correction via selective bimolecular quenching (81); cationic and anionic surfactants as micellar mobile phase in HPLC (82); HPLC-micellar RTP detector (83); and analysis of nitrogen heterocycles (84).

Although the micellar RTP has several advantages of excellent detection limits (nM in some cases (85)), use in aqueous solutions, fewer interferences, enhanced phosphorescence vs. fluorescence, and a phosphoroscope-free instrument as reported by Cline-Love and Skrilec (85), micellar RTP does have drawbacks; it has a tedious and

time consuming sample preparation procedure and many fewer compounds can be measured by use of this technique. In comparison, solid substrate RTP has the merit of being much simpler, entailing a time-saving procedure, and measuring more compounds. The methods have similar detection powers.

In 1981, Frei et al. (86) studied RTP in liquid solution by use of analytes as donors of triplet energy and α -diketones as acceptors to observe sensitized phosphorescence. The sensitivity of this technique is a little bit inferior to that of LTP, with LOD in the range of 10^{-7} to 10^{-9} M which rivals micellar RTP and solid substrate RTP, for polychlorinated biphenyl (PCB) and naphthalene (PCN) and polybrominated biphenyl (PBB) and naphthalene (PBN) etc. However, deoxygenation with a complicated apparatus and a very pure solvent are essential for sensitized phosphorescence observation. The continued work on this by Frei et al. (87,88) including an HPLC detection system by use of this RTP technique to study PCB, PBB, PCN, and PBN by use of diacetyl as the acceptor (87). In this LC system, a 100 μ l sample volume and a pure eluent from the column are essential for detection. However, the LODs lie in the range of 10^{-7} to 10^{-9} M which is about the same as the static system. The advantages of this technique compared to micellar and solid substrate RTP are the same, i.e., excellent sensitivity and selectivity, but it does require a phosphoroscope as solid substrate RTP. However,

it can be used in normal-phase HPLC which is not accessible to micellar RTP at this moment. The disadvantages of liquid RTP are the same as those of micellar RTP, namely, deoxy- genation and pure solvents necessary which cause problems of tedious, time consuming sample preparation.

Theories of Solid Substrate RTP

There are several known factors affecting the RTP observation. First, the degree of rigidity of an analyte held on a solid substrate either through hydrogen bonding formation between analyte and substrate or via ionic or chemical adsorption; second, the presence of heavy atom perturber enhancing the phosphorescence intensity; third, the dryness of the substrate; and fourth, the freedom from molecular oxygen. Once the analyte is adsorbed firmly on the solid substrate, the thermal deactivation probability decreases and intersystem crossing increases. The heavy atom perturber also increases the intersystem crossing rate in addition to enhancing the rate of phosphorescence emission from T_1 to S_0 (39,89,90). Since hydrogen bonding formation between analyte and substrate is one of the main factors (15, 54,64) which fulfills the rigidity factor, the presence of a trace amount of water will compete with the analyte for the possible hydrogen bonding sites to reduce rigidity thus decreasing the phosphorescence intensity. Oxygen is a potent quenching agent of the excited triplet state molecules (91,92); however, the RTP early reports (14,16) suggested that RTP was nearly completely insensitive

to oxygen quenching in dry atmosphere. Subsequent studies (29,51) with filter paper showed that RTP is quenched to some degree by oxygen, although it is not serious in a dry atmosphere. It is also noticed that RTP signals are slightly lower in air than in other inert gases, such as nitrogen or helium (45). Certainly, there may be other mysterious factors still unexplored which may affect the success and usefulness of RTP as an analytical tool.

Solid Substrates

A rigid media, such as glass matrices at 77°K, solid substrates, or micelles is essential for RTP observation. At the current stage, varieties of filter papers (36,55) are the most popular and simplest solid substrate for RTP studies. However, there is a serious background luminescence problem inherent with papers interfering with analyte phosphorescence observation especially in the emission wavelength range of 450 to 550 nm. There have been hundreds of compounds studied by use of various filter papers. Sodium acetate solid substrate introduced by Hurtubise et al. (1,15), produces a lower background luminescence but is not as popular as filter paper so far and fewer compounds have been studied on it. Silica gel, also introduced by Hurtubise et al. is the main constituent of thin layer chromatography (TLC) possessing the same advantages and disadvantages of those of the sodium acetate substrate. Inorganic compound plates (19), introduced by Su and Winefordner, produces lower background luminescence but

unfortunately, also lower phosphorescence signals for the analytes compared to paper substrates. Since there are many potential inorganic or organic compounds to be used as the constituent of plate substrates and the optimal composition between binder and inorganic or organic compounds has not been optimized, it is too soon to decide the fate of inorganic or organic plate solid substrates.

Bateh and Winefordner (20) reported that DTPA (diethylene triamine pentaacetic acid) treated S & S 903 filter paper as a better substrate than S & S 903 filter paper in terms of background luminescence and analyte signal. Dalterio and Hurtubise (44) studied the possibility of utilizing polymer-salt mixtures as solid substrates for analysis of hydroxyl-substituted aromatics and found that the LODs of eight compounds on 1% PAA (polyacrylic acid)-NaBr substrate are two to fifteen times worse than those on Whatman No. 31 filter paper. Su and Winefordner (21) reported the work of evaluating ion exchange filter papers as solid substrate for RTP and found that the anion exchange filter paper is quite successful for analysis of anionic species in the presence or absence of heavy atoms, and they expected that cationic exchange filter papers are a very promising substrate for cationic analytes with or without heavy atoms.

Instrumentation

The main components of spectrophotofluorimeter used to observe RTP consists of an intense light source (either continuous wave (cw) or pulsed Xenon lamp or laser light source); two monochromators select excitation and emission wavelengths suitable for the analyte; a sensitive detection system, generally a photomultiplier tube is used; a phosphoroscope is used to discriminate the phosphorescence from fluorescence and/or scattering light; and the solid substrate holder holds the solid substrates in alignment with the optical path of the spectrophotofluorimeter. There are various solid substrate sample holders used in different research laboratories at the present time: a rotatable hollow copper drum with filter paper or TLC plate being wrapped around (64); a brass plate with a series of circular depressions for powder or paper substrates (44); and an aluminum bar with a four opening hole cover plate for the paper substrate (33). Two systems incorporating a continuous role of filter paper as the substrate were designed by Winefordner and coworkers (29,31) to be employed for routine analysis.

CHAPTER 3
DEVELOPMENT OF NEW SOLID SUBSTRATES FOR RTP

Introduction

The development of a good solid substrate which produces higher analyte luminescence intensities and lower background luminescence than the present solid substrates, i.e., filter paper (14,16,22-24,28,37), silica gel (42,45), sodium acetate (1,15) is the most important critical factor affecting the success of room temperature phosphorescence (RTP) as an analytical tool. Many efforts have been made to minimize the background luminescence of filter paper by a rinsing, chemical treatment, heating procedure in our laboratory (18). Recently, Bateh and Winefordner (20) reported the study of cellulose as a solid substrate for RTP. They suggested that hemicellulose and/or lignin is the main species inducing the background luminescence. Unfortunately, such species can not be removed from the filter paper without degrading it, and so these materials will always hamper the RTP observation as long as the phosphorescence emission is in the range of 450-550 nm. In addition, they reported DTPA treatment of S & S 903 filter paper may fill the voids in S & S 903 which will minimize absorption of the analyte into the filter paper and will maximize the adsorption of analyte onto the surface.

Therefore, the analyte phosphorescence intensity will be enhanced. Based on the proposed theories of RTP, the rigidity of the analyte held on the solid substrate is critical to RTP observation. It is believed that the probability of nonradiative deactivation is minimized by the rigidity factor, thus enhancing the probability of intersystem crossing (54,64). So far, hydrogen bonding (15,54,64) of the analyte to the substrate is believed to be the main mechanism in filter paper and sodium acetate substrates responsible for the rigidity factor.

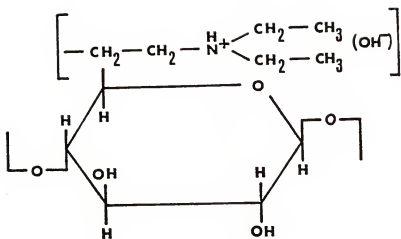
In the present case, inorganic compound plate substrates were developed by blending certain amounts of inorganic compounds which possess one or more possible hydrogen-bonding sites, with one or more binding materials such as T-7 clay (93), corn starch (93), etc. The limits of detection (LODs) of PAHs and PABA were studied by use of several inorganic compound plates and the results are shown in Table 4. Since filter paper is so far the best solid substrate for RTP due to its possession of multi-hydrogen bonding sites in each cellulose molecule, any decrease in the background luminescence and/or increase in the analyte signal intensity of paper certainly leads to the development of a better solid substrate. This thought leads to the exploration of ion exchange filter papers as RTP substrates. If there is an ionic exchange group, in addition to the hydroxyl groups in the substrate, ionic compounds will be held even more rigidly than with substrates

not containing ion exchange groups. Therefore, commercially available anionic exchange filter paper which has free OH^- as well as an NH^+X^- functional groups (Figure 2) (anion exchange filter paper) is evaluated in the present study. Cationic exchange ($-\text{COO}^-\text{Na}^+$) filter papers are not commercially available in filter paper form and so could not be included in this study; in the future, we hope to evaluate cationic exchange papers, especially for those analytes which require Ag^+ or Tl^+ or other cationic heavy atoms to induce RTP. The analytical figures of merit (detection limit, linear dynamic range, slopes of calibration curves) of several model compounds of drugs, pesticides, and PAHs are investigated by use of Whatman DE-81 anion exchange filter paper, and the results are compared with those with S & S 903 filter paper as the substrate.

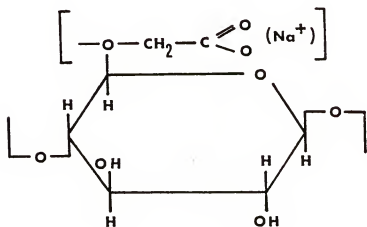
Experimental

Instrumentation

All RTP observations are performed with an Aminco-Bowman spectrophotofluorimeter and ratio photometer (American Instrument Co., Silver Springs, MD), with a Hamamatsu 1P21 photomultiplier tube (Whatman, MA), a 150 W Xe arc lamp, an X-Y recorder (Bolt, Beranek, and Newman, Inc.), and a laboratory-constructed phosphoroscope for use with the sampling bar system (33). A block diagram of instrument and a table of components are given in Figure 3 and Table 2, respectively.



DIETHYLAMINOETHYL CELLULOSE (ANION)



CARBOXYMETHYL CELLULOSE (CATION)

Figure 2. Structure of anion (top) and cation (bottom) exchange filter papers

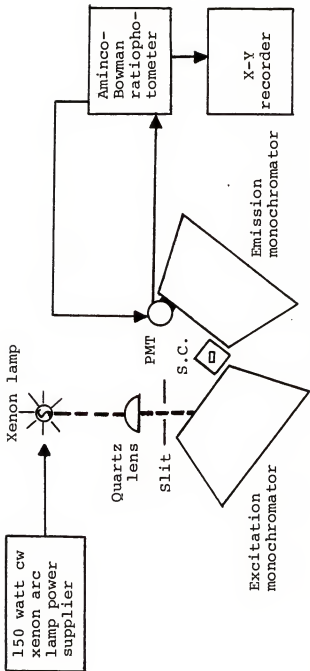


Figure 3. A block diagram of instrument for RTP study

S.C. = sample compartment
PMT = photomultiplier tube

Table 2. A Table of Components of Instrument for RTP study

<u>Components</u>	<u>Manufacturer</u>
Aminco-Bowman Spectrophotofluorimeter/ratiophotometer	American Instrument Co., Silver Spring, MD
Plotamatic X-Y recorder	Bolt, Beranek and Newman Inc., Santa Ana, CA
1P21 photomultiplier tube	Hamamatsu Co., Whatman, MA
150 W cw xenon arc lamp power supplier	Schoeffel Instrument Co., Westwood, NJ
Rotating can phosphoroscope	Laboratory built
4-Hole sampling bar system	Laboratory built
Fisher Recorderall Series 5000 recorder	Fisher Scientific Inc., Pittsburgh, PA
Apple II computer system	Apple Computer Inc., Cupertino, CA
12-Bit analog-to-digital converter	Laboratory built
Scaler (0-10 volt full scale)	Laboratory built
10-Hertz low pass Sallen-Key equal component active filter	Laboratory built
Hiplot digital plotter DMP-4	Houston Instrument, Austin, TX
Paper Tiger printer	Integral Data Systems, Milford, NH

Chemicals

The compounds determined were obtained from commercial sources (Table 3) except the pesticides which were obtained from the Environmental Protection Agency (EPA) (Research Triangle Park, NC 27711, analytical reference standards). All chemicals were analytical grade except PABA was practical grade and all used without further purification upon receiving. The solvents used for sample preparations were PAHs and pesticides in pure ethanol (U.S. Industrial Chemical Co.); drugs and PABA in 1:1 ethanol/water (Barnstead nanopure water, Barnstead/Sybron Co.). The filter papers used were S & S 903 (Schleicher & Schuell Inc., Keene, NH) in both studies; DE-81 (Whatman Chemical Separation Inc., Clifton, NJ); and DTPA treated S & S 903 (preparation procedure was described by Bateh and Winefordner (20)).

Procedure

Inorganic compound plates. At the very beginning of the study, chalk was cut and shaved to produce thin plates approximately 1-2 mm thickness and 6-8 mm square; unfortunately, these plates were quite fragile. In addition, this procedure was too time consuming and tedious. Alternatively, a paste of chalk powder was thus used and was prepared as described below. Because the main components of all chalk are CaCO_3 and a binder, we also felt a study of other substrates, including H_3BO_3 , CaHPO_4 , Na_2HPO_4 , and CaSO_4 was desirable. These compounds have at least one

Table 3. Compounds Studied by RTP and Their Sources

<u>Compound</u>	<u>Source</u>
Privine HCl	Ciba-Geigy Corp., Summit, NJ
Procaine HCl	
Chrysene	Eastman Kodak, Rochester, NJ
Phenanthrene	
Coronene	
p-Aminobenzoic acid	
Biphenyl	
Fluoroanthene	Chem Service, Media, PA
Pyrene	
1,2,5,6-Dibenzanthracene	K & K Laboratories, Inc. Plain View, NY
Carbazole	Aldrich Co., Milwaukee, MI
Diethylene triamine pentaacetic acid	Sigma Chemical Co., St. Louis, MO
Naphthalene acetic acid Oxythioquinox	Environmental Protection Agency (EPA) Research Triangle Park, NC
2-Aminobenzimidazole	
Ancymidol	

active site, such as carboxyl or hydroxyl groups in each of them; CaCO_3 has only one free carboxyl group which appeared to interact with the analytes via hydrogen-bonding. The excitation and emission wavelengths and limits of detection of PABA and PAHs have been studied using these new inorganic compound plate substrates and results are reported in this chapter. External heavy atoms TlNO_3 , AgNO_3 and NaI were also used in the study. The chalk plates were made by the following procedure: chalk powder which was shaved from chalk and was mixed with Barnstead deionized water to make chalk paste which was then spread on a plastic plate (approximately 20 cm x 15 cm x 3 mm) with 1-2 mm thickness and was dried under an infrared (IR) heat lamp. After being dried, a blade was used to trim the chalk into 6-8 mm square plates. The H_3BO_3 /T-7 clay/NaOH and CaHPO_4 /T-7 clay/corn starch/NaOH plates were made by the same procedure as the chalk plates except the materials were already in powder form. (T-7 clay and corn starch were obtained from Weber Costello Co.)

Ion exchange filter paper. A 1 μl sample solution or solvent or heavy atom solution was introduced by use of an SMI micropettor (Emeryville, CA) onto one of the 1/4 in diameter filter paper discs which were held in the sampling bar under an IR heating lamp (c.a. 65°C) for 5 min (ethanol as solvent) or 10 min (ethanol/water as solvent). Afterwards, the sampling bar was inserted into the sample

compartment of the spectrophotofluorimeter with N_2 stream passing downward over the samples. After a 7 min cooling time, the RTP observation was made and recorded.

Results and Discussion

Inorganic Compound Plates

The LODs of analytes studied are listed in Table 4 together with their characteristic excitation and emission wavelengths. Generally speaking, this inorganic compound plate produced a much lower background luminescence but a much smaller analyte signal than the S & S 903 filter paper. The LODs of the same analytes on S & S 903 filter paper are much better than those on the new substrates (see Table 4). However, there are a number of parameters that still need to be optimized in the case of the new substrates for RTP, including the composition of the substrate, i.e., the fractions of inorganic substances, clay, and NaOH; insufficient time prevented optimization of these parameters in the present study. Also, the amounts of heavy atoms used may not be optimal for these new substrates because they are chosen based upon the results for filter paper. It may be interesting to point out that there is an additional phosphorescence emission peak at 460 nm for coronene on H_3BO_3 plate as shown in Figure 4. This additional emission peak is believed to be the delayed fluorescence (66-68,94) of coronene; it is observed when anionic exchange filter paper (DE-81) is used for RTP of coronene.

Table 4. Excitation and Emission Room Temperature Phosphorescence Wavelengths and Corresponding Limits of Detection for Several PAHs in the Presence of Various Heavy Atoms and with Several Inorganic Compound Plate Substrates

Compound	Conditions	Filter Paper				Chalk				$\text{H}_3\text{BO}_3/\text{T}-7/\text{NaOH}$				$\text{CaHPO}_4/\text{T}-7/\text{Corn Starch}$			
		λ_{ex}	λ_{em}	<u>LOD</u>	λ_{ex}	λ_{em}	<u>LOD</u>	λ_{ex}	λ_{em}	<u>LOD</u>	λ_{ex}	λ_{em}	<u>LOD</u>	λ_{ex}	λ_{em}	<u>LOD</u>	
PABA	1M NaI	284	432	.02	284	432	0.2	284	432	NA	284	432	1.0				
Phenanthrene	0.1M TiNO_3	284	505	0.2	290	480	25	284	505	10	290	480	25				
	1M AgNO_3	284	505	0.4	294	480	32	284	505	16	290	480	NA				
Chrysene	0.1M TiNO_3	272	515	0.3	280	525	NA	280	515	30	280	525	NA				
	1M AgNO_3	272	515	0.7	280	525	15	280	515	15	280	525	NA				
Coronene	0.1M TiNO_3	310	530	1.4	310	530	NA	310	460	NA	310	530	NA				
	1M AgNO_3	310	530	0.1	310	530	4.0	310	460	NA	310	530	NA				
Fluoranthene	0.1M TiNO_3	284	555	3.7	350	500	350	350	555	NA	350	555	NA				
	1M AgNO_3	284	555	4.0	360	565	35	350	555	NA	350	555	NA				
Pyrene	0.1M TiNO_3	330	600	4.0	340	600	17	330	600	80	330	600	70				
	1M AgNO_3	340	600	6.0	340	600	NA	330	600	24	330	600	NA				

Table 4-continued

Compound	Conditions	Filter Paper				Chalk				$\text{CaHPO}_4/\text{T}-7/\text{NaOH}$				$\text{CaHPO}_4/\text{T}-7/\text{Corn Starch}$			
		<u>λ_{ex}</u>	<u>λ_{em}</u>	<u>LOD</u>	<u>λ_{ex}</u>	<u>λ_{em}</u>	<u>LOD</u>	<u>λ_{ex}</u>	<u>λ_{em}</u>	<u>LOD</u>	<u>λ_{ex}</u>	<u>λ_{em}</u>	<u>LOD</u>	<u>λ_{ex}</u>	<u>λ_{em}</u>	<u>LOD</u>	
Carbazole	1M NaOH/NaI	323	440	.07	323	440	3.0	323	440	NA	323	440	0.4				
1,2,5,6-Dibenzanthracene	0.1M TlNO_3 1M AgNO_3	300	565	5.0	300	555	NA	300	555	NA	300	555	NA				
Biphenyl	0.1M TlNO_3 1M AgNO_3	266	486	10	286	486	NA	286	486	NA	286	486	NA				

a. LOD in ng is determined by $\text{S}/\text{N} = 3$ and analyte volume = 5 μl ; λ_{ex} and λ_{em} are peak excitation and emission values in nm. If more than one wavelength is given, the peak value is underlined; NA = not analytically useful.

LOD of carbazole on $\text{CaSO}_4/\text{Na}_2\text{HPO}_4/\text{Kaolinite clay/NaOH}$ plate is 0.7 ng; LOD of PABA on it is 0.4 ng.

LOD of carbazole on $\text{CaHPO}_4/\text{Kaolinite clay}$ is 1.0 ng.

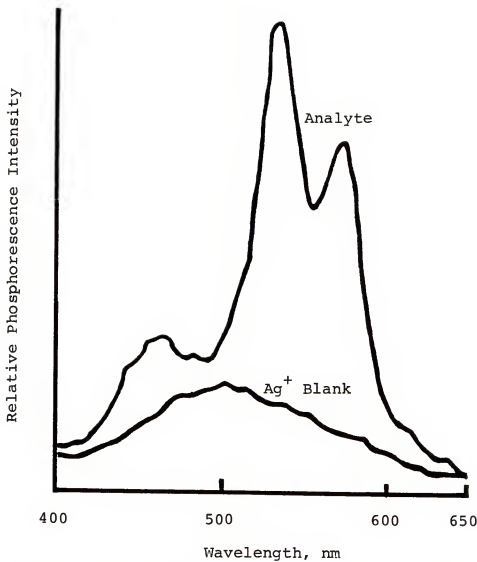


Figure 4. RTP spectrum of coronene in 1 M AgNO_3 and on boric acid inorganic compound plate ($\lambda_{\text{ex}} = 310 \text{ nm}$)

Ion Exchange Filter Papers

Background luminescence and the presence of heavy atoms. The critical figures of merit in evaluating a solid substrate for RTP observation are the background luminescence and analyte intensities compared with a reference substrate, e.g., S & S 903. In Table 5, DE-81 has the lowest background luminescence except for the presence of I^- , i.e., after I^- exceeds approximately 2 μ mole I^- . In addition, the background luminescence of DE-81 increases in the case of I^- , whereas, those of S & S 903 and DTPA treated S & S 903 filter paper decrease. However, in the case of Ag^+ , the background luminescence of DPTA treated S & S 903 increases whereas S & S 903 and DE-81 decrease. The decrease of background luminescence of DE-81 when Ag^+ is used is probably due to the deposition of silver metal and oxides by the basic environment of DE-81 and the catalysis of UV light. DE-81 filter paper becomes grayish brown in color if more than 0.07 μ mole Ag^+ is applied on it. However, Tl^+ does not have a similar problem with deposition of the metal or oxide.

Analytical figures of merit. If minimization of background luminescence results at the expense of reduced analyte intensity, the substrate is not then so desirable for analytical RTP studies. In fact, DE-81 not only minimizes the background luminescence, but also enhances the analyte intensities of drugs, pesticides, and PABA to some extent as compared with S & S 903. In the case of

Table 5. Background Luminescence of Substrates DE-81, S & S 903, and DTPA Treated S & S 903 Filter Papers

		Blank Solutions							
Solvent	0.1 M	0.02 M	0.1 M	1 M	2 M	0.0035 M	0.007 M	0.35 M	
Substrate	EtOH/H ₂ O	Tl ⁺	I ⁻	I ⁻	I ⁻	Ag ⁺	Ag ⁺	Ag ⁺	
DE-81	6.7	22.8	6.4	10.7	13.8	20.6	7.1	5.7	1
DTPA treated S & S 903	20.6	40.0	20.6	20.6	17.3	15.6	23.2	24.2	25.7
S & S 903	51.7	105.2	48.9	48.2	35.6	34.0	64.3	70.9	50.7

35

a. All the luminescence intensities are normalized to that of 0.35 M Ag⁺ on DE-81. The wavelengths used to take the above data are: $\lambda_{ex} = 310$ nm, $\lambda = 496$ nm for Ag⁺ and Tl⁺; $\lambda_{ex} = 300$, $\lambda_{em} = 490$ for I⁻. The intensity of the solvent blank is taken at these two wavelength combinations and average values used.

2-aminobenzimidazole pesticide, DE-81 enhances the signal approximately 20 times (compared to S & S 903) and 40 times (compared to DTPA treated S & S 903). In Table 6, limits of detection of drugs and pesticides using DE-81 are usually better than with S & S 903 and about the same as or better than DTPA treated S & S 903. However, for PAHs, DE-81 with Ag^+ or Tl^+ generally results in somewhat poorer detection limits compared to S & S 903 or DTPA treated S & S 903; this is to be expected since DE-81 is an anionic exchange filter paper. However, slightly greater linear dynamic ranges for drugs and pesticides, occur with DE-81 than with S & S 903.

Special characteristics of some PAHs. Coronene on DE-81 (Figure 5) is observed to induce additional emission peaks at approximately 435 nm and 465 nm in addition to the normally present 530 nm and 570 nm emission peaks as reported previously for a boric acid plate; it is believed that the additional peaks are delayed fluorescence of coronene (94). Therefore, a further study was carried out for coronene on DE-81. First, RTP of coronene without the addition of Ag^+ on DE-81 and S & S 903 is observed, and the results are listed in Table 7 (a), and shown in Figure 6, which shows that the maximum phosphorescence occurs at 570 nm for both cases; also, the phosphorescence intensities on DE-81 are smaller at 530 nm than at 570 nm and the phosphorescence intensity at 530 nm on S & S 903 is not detectable. However, the RTP signal of coronene at 570 nm

Table 6. Analytical Figures of Merit of Several Model Compounds Evaluated Using DE-81, S & S 903 and DTPA Treated S & S 903 Filter Papers

Compound	Heavy Atom	Substrate	λ_{ex} (nm)	Absolute		
				λ_{em} (nm)	LOD (ng) ^b	Slope ^c
Carbazoled	I ⁻	DE-81	323	436	0.054	1.02
	I ⁻	S & S 903	323	436	0.059	0.98
Biphenyl	Ag ⁺	DE-81	266	486	9.0	0.94
	Ag ⁺	S & S 903	266	486	3.7	1.01
Tl ⁺	DE-81	266	486	7.7	1.03	15
	Tl ⁺	S & S 903	266	486	6.9	0.96
Chrysene	Ag ⁺	DE-81	272	515	2.6	0.97
	Ag ⁺	S & S 903	272	515	1.1	1.07
Tl ⁺	DTPA ^e	272	515	1.1	0.88	>50
	Tl ⁺	DE-81	272	515	0.20	----
Tl ⁺	S & S 903	272	515	0.18	----	50
	Ag ⁺	DE-81	304	530	0.39	0.98
Coronene	Ag ⁺	S & S 903	304	570	0.76	1.09
	Ag ⁺	DE-81	304	570	0.33	1.01
Tl ⁺	DE-81	304	530	0.08	1.08	10
	Tl ⁺			570	0.21	0.99

Table 6-continued

Compound	Heavy Atom	Substrate	λ_{ex} (nm)	λ_{em} (nm)	Absolute LOD (ng) ^b	Slope ^c	LDRC
Coronene- (continued)	Tl ⁺	S & S 903	304	530	0.11	1.08	20
				570	0.25	1.03	20
Phenanthrene	Ag ⁺	DE-81	260	505, 476 ^f	1.5	0.89	27
	Ag ⁺	S & S 903	260	505, 476 ^f	0.6	0.99	>100
	Ag ⁺	DTPA	260	505, 476 ^f	1.0	0.94	>60
	Tl ⁺	DE-81	260	476	0.4	0.96	12
	Tl ⁺	S & S 903	260	505	0.5	0.97	12
				476	0.2	1.13	10
				505	0.2	0.98	10
Privine HCl	I ⁻	DE-81	280	490, 510	0.32	1.02	>400
	I ⁻	S & S 903	280	490, 510	0.33	0.92	>400
	I ⁻	DTPA ^e	280	490, 510	0.44	1.09	>300
Procaine HCl	I ⁻	DE-81	300	440	0.23	1.09	>780
	I ⁻	S & S 903	300	440	0.34	0.93	18
	I ⁻	DTPA ^e	300	440	0.22	0.90	>800
2-Aminoben- zimidazole	I ⁻	DE-81	280	410	2.3	1.06	50
	I ⁻	S & S 903	280	410	50.	----	----
	I ⁻	DTPA ^e	280	410	110.	----	----

Table 6-continued

Compound	Heavy Atom	Substrate	λ_{ex} (nm)	λ_{em} (nm)	Absolute LOD (ng) ^b		Slope ^c	LDR ^c
					LOD (ng)	Absolute LOD (ng)		
Naphthalene Acetic Acid	I ⁻	DE-81	290	490, 515	0.2	1.01	>500	
	I ⁻	S & S 903	290	490, 515	0.4	0.92	10	
	I ⁻	DE-81	290	490, 515	0.12 ^g	1.00 ^g	>1000	
	I ⁻	S & S 903	290	490, 515	0.21 ^g	0.96 ^g	>500	
	---	DE-81	290	490, 515	3.5 ^g	0.99 ^g	5	
	---	S & S 903	290	490, 515	3.5 ^g	1.04	5	
Oxythioquinox ^h	I ⁻	DE-81	396	470	17.	0.94	3	
	I ⁻	S & S 903	396	546	8.	----	----	
	I ⁻	DE-81	396	470	11.	0.89	>10	
	---	DE-81	396	546	13.	0.87	>8	
	---	S & S 903	396	470	17.	0.91	>6	
	---	DE-81	396	546	8.	----	>14	
PABA	I ⁻	DE-81	280	432	0.02	0.94	>5000	
	I ⁻	S & S 903	280	432	0.06	0.95	>2000	
	---	DE-81	280	432	0.15	1.05	>600	
	---	S & S 903	280	432	0.20	0.89	>500	
	---	DE-81	280	432	0.20	0.89	>500	

a. Sample volume = 1 μ l; concentrations of I⁻ = 1 M, of Ag⁺ = 0.035 M, of Tl⁺ = 0.1 M; no heavy atom means solvent only; signal-to-noise ratio for LOD determination = 3

Table 6-continued

- b. Absolute LOD (ng) = $1 \mu\text{l} \times \text{LOD } (\mu\text{g/ml})$; the LODs in the Table are the average values of those within linear dynamic range.
- c. Linear dynamic ranges (LDRs) are the ratios of the upper concentration of linearity (within 5%) and the LOD (">" symbol used for those LDRs which may extend over the upper concentrations used in the study; no symbol used for all others with certain concentration limits);
- The slopes are taken for the analytical calibration curves of log RPI vs log concentration of analytes.
- d. I^- is the best heavy atom so far for carbazole²⁷.
- e. DTPA stands for diethylenetriamine pentaacetic acid treated S & S 903 filter paper.
- f. The two peaks are not well-resolved.
- g. Data obtained with infrared lamp heating procedure in all cases, except those denoted with g superscript, and then the procedure was with 6 min in measurement position at room temperature in a dry N_2 stream.
- h. Ancymidol pesticide did not phosphoresce and so is not included in the Table.

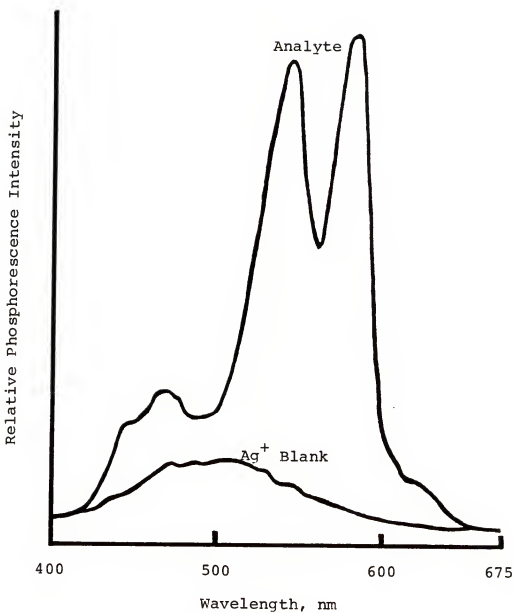


Figure 5. RTP spectrum of coronene in 0.0035 M AgNO_3 and on DE-81 filter paper ($\lambda_{\text{ex}} = 310 \text{ nm}$)

Table 7. RTP Net Analyte Intensities of Coronene^a

(a) Without heavy atoms

Substrate	[Coronene], $\mu\text{g/ml}$				
	2.2	5.5	10.9	27.3	54.5
DE-81	-/0.8	1.3/1.9	2.4/4.6	6.7/13.1	4.6/9.5
S & S 903	-/-	-/-	-/1.3	-/4.2	-/3.6

(b) With Ag^+ as heavy atom (DE-81)

[Ag^+], M	[Coronene], $\mu\text{g/ml}$				
	2.2	5.5	10.9	27.3	54.5
1	8.4/3.5	19.9/7.7	45.5/18	67.7/26.6	89.1/35.4
0.7	7.2/2.5	17.6/6.4	39.5/14.4	73.6/28.6	100.5/37.7
0.007	2.6/2.0	6.9/5.4	11.3/9.4	17.4/16.3	22.6/21.7
0.0035	1.8/1.4	4.5/4.7	9.7/10.9	14.2/13.8	16.8/15.8
0.00035	1/1	3.5/4.5	4.4/6.0	7.8/10.8	7.8/10.3

a. The numbers in the Table are the phosphorescence intensities of coronene at 530 nm to the left hand side of slash and at 570 nm to the right hand side of the slash. All the intensities are normalized to the intensity of 2.2 $\mu\text{g/ml}$ coronene in 0.00035 M Ag^+ .

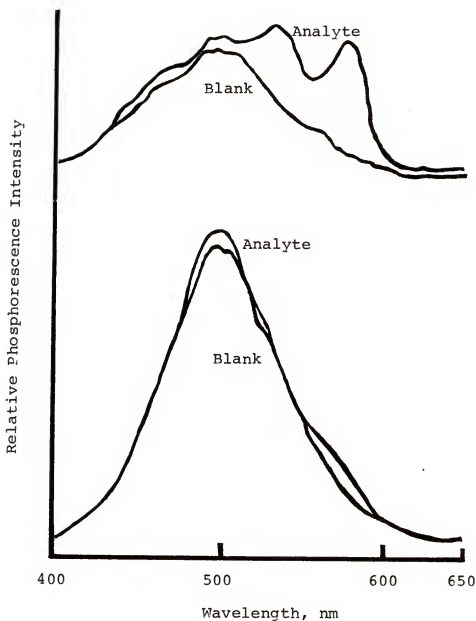


Figure 6. RTP spectra of coronene (5.5 $\mu\text{g}/\text{ml}$) without heavy atom on DE-81 (top) and S & S 903 (bottom) filter papers
($\lambda_{\text{ex}} = 310 \text{ nm}$)

results in the maximum emission peak up to 0.0035 M Ag^+ but the 530 nm peak becomes maximal for all higher Ag^+ concentrations as shown in Table 7 (b) and Figure 7. The inversion of the order of intensities at 530 nm and 570 nm is believed to be due to the Ag^+ heavy atom perturbing the excited triplet state corresponding to the shorter wavelength of coronene to a larger degree than the longer wavelength one (570 nm). With phenanthrene, on the other hand, 0.035 M Ag^+ results in poorly resolved 476 nm and 505 nm peaks (Figure 8). However, with 0.1 M Tl^+ well separated peaks occur at 476 nm and 505 nm (Figure 8).

Conclusions and Future Work

According to the studies, inorganic compound plates minimize background luminescence, but do not enhance the analyte phosphorescence intensity enough to be useful as a better substrate than filter paper. Of course, changing the heavy atom concentration and/or species and optimizing the compositions of the inorganic compound and binding material as well as choosing the suitable inorganic species may make things different. Besides, organic compounds possessing possible hydrogen bonding sites, e.g., DTPA may be used to make plate substrates. Certainly, it is more tedious and time consuming for preparing the plates than the commercially available filter paper, but it is hoped that eventually a good plate substrate can be made to surpass these drawbacks and make RTP a more useful technique.

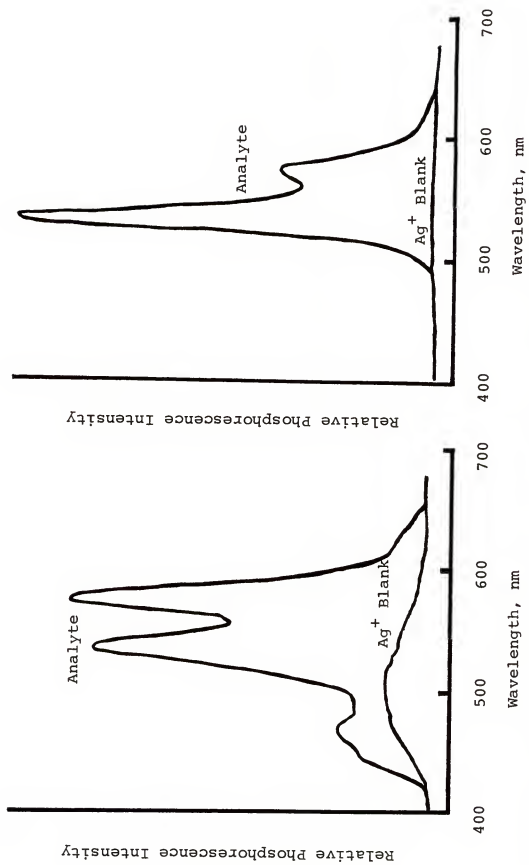


Figure 7. RTP spectra of coronene (10.9 $\mu\text{g}/\text{ml}$) in 0.0035 M (left) and 0.7 M (right) AgNO_3 and on DE-81 filter paper ($\lambda_{\text{ex}} = 310 \text{ nm}$)

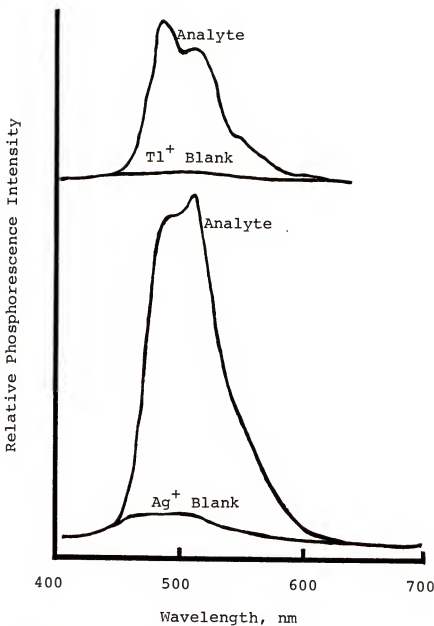


Figure 8. RTP spectra of phenanthrene (63 $\mu\text{g}/\text{ml}$) in 0.1 M TlNO_3 (top) and 0.0035 M AgNO_3 (bottom) and on DE-81 filter paper ($\lambda_{\text{ex}} = 260 \text{ nm}$)

The cationic exchange filter paper is not commercially available in filter paper form at the present time. However, it is reasonable to predict, based on the results of anionic exchange filter paper, that cationic exchange filter paper will be a very promising solid substrate to study cationic analytes and analytes which use cationic heavy atom perturbers. It is also reasonable to foresee the possible improvement of ion exchange filter papers by using DTPA to fill the voids and enhancing the analyte phosphorescence intensity.

CHAPTER 4
ROOM TEMPERATURE PHOSPHORESCENCE BACKGROUND
CORRECTION BY USE OF COMPUTER APPROACH

Introduction

RTP is a very selective, sensitive, and simple analytical technique which can be used to do real sample analyses without separation. However, the background luminescence of filter paper produces some difficulties in identification and quantification of the analytes as well as hampers the LOD and LDR improvement.

Although the background luminescence of the silica gel, sodium acetate, and other substrates is less than that of filter paper, it still exists and produces problems for RTP measurements. The best solution to this problem would be the discovery of a lower background luminescence substrate than the previously used solid substrates. In the meantime, correction of the sample spectrum from the background spectrum gives the analyte spectrum which is suitable for qualitative analysis purposes and for precise, fast routine measurements. In this work, this is accomplished by acquiring RTP spectra via a computer interfaced spectrophosphorimeter; the spectra were subsequently retrieved and blank corrected. At the same time, the

LODs and LDRs were also determined by using the blank corrected signals. PABA, privine HCl, biphenyl, and benomyl were studied and their LODs, LDRs, and spectra are given in this chapter.

Experimental

Instrumentation

An Aminco-Bowman spectrophotofluorimeter and ratio photometer with a Hamamatsu 1P21 photomultiplier tube, a 150 W Xe arc lamp, an X-Y recorder, and the sampling bar and phosphoroscope system were the same ones as described in Chapter 3 instrumentation section. An Apple II computer system (Apple Computer Inc., Cupertino, CA) was used to interface via a laboratory-built 12-bit A/D converter, a scaler, and a 10 Hz low pass Sallen-Key equal component active filter with the fluorimeter. Also a Houston Hiplot digital plotter DMP-4 (Houston Instrument, Division of Bausch & Lomb, Austin, TX) and a paper tiger printer (Integral Data Systems, Milford, NH) were used to plot the spectra and print the program or outputs. All these components were listed in Table 2 of Chapter 3. The circuitry diagrams of the low pass filter and Applesoft BASIC programs used to handle the data are shown in Appendix B.

Chemicals

All the reagents used are the same as those used in Chapter 3 and listed in Table 3, except that benomyl (Methyl-1-[butylcarbamoyl]-2-benzimidazole carbamate) was purchased from Chem. Service Co.

Procedure

Sample preparation. Solutions were made in the following solvents: PABA and benomyl in 1:1 ethanol/water; privine HCl in water; and biphenyl in pure ethanol. All solutions except biphenyl (143 μ g/ml) were prepared and run on the same day. An SMI 5 μ l micropettor (Scientific Manufactory Industries, Emeryville, CA) was used to spot the sample on the filter paper disc (1/4 in diameter). The disc then was dried under the IR radiation heating lamp for 10 min (water as solvent) or 5 min (ethanol as solvent). After 5 min cooling with the stream of nitrogen over it, RTP spectrum was scanned and stored/recorded.

Instrument/computer operation. A block diagram of the computer and fluorimeter is shown in Figure 9. Because wavelength scanning in the fluorimeter is controlled by a linearly increasing voltage, the voltages of 210 nm and 620 nm were determined and used as thresholds for initiating and terminating the collection of data (in photocurrent) from the fluorimeter into the computer. Gains used in both fluorimeter and scaler were stored in the data file to normalize all the data. The concentrations of solutions run were also stored in the data file. After correction

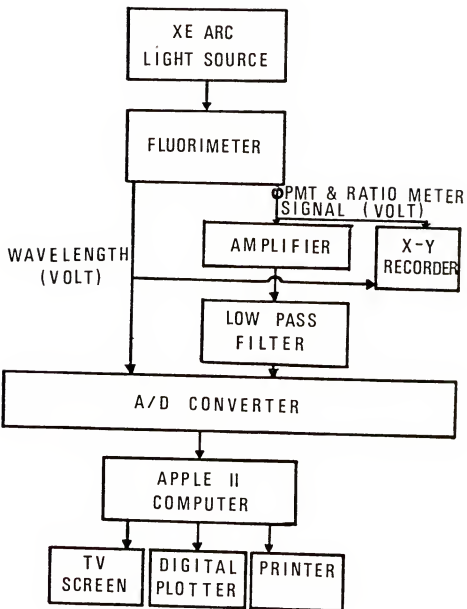


Figure 9. Block diagram of computer and fluorimeter

of the sample spectrum from the blank spectrum point by point, all data were stored on the diskette. The maxima of signals and corresponding concentrations were retrieved and used to calculate the slope and intercept in ln-ln plot by the least square method. In addition, the slope of signal vs. concentration was calculated at the same time, the slope (S = signal/concentration, in $\mu\text{g}/\text{ml}$) and the standard deviation (s) of 50 or 16 consecutively stored blank readings were used to calculate the LOD by use of the equation:

$$\text{LOD, } \mu\text{g}/\text{ml} = \frac{3s}{S} \text{ (}\mu\text{g}/\text{ml}\text{)} \quad (8)$$

Calculation of LOD, slope from conventionally recorded spectra. The difference between the peak signal for the analyte and the blank signal at the same wavelength was measured and used as the signal of the analyte. Afterwards, these data and the corresponding concentrations were used to obtain the slope of the ln-ln plot by the least square method which was a built-in program of the TI-55 calculator. The LOD was calculated using an S/N of 3 where the noise, N , was taken as 1/5 of the blank peak-to-peak noise (measured at 350 nm)

Calculations of LOD by peak-to-peak noise method and the computer stored data. The LOD was determined by use of Equation (8), where S is the blank corrected signal and the standard deviation was either found by dividing the

peak-to-peak noise (obtained over a time period equal to the 50 blanks) by 5 or by taking the standard deviation of the 50 blank signals. The computer estimated LODs for the peak-to-peak noise method and the standard deviation method are given in columns 7 and 8, respectively, of Table 8.

Results and Discussion

The characteristics of model compounds chosen to do the study are presented in Table 8. The model compounds consisted of a drug, a pesticide, a PAH, and the best compound to phosphoresce at room temperature (PABA). The slopes of the ln- \ln plots obtained by using the computer or by conventional means are similar except for benomyl which has larger random errors in the measured signals. The LODs calculated by the computer (standard deviation method) is about four times worse than those by the conventional calculation (use of noise), which may be caused by the difference of the methods used between conventional calculation (peak-to-peak of noise of blank) and computer calculation (standard deviation of blank readings). But the LODs calculated by the computer using peak-to-peak noise method are about the same as those by the conventional method. There is almost no difference between the LOD values calculated from 50 blank readings or from 16 blank readings.

Table 8. Analytical Figures of Merit for Several Model Compounds
Using the Conventional and Computer Approaches

Compound ^a	Conditions			LOD (µg/ml) ^c		Slope (S), Intercept (I) ^f		
	Solvent	Heavy Atom	λ_{ex}	λ_{em}	Conven-tional	Computer	Conven-tional	Computer
PABA ^b (4.9-112)	1:1 EtOH/H ₂ O	No	288	432	----	0.13	0.17	0.94 (S) 0.54 (I)
Benomyl ^c (9-144)	1:1 EtOH/H ₂ O	I ⁻ (0.5 M)	280	410	----	1.63	2.33	0.85 (S) -2.46 (I)
Biphenyl ^c (9-143)	Ethanol	Ag ⁺ (1 M)	266	486	----	2.30	2.29	1.09 (S) -2.20 (I) -3.12 (I)
Priveine HCl ^d (4.9-112)	Water	No	280	490, 510	----	3.69	3.01	1.17 (S) 1.15 (S) -3.77 (I)

- a. Numbers in parenthesis are the range of concentrations in µg/ml used in study.
- b. LOD and slope are calculated with the omission of the two lowest concentrations.
- c. LODs and slopes are calculated with the omission of the highest concentrations.
- d. S = 1.01, I = -2.08 (Conventional) and S = 1.09, I = -3.49 (Computer) for top three points only.
- e. LODs calculated by Conventional means are based on peak to peak noise of blank near 350 nm; and calculated by Computer are based (in 1st column) upon estimating the blank standard deviations by means of the maximal peak to peak signal fluctuations

Table 8-continued

and based (in 2nd column) upon the blank standard deviations which are estimated from the 50 blank readings at peak maxima (top) and 350 nm (bottom) respectively; p-p is peak to peak and s.d. is standard deviation.

f. Slopes of ln-ln plot: by Conventional means use cm as unit for signal and measured from peaks on recorded paper; by Computer utilize photocurrent as unit of signal after being corrected from blank.

Blank Corrected Spectra

The biggest advantage of this approach is to obtain the blank corrected analyte spectra, which gives more information for qualitative analysis. From the blank corrected spectrum of privine HCl (Figure 10), the two peaks (490 nm and 510 nm) can be seen at almost every concentration level studied, which is not true in the case of blank uncorrected spectrum. The spectra of model compounds obtained from both computer-plotter and X-Y recorder are shown in Figures 11,12,13, and 14.

Calibration Curve

Figure 15 shows the \ln signal (cm) vs. \ln concentration ($\mu\text{g/ml}$) plot (Figure 15 (a)) and the \ln signal (photocurrent) vs. \ln concentration ($\mu\text{g/ml}$) plot (Figure 15 (b)). The former is conventionally calculated with a TI-55 calculator, and the latter by the computer. At the first glance, they appear to be identical, but subtle differences, especially for benomyl (curve b), are found. Which is indicated in Table 8 from the slope calculated by conventional means (0.85) which is largely different from that by computer (0.95).

Conclusions and Future Work

Computer assisted background correction for RTP has several advantages: less time for calculations; higher precision (in digital form); greater reliability; and ability to obtain blank corrected analyte spectra. In

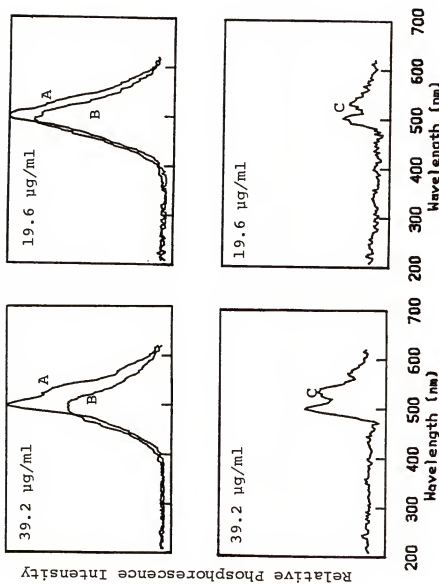


Figure 10. Analyte (A), blank (B), and blank corrected analyte (C) spectra of pravine HCl

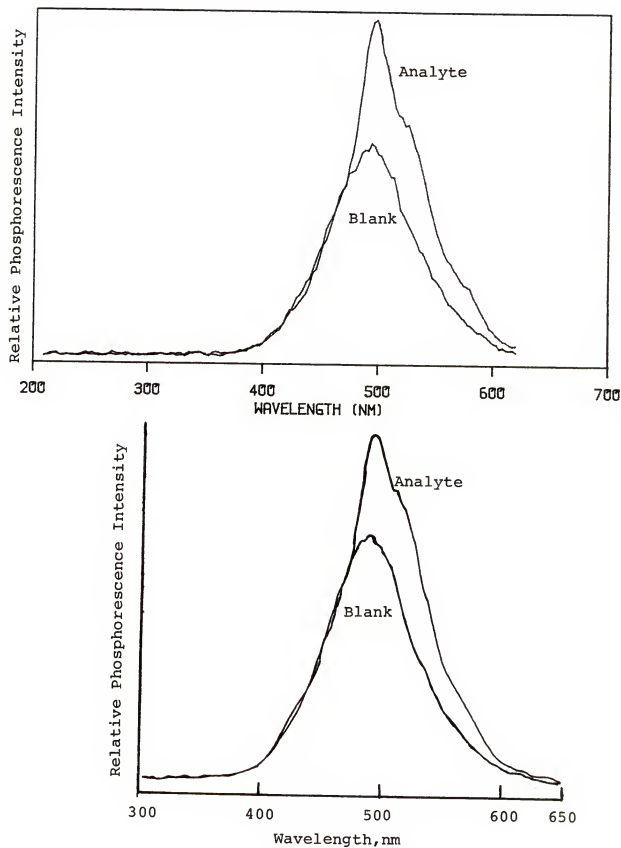


Figure 11. RTP spectra of privine HCl (28 $\mu\text{g}/\text{ml}$) obtained from computer-plotter (top) and X-Y recorder (bottom)

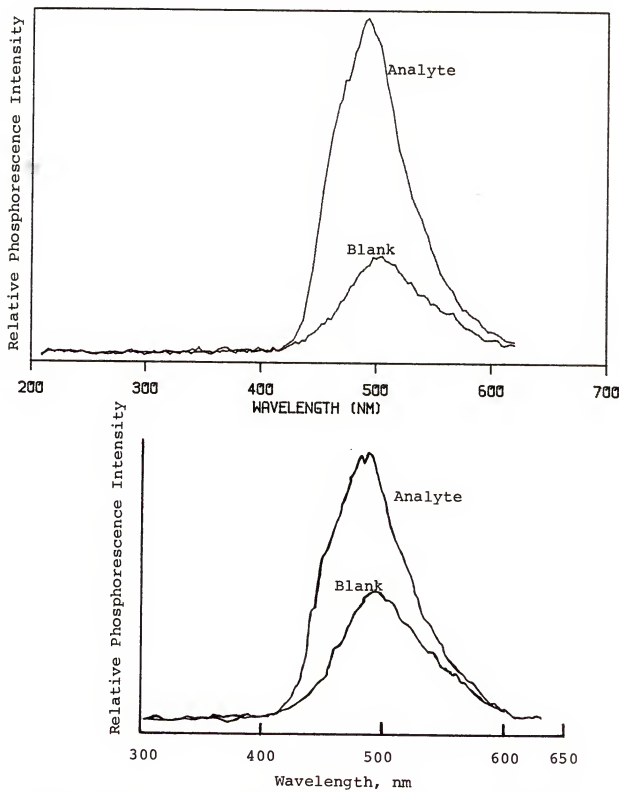


Figure 12. RTP spectra of biphenyl (72 $\mu\text{g}/\text{ml}$) obtained from computer-plotter (top) and X-Y recorder (bottom)

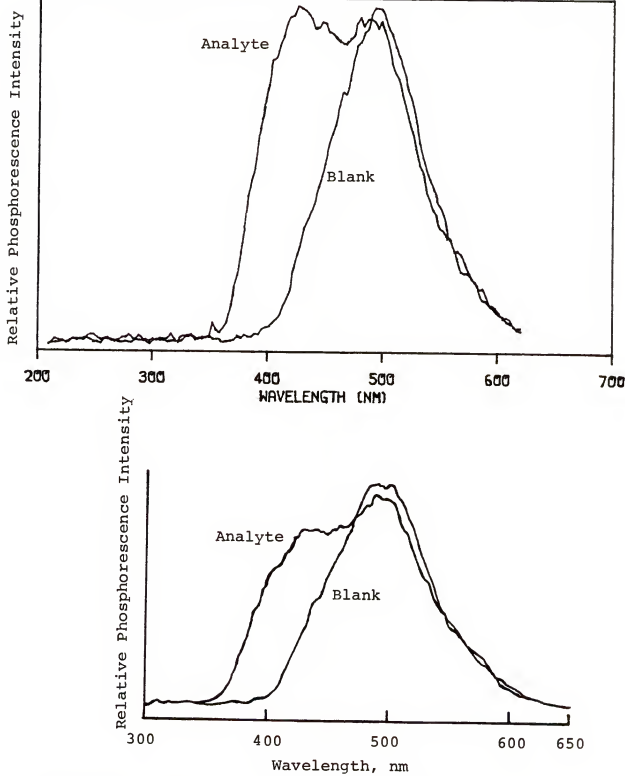


Figure 13. RTP spectra of benomyl (36 $\mu\text{g/ml}$) obtained from computer-plotter (top) and X-Y recorder (bottom)

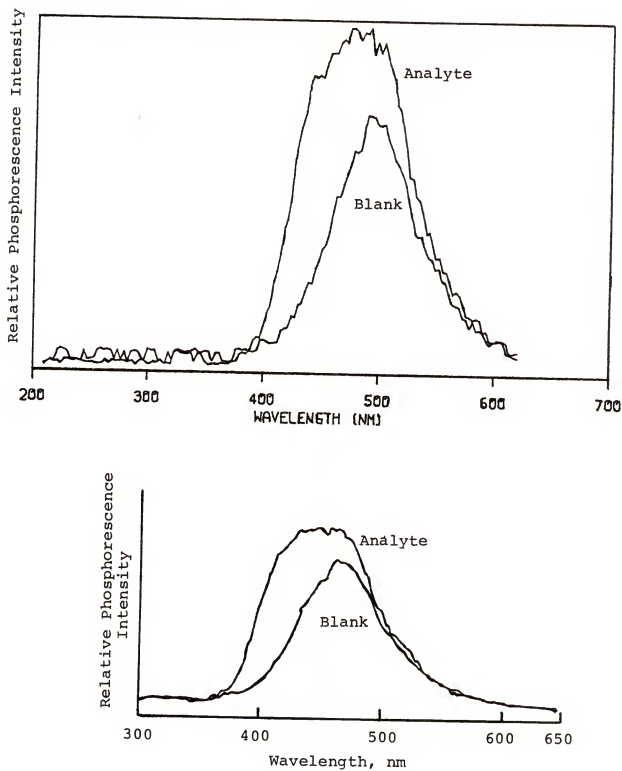


Figure 14. RTP spectra of PABA (0.8 μ g/ml) obtained from computer-plotter (top) and X-Y recorder (bottom)

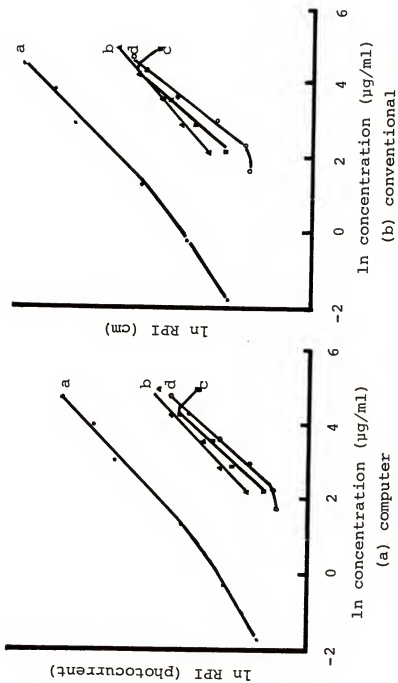


Figure 15. Calibration curves of four model compounds by (a) computer and (b) conventional outputs
 Curves identified as: a. PABA; b. benomyl; c. biphenyl;
 d. pridine HCl

addition, the programs are designed in a very general way and may allow correction of a synthetic mixture spectrum (as background) from the sample spectrum and enable calculation of the LOD and slope of the analyte.

The reproducibility of RTP lies between 2% to 10% or so and is caused mostly by the light source drift, sample introduction variation, inhomogeneity of different batches of solid substrate, the alignment of sampling bar, and the prejudice of the operator.

In an ideal RTP system a computer is used to automate the sample introduction by spraying sample solution on a definite substrate area with a certain volume of solution; the precise alignment of the sample holder system; and the data storage, reduction, and handling (LOD, LDR calculations). In this case, the excellent selectivity, good sensitivity, good reproducibility, reliability, and automated system of RTP will lend itself to a very useful analytical technique for routine analyses. The automatic sample holder systems introduced by Winefordner et al. (29, 31) are satisfactory for handling filter paper as solid substrates. They are, however, by no means a versatile sample holder which can handle powder substrates. A versatile luminescence sample holder is thus designed and currently under investigation by Su, Wittman, and Winefordner (work in progress) for handling all kinds of solid substrates and even liquids and for carrying out luminescence studies at room or low temperatures. Besides, no quartz

apparatus should be needed for this system to study the luminescence; thus it is free from one of the major disadvantages of LTP. The mechanical drawings of this new system is shown in Appendix C.

Chapter 5
STUDIES OF HEAVY ATOM EFFECT AND SAMPLE DRYING
PROCEDURE FOR RTP

Introduction

Thorough drying of the sample was found essential by Schulman and Walling (14,16) for RTP observation of analytes adsorbed on paper and other supports. However, RTP of PABA adsorbed on sodium acetate was reported by von Wandruszka and Hurtubise (1,15) as insensitive to quenching by moisture in humid air. In many cases, drying the sample under a hot-air blow dryer or in an oven for a few minutes was sufficient. However, air drying followed by a period in a desiccator provided more reproducible and more intense analyte phosphorescence measurement (17). It was reported later by vo-Dinh, Yen, and Winefordner that sample drying for approximately 30 min by infrared heating lamp was more efficient than other methods using desiccators, blowers, or ovens (22,27). A 10 min infrared heating method was then used by Aaron, Kaleel, and Winefordner to study pesticides (25); by Yen-Bower and Winefordner to investigate pharmaceutical compounds (23) and PAHs (28); and by Mohamed (3) to analyze mebendazole and flurendazole drugs. Recently, Bateh and Winefordner (2) reported that 7 min sample drying under a flow of dehumidified nitrogen gas (~20 L/min) was enough to observe RTP

of theophylline pharmaceutical preparations. The sample drying procedure was then studied further by Su and Winefordner (21) to compare both infrared heating and dehumidified N_2 stream drying procedures, and the results are discussed in this chapter.

The influence of heavy atoms on RTP has been studied by several workers (22,23,27,28,38-41,61,62,89,95,96). The heavy atom effect, by perturbation of analyte to enhance the intersystem crossing rate and radiation rate of triplet state deactivation (39,89,90) results in an increase in phosphorescence intensity, a decrease in the fluorescence intensity, and a decrease in the phosphorescence lifetime (97). The heavy atom effect is most striking for non-ionic organic compounds, such as PAHs, where phosphorescence appears only if the heavy atom is present (27,28). According to the SEHAP (selective heavy atom perturbation) technique reported by vo-Dinh and Hooyman (61), the heavy atom species will affect the phosphorescence enhancement of PAHs. By taking advantage of this, they were able to do multi-component analysis of PAHs by selective measurement of specific target PAH compounds in a synthoil sample. However, in addition to the heavy atom type, the concentration of it also affects the phosphorescence intensity of analytes. A further study on this was carried out by Su and Winefordner (21), and the results are given in this Chapter.

ExperimentalInstrumentation

The same Aminco-Bowman spectrophotofluorimeter and the other attachments were used and described in Chapters 3 and 4 previously. The only additional equipment to those used was a Fisher Recordall Series 5000 recorder (Fisher Scientific, Pittsburgh, PA) coupled with the above system to do the sample drying procedure study.

Chemicals

All the components used for both heavy atom and sample drying procedure studies were the same as those used in Chapter 3.

Procedure

For the sample drying procedure studies, a 1 μ l heavy atom solution and a 1 μ l sample solution were introduced consecutively onto the DE-81 or S & S 903 filter paper disc substrates. The sampling bar with sample on substrate was then dried under infrared heating lamp for 5 min (ethanol as solvent) or 10 min (water in solvent); or without any infrared heating (use of a dry gas flowing over substrate). After any of the above drying procedures, the sampling bar was inserted into the sample compartment where dehumidified N_2 stream flowed continuously downward over the substrate. After placing the sampling bar in the sample compartment, the rotating can phosphoroscope was turned on, shutters

were opened, and the recorder was turned on to record the histogram. The whole system was on until the suitable analytical results were obtained.

The procedure for the heavy atom study is similar to that of Chapter 3.

Results and Discussion

Sample Drying Procedure

Drying the analyte on the substrate will get rid of most of the water content of the substrate enhancing the degree of rigidity of analyte and the intensity of phosphorescence as well. Normally, "heat" is used to dry the sample. After a definitive study, it was found that an optimal drying procedure is needed for each analyte to be measured. A typical drying histogram, as shown in Figure 16, consists of a curve of relative phosphorescence intensity (RPI) vs. time, which is divided into three time zones, namely, rise, plateau, and fall times. The histograms of several compounds are included in Appendix D. The characteristics of the sample drying procedure of several model compounds, as shown in Table 9, imply that the optimal drying and sampling times for an analyte depend on the substrate material and the analyte itself. Heating the sample with an infrared heating lamp lengthens the plateau time without changing the phosphorescence intensity significantly in most cases ($\pm 10\%$ FSI) (Table 10); however, heating is more laborious and takes a long time. Therefore, in an optimized RTP procedure, it is necessary to determine

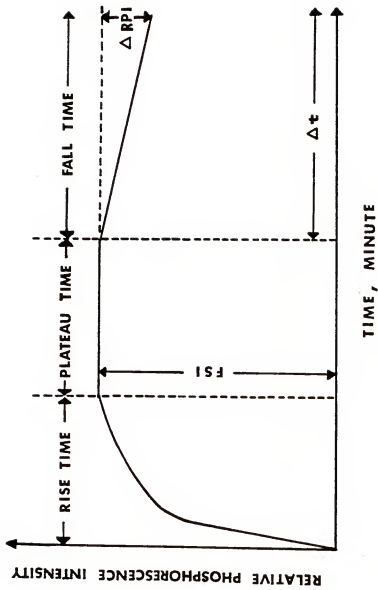


Figure 16. Typical histogram of RTP sample drying procedure

plateau time zone consists of all the points whose RPI lies at the vicinity of the maximum phosphorescence intensity and within the range of (RPI/FSI) = 0 to 0.1, where FSI stands for full scale Relative phosphorescence Intensity
 Fall time zone consists of all the points whose RPI does not lie in the plateau time zone and is decreasing, but is increasing for rise time zone

Table 9. Characteristics of Sample Drying Study for Several Model Compounds

Compounds ^a	Substrate	IR Lamp ^b Heating	Rise Time (min)	Plateau Time ^c (min)	Fall Rate ^d (Fall Time (min))
Carbazole (120 μ g/ml)	S & S 903	No	2.1	2.1-3	4.7 (3-8.8)
	S & S 903	Yes	1.1	1.1-2	3.8 (8.8-12.3)
DE-81	No	1.8	1.8-2.6	6.3 (2.6-8)	3.8 (2-8.5)
	Yes	1.5	1.5-3.5	4.9 (8-12)	3.3 (8.5-12.5)
Biphenyl (143 μ g/ml)	S & S 903	No	3	3-7	1.0 (7-26)
	S & S 903	Yes	7	7-21	----
DE-81	No	1.4	1.4-8	1.1 (8-22)	----
	Yes	10	10-22	----	----
Chrysene (63 μ g/ml)	S & S 903	No	1.2	1.2-5.2	1.2 (5.2-24)
	S & S 903	Yes	7.2	7.2-20	----
DE-81	No	2	2-8	0.8 (8-21)	----
	Yes	8.2	8.2-21	----	----

Table 9-continued

<u>Compounds^a</u>	<u>Substrate</u>	<u>IR Lamp^b</u>	<u>Rise Time^c (min)</u>	<u>Plateau Time^c (min)</u>	<u>Fall Rate^d (Fall Time (min))</u>
Coronene (27.3 $\mu\text{g/ml}$)	S & S 903	No	0.8	0.8-1.8	10.0 (1.8-4) (4.6) ^e
	S & S 903	Yes	1.2	1.2-5.2	3.7 (5.2-8.2) (8.2-10.2)
DE-81	No	0.2	0.2-2.2	5.0 (2.2-10.7) (10.7-19) ^e	
DE-81	Yes	4	4-9	2.0 (9-19) (19-24) ^e	
Phenanthrene (63 $\mu\text{g/ml}$)	S & S 903	No	2	2-3	2.6 (3-9.5) 2.5 (9.5-16)
	S & S 903	Yes	7	7-13	1.2 (13-16)
DE-81	No	1	1-2	2.4 (2-11)	
DE-81	Yes	5	5.9	2.0 (11-18) 1.1 (9-20)	
Privine HCl (134 $\mu\text{g/ml}$)	S & S 903	No	3.6	3.6-8	0.4 (8-16)
	S & S 903	Yes	5	5-13	----

Table 9-continued

<u>Compounds^a</u>	<u>Substrate</u>	<u>IR Lamp Heating</u>	<u>Rise Time (min)</u>	<u>Plateau Time^c (min)</u>	<u>Fall Rate^d (Fall Time) (min)</u>
	DE-81	No	4	4-9	0.6 (9-16)
	DE-81	Yes	9	9-16	----
Procaine HCl (179.4 μ g/ml)	S & S 903	No	28	28-33	----
	S & S 903	Yes	14	14-31	----
	DE-81	No	6.6	6.6-10	1.1 (10-20)
	DE-81	Yes	7	7-12	1.0 (12-15)
2-Aminobenzimidazole (110 μ g/ml)	S & S 903	No	5.0	5.0-15	----
	S & S 903	Yes	1.4	1.4-10.4	----
	DE-81	No	5.2	5.2-11.2	2.5 (11.2-14.2)
	DE-81	Yes	4	4-9	2.0 (9-12)
Naphthalene acetic acid	S & S 903	No	3	3-8	0.2 (8-31)
(105 μ g/ml)	S & S 903	Yes	3.4	3.4-27.4	----
	DE-81	No	5.2	5.2-11.2	0.3 (11.2-17)
	DE-81	Yes	11	11-20	----

Table 9-continued

Compounds ^a	Substrate	IR Lamp ^b Heating	Rise Time		Plateau Time ^c (min)		Fall Rate ^d (Fall Time) (min)
			(min)				
PABA (100 μ g/ml)	S & S 903	No	7		7-13		----
	S & S 903	Yes	5		5-12		2.4 (12-14)
	DE-81	No	3.6		3.6-8		1.8 (9-16)
	DE-81	Yes	3		3-6		1.4 (6-12)

a. Excitation and emission wavelengths and the heavy atom species and concentrations used for each compound are the same as those in Table 3.

b. "No" stands for the case of sample drying by room temperature N₂ stream.

c. Plateau time zone consists of all the points whose RPI lies at the vicinity of the maximum phosphorescence intensity and within the range of $(\Delta RPI/FSI) = 0$ to 0.1 , where FSI stands for Full Scale Relative Phosphorescence Intensity.

d. Fall time is shown inside the parenthesis and fall rate is calculated by use of $(\Delta RPI/FSI) \times 100\%/\Delta t$ in (% per min); the value is shown in front of the parenthesis.

e. The curve levels off at this time interval.

Table 10. Intensity Comparison With and Without Infrared Lamp Heating

<u>Compounds</u>	<u>Substrate</u>	<u>(RPI_{IR}/RPI_{N₂}), cm</u>
Biphenyl	S & S 903 DE-81	7.4/8.2 = 0.90 2.3/2 = 1.14
NAA	S & S 903 DE-81	7/7 = 1.00 13/13.6 = 0.96
Privine HCl	S & S 903 DE-81	10.1/10 = 1.01 13.6/14 = 0.97
Chrysene	S & S 903 DE-81	2/2.4 = 0.83 2.7/1.8 = 1.50
PABA	S & S 903 DE-81	6.4/6.6 = 0.97 5/4.9 = 1.02
Procaine HCl	S & S 903 DE-81	9.4/10 = 0.94 10.3/11.4 = 0.90
2-Aminobenzimidazole	S & S 903 DE-81	0.6/1.0 = 0.60 5/4 = 1.25
Phenanthrene	S & S 903 DE-81	13.8/13.6 = 1.01 4.2/4.2 = 1.00

the optimal sample drying procedure and sampling time via a drying histogram of the analyte obtained in the presence of the heavy atom with the heating procedure or with flowing N_2 .

Effect of Heavy Atom Effect on Response and Calibration Curves

The effect of external heavy atoms on RTP response curves (log I vs. log concentration of heavy atom at a given analyte concentration) and calibration curves (log I vs. log concentration of analyte at a given heavy atom concentration) were carried out by variation of concentrations of both heavy atoms and analytes on DE-81 and S & S 903 substrates; the effect of I^- is evaluated for PABA, procaine HCl, NAA, and carbazole; the effect of Ag^+ for phenanthrene and chrysene. The response and calibration curves of procaine HCl, carbazole, and phenanthrene are shown in Figures 17 and 18, 19 and 20, 21 and 22, respectively, and the others are shown in Appendix E. Several interesting points should be noted from this study: first, the heavy atom response curves for various analyte concentrations give straight segments (segments are linear only for procaine HCl, carbazole, and NAA) of about one order of magnitude for each compound studied; second, the best LOD for each compound occurs at different heavy atom concentrations with various substrates; this implies that a comparison of substrates based on enhancing RTP signals by the use of the same heavy atom concentration may not

Figure 17. RTP response (left) and calibration (right) curves of procaine HCl on DE-81

Curves identified as:

(left) a. 179.4 $\mu\text{g/ml}$; b. 90 $\mu\text{g/ml}$; c. 45 $\mu\text{g/ml}$; d. 23 $\mu\text{g/ml}$; e. 11 $\mu\text{g/ml}$; f. 2 $\mu\text{g/ml}$ of procaine HCl

(right) a. 2 M, 1.4 M, and 1 M; b. 0.5 M; c. 0.1 M; d. 0.05 M of I^-

RPI = relative phosphorescence intensity

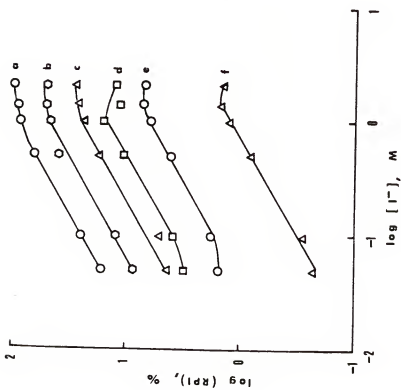
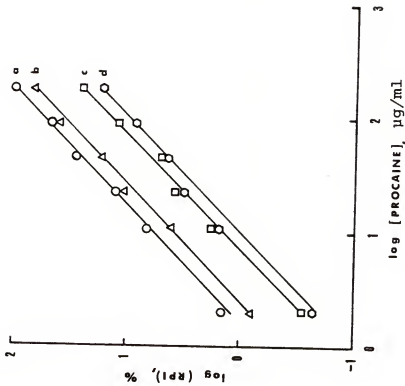


Figure 18. RTP response (left) and calibration (right) curves of procaine HCl on S & S 903

Curves identified as:

(left) same as Figure 17(a)

(right) a. 2 M; b. 0.5 M; c. 0.1 M and 0.05 M of I^- ; 1.4 M and 1 M lie in between curves a and b

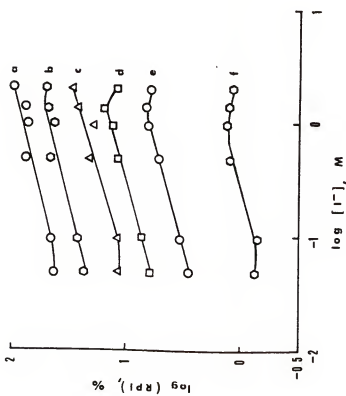
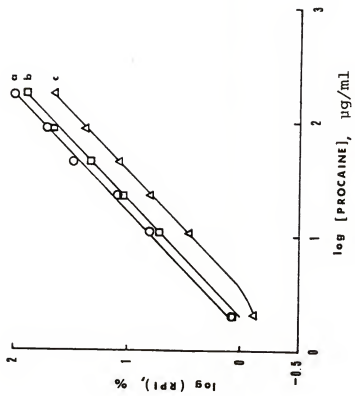


Figure 19. RTP response (left) and calibration (right) curves of carbazole on DE-81

Curves identified as:

(left) a. 116.4 $\mu\text{g/ml}$; b. 46.5 $\mu\text{g/ml}$; c. 18.6 $\mu\text{g/ml}$; d. 3.7 $\mu\text{g/ml}$; e. 0.74 $\mu\text{g/ml}$ of carbazole

(right) a. 2 M; b. 1.4 M and 1 M; c. 0.5 M; d. 0.1 M; e. 0.05 M of I^-

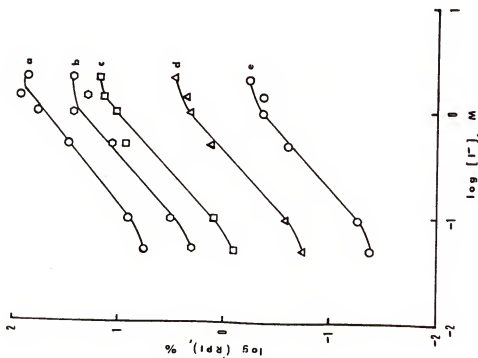
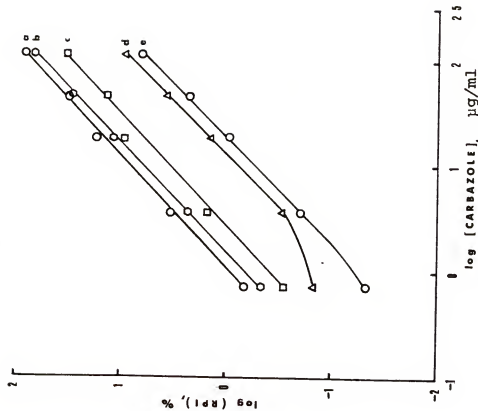


Figure 20. RTP response (left) and calibration (right) curves of carbazole on S & S 903

Curves identified as:

(left) a. same as Figure 19(a)

(right) a. 1 M; b. 0.5 M; c. 0.1 M of I⁻; 1.4 M and 2 M lie in between curves a and b

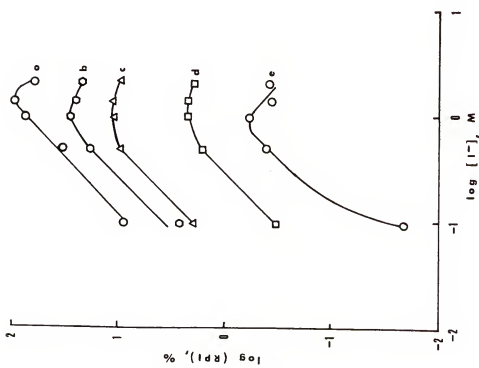
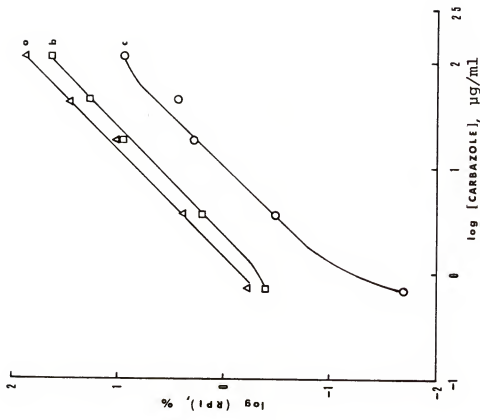


Figure 21. RTP response (left) and calibration (right) curves of phenanthrene on DE-81

Curves identified as:

(left) a. 63 $\mu\text{g}/\text{ml}$; b. 25.2 $\mu\text{g}/\text{ml}$; c. 10 $\mu\text{g}/\text{ml}$;
d. 4 $\mu\text{g}/\text{ml}$ of phenanthrene
(right)a. 0.35 M; b. 0.035 M, 0.007 M, and
0.0035 M; c. 1 M of Ag^+

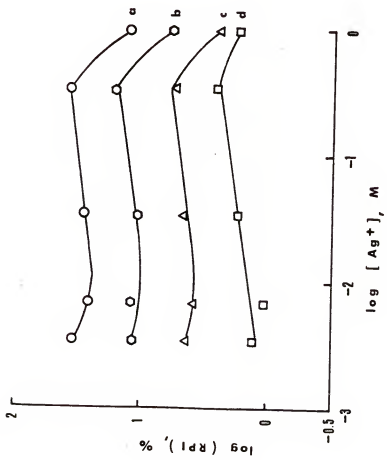
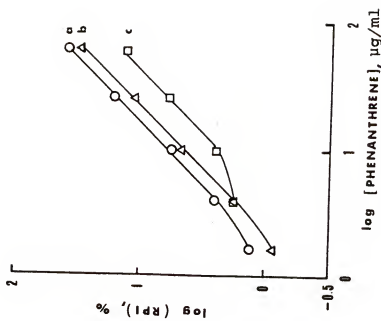
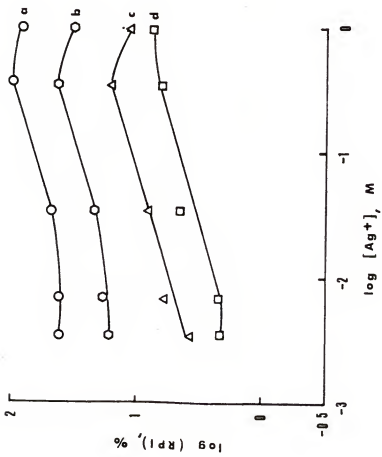
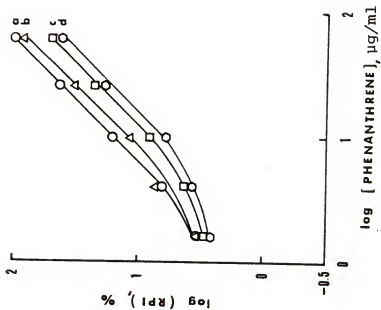


Figure 22. RTP response (left) and calibration (right) curves of phenanthrene on S & S 903

Curves identified as:
(left) same as Figure 21(a)
(right) a. 0.35 M; b. 1 M; c. 0.0035 M; d.
0.007 M and 0.0035 M of Ag^+



be optimal for a given analyte for each substrate, e.g., 1 M Ag⁺ used for comparison of DE-81 and S & S 903 by use of phenanthrene as the analyte (Figures 21 and 22 (b)) is certainly not optimal for the DE-81 filter paper test; and third, the change in the log RPI values between the response curves within the straight line regions is proportional to the differences of analyte concentrations.

Conclusions and Future Work

The histogram of each analyte is rather important for an analytical chemist to decide when is the best time to observe and record the analyte phosphorescence. Of course, it is best to observe the phosphorescence signal during the plateau time, i.e., the most intense and reproducible signal is obtained then.

It is also critical for an analyte to be measured by using the best heavy atom species and concentration. For a complicated multicomponent real sample analysis, it is possible to identify selectively and quantify the analytes by taking advantage of different combinations of plateau time, heavy atom species (61), concentrations of heavy atoms, lifetime, and the excitation/emission wavelengths.

CHAPTER 6
SPIKED MOBILE PHASE FLUORESCENCE DETECTOR FOR HPLC

Introduction

Current state-of-the-art HPLC is a very useful separation technique to analyze samples which are thermally unstable, nonvolatile, and soluble in the mobile solvent used for the separation. Although HPLC is one of the most popular and useful analytical techniques, no present HPLC detector is as versatile or as universal as desired (98). There is no LC detector equivalent to the thermal conductivity or flame ionization detectors of GC. However, HPLC applications are not seriously limited by the detector at the present time. If this does happen, two or more detectors (hyphenated) can be utilized to ensure the analysis of the analyte. However, it is more favorable to have a simple, single detector which is sensitive and universal to the components eluted from the HPLC column. This is the goal of this work reported in this chapter.

Theoretical Background

To develop detectors for HPLC, several characteristics of ideal HPLC detector should be known and fulfilled most of them. According to Snyder and Kirkland (98) with some other additions, the characteristics of an ideal HPLC detector are listed in Table 11.

Table 11. Characteristics of an Ideal HPLC Detector

High sensitivity and reproducibility
Universal or selective response
Wide LDR
Independent of column parameters
Not affected by mobile phase
Reliable and convenient to use
Linear response with the amount of analyte
No dead volume
Nondestructive
Fast response
On-line detection
Automation

When evaluating detectors for HPLC, one feature to be considered is the "detector noise level" which is determined by the high frequency (flicker) noise and random baseline fluctuation (shot) noise arising from instrument electronics, temperature fluctuations, line voltages, and other effects not directly attributable to the solute, e.g., flow changes, pump pulsations and so on. Detector noise makes difficult the sensing of very small peaks, it is often given as the random baseline variation in units of detector response (e.g., absorbance units for UV or RFI for fluorescence detector) at a specified sensitivity. Detector drift will

interfere with the measurements of small peaks; it is mostly caused by the total HPLC system rather than only by the detector. The sensitivity of a detector is also important, for example, 10 ng or less analyte in a sample should be measured without difficulties. LOD is usually used to show the minimum concentration (or mass) of a solute that can be detected, and is generally taken as the concentration (or mass) of a solute entering the detector per unit time that will provide a signal-to-noise ratio of 3. For a detector to be used in routine quantitative analysis, a wide LDR of four or more orders of magnitude is desired, and the on-line detection feature is critical for maintaining the analyte free from contamination and degradation and for saving analysis time. The detector cell volume V_d should be smaller than V_p , $V_d < 10\% V_p$ (99), where V_p is the volume of the peak interest. It is also very desirable to operate the detector cells under moderate pressure of 5-10 atm. Air bubbles may also cause problems for detection if fittings are not tightened sufficiently or the mobile phase is not degassed completely. The detector response should be fast enough to ensure that an analyte peak is not broadened due to time constant of the detector-amplifier system. According to Sternberg (99), the maximum detector time constant τ (s) that can be tolerated is about one-third that of the standard deviation of the peak σ (s).

Current commercially available HPLC detectors are based on a number of detection principles, including absorbance, fluorescence, refractive index, electrochemical, and mass spectrometry detection (100). According to the survey of 365 published scientific papers on popularity of HPLC detectors, conducted by R. Major of Varian Associates (100), the UV absorbance detector was utilized in 71% of the papers surveyed, the fluorescence (FL) detector in 15%, refractive index (RI) detector in 5.4%, and the electrochemical (EC) detector in 4.3%. Table 12 lists the characteristics of the four currently most popular HPLC detectors.

According to the information in Table 12, the only universal detector is the RI detector, but it suffers from the drawbacks of incapability with gradient elution, poor LODs, and sensitivity to temperature of the flowing system. None of the other three detectors (UV, FL, and EC) is universal without modification. The fluorescence detector is more sensitive than the UV and RI modes; if the fluorescence detector cell is made as small as 1 μ l, the LOD and LDR improve due to minimization of detector dead volume. By maintaining the merits of the fluorescence detector, including selectivity, sensitivity, and gradient elution ability, etc., a modification of a spiked mobile phase of HPLC with a fluorophor at a low concentration (c.a. $1\text{--}10 \mu\text{g/ml}$) enables the detection of nonfluorescent compounds as negative peaks by the fluorescence detection

Table 12. Characteristics of the Four Currently Most Popular HPLC Detectors

<u>Character</u>	<u>UV (absorbance)</u>	<u>RI (RI unit)</u>	<u>FL (RFI)</u>	<u>ECA (μA)</u>
specificity	selective	general	selective	selective
gradient elution	yes	no	yes	no
LOD	2×10^{-10} g/ml	1×10^{-7} g/ml	10^{-11} g/ml	10^{-12} g/ml
LDR (orders of magnitude)	5	4	3	6
detector cell volume	8 μl	3 μl	20-30 μl	<1 μl except for 20 μl for coulometric
temperature sensitivity	low	10^{-4} °C	low	1.5% / °C
inherent flow sensitivity	no	no	no	yes
sensitivity at t1% noise, full scale	0.002	2×10^{-6}	0.005	2×10^{-9}

a. Characteristics listed are mainly for amperometric detection system except specially mentioned.

system. The capability of detecting fluorescent compounds as positive peaks and of detecting non- and weak fluorescent compounds as negative peaks lends the spiked mobile phase fluorescence detector a candidate of promising universal HPLC detectors.

The working theory behind the spiked mobile phase negative peak fluorescence detector is believed to be an absorption mechanism for compounds producing negative peaks (non- or weak fluorescent), i.e., compounds possessing fluorescence quantum efficiencies smaller than those of the spiking fluorophor. If $I_o \gg (I_o - I')$, then the relation of $(I_o - I') \propto C$ (concentration) is followed; otherwise, by $\log \frac{I_o}{I'} \propto C$ is valid, where I_o is the spiked mobile phase baseline fluorescence intensity and I' is the negative peak fluorescence intensity less intense than the baseline (see Figure 23). Because the flow cell has a 1 mm inside diameter quartz tube, the absorption light path is very short, it is most likely that $(I_o - I') \propto C$ relationship is valid, and it is true for acridine and 7,8-benzoflavone negative peak PAHs (as seen in Table 16). As to the positive peak (fluorescent) compounds with quantum efficiencies > 0.01 , the relationship of $(I - I_o) \propto C$ is followed, where I is the positive peak compound fluorescence intensity above the baseline fluorescence intensity of the spiking fluorophor (as seen in Figure 23).

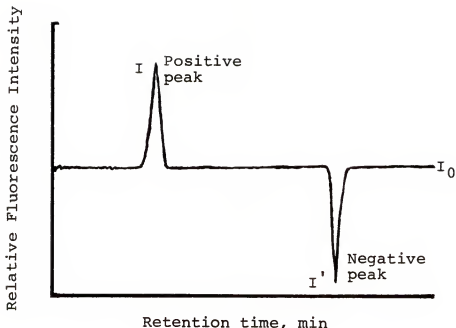


Figure 23. A postulated chromatogram with positive and negative peaks detected by the spiked mobile phase fluorescence detector

Positive peak: fluorescent compounds with quantum efficiencies > 0.01

$(I - I_0) \propto$ concentration (C)
 Negative peak: nonfluorescent compounds with quantum efficiencies (Q) $< Q$ of spiking fluorophor

a. $I_0 \gg (I_0 - I')$ then

$$(I_0 - I') \propto C$$

b. otherwise

$$(A = \log \frac{I_0}{I'}) \propto C$$

The main factors responsible for negative peaks of non- or weak fluorescent compounds is believed to be absorption of exciting or emitting radiation of the spiking fluorophor by the analyte. Quenching effect on the spiking fluorophor by analyte is another possible major factor causing the negative peaks. Some other effects, such as interaction between analyte and spiking fluorophor also decrease the fluorescence intensity of baseline to enhance the negative peak. The UV absorbance detection system as well as most any other detector type also gives negative peaks for analytes if a suitable spiked chromophor is mixed with the mobile phase. However, fluorescence is a more sensitive technique and is thus chosen to do the study. The spiking fluorophor, which must give a stable baseline of certain fluorescence intensity, can be chosen from any fluorophor which is miscible with the mobile phase of the HPLC system, nontoxic, noncarcinogenic, and inert to analyte and solvent. The possible candidates of the spiking fluorophor are listed in Table 13 with their excitation and emission wavelengths. Aniline was used in the present studies and was found to be successful; the LODs are given in Tables 14 and 16. This detection system should be able to detect effluents from reversed-phase, normal-phase, ion-exchange HPLC systems and flow injection analysis (FIA) technique.

Table 13. Some Possible Candidates of the Spiking Fluorophor with Their Characteristic Wavelengths and Solvents

<u>Compound</u>	<u>Solvent^a</u>	<u>pH</u>	<u>λ_{ex} (nm)</u>	<u>λ_{em} (nm)^b</u>
PABA	water (R) (I)	8	295	345 (F)
Aminopterin	water (R) (I)	7	280 370	460 (F)
Aniline	water (R) (I)	7	280 291	344 (F) 361
Anthracene	pentane (N)	---	420	430 (G)
Biphenyl	water (R) (I)	7	270	318 (P)
Codeine	water (R) (I)	7	285	350 (P)
Deserpidine	water (R) (I)	1-2	280	365 (F)
Desipramine	water (I)	~14	295	415 (F)
1,4-Diphenylbutadiene	pentane (N)	---	328	370 (G)
Gentisic acid	water (I) (R)	7	315	440 (F)
Griseofulvin	water (I) (R)	7	295 335	450 (G)
Indole	water (I) (R)	7	269 315	350 (F)
Indole acetic acid	water (I) (R)	8	295	345 (F)
Morphine	water (I) (R)	7	285	350 (P)
Phenobarbital	water (I)	13	265	440 (P)
Picene	pentane (N)	---	281	398 (G)
Quinine	water (I) (R)	1	250 350	450 (G)

a. R = reversed phase; I = ion exchange; N = normal phase.

b. G = good fluorophor; F = fair fluorophor; P = poor fluorophor

Experimental IInstrumentation

An Aminco-Bowman spectrophotofluorimeter was used as the detection system for an Altex high performance liquid chromatograph (Model 312). The liquid chromatograph was interfaced to the spectrophotofluorimeter via a flow cell (Figure 24). The flow cell consisted of a quartz tube (1.0 mm ID and 3.0 mm OD) connected to the LC effluent with a 4. μ l volume irradiated; the flow cell was held in a holder machined from a bakelite block (Figure 24). The quartz tube was held rigidly within the bakelite holder with a swagelock connector. The bakelite holder was machined to contain conical parts with three slit-like baffles to minimize stray light and pre- and postfilter effects during the excitation and emission processes. The fourth side of the bakelite holder had a slot to allow connection to the tygon waste tube connection to the quartz tube. The bakelite holder with a quartz cell fit into the conventional fluorescence attachment of the Aminco-Bowman spectrophotofluorimeter.

Chemicals

The aniline was Analytical Reagent Grade, and the methanol and acetonitrile were chromatographic grade solvents. The water was demineralized (16 m Ω) via a Nanopure Barnstead exchanger. The other chemicals, including o-bromobenzoic acid, 2,4-dinitro phenol, ethanol, carbazole,

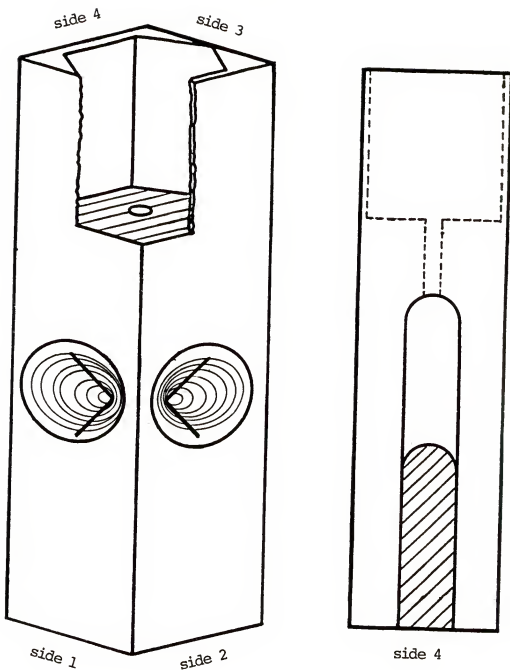


Figure 24. Diagram of flow cell

indole, Tegretol, and Dianabol were obtained from Matheson Coleman & Bell, Fisher Scientific, U.S. Industrial Chemical Co., Aldrich Co., Nutritional Biochemical Co., and CIBA Pharmaceutical Co., respectively.

Procedure

In order to avoid analyte solvent peaks interfering with analyte sample peaks, the mobile phase was also used as the solvent to prepare all sample solutions. The mobile phases consisted of 1, 10, or 1000 $\mu\text{g}/\text{ml}$ aniline in 60% methanol/40% water and 9.8 $\mu\text{g}/\text{ml}$ aniline in 80% acetonitrile/20% water, and 5.0 $\mu\text{g}/\text{ml}$ aniline in 70% acetonitrile/30% water.

The most significant experimental parameters were HPLC-isocratic operation, 4.6 mm x 25 cm column with Spherisorb ODS, 10 μm packing, flow rate of 1.0 ml/min, 20 μl sample loop; fluorimeter- $\lambda_{\text{ex}} = 290 \text{ nm}$, $\lambda_{\text{em}} = 340 \text{ nm}$ (set for aniline), PM high voltage -750 V, and a spectral band-pass of 12 nm.

Results and Discussion I

According to the results in Table 14, it is clear that the new fluorescence detector will give 4-10 $\mu\text{g}/\text{ml}$ detection limits for negative peaks and 20-100 ng/ml detection limits for positive peaks. The detection limits of species having positive peaks could have been improved by using more optimal excitation and emission wavelengths on the spectrophotofluorimeter (set for optimal excitation and emission of aniline). Although there are several anomalies in Tables 14

Table 14. Detection Characteristics of New Fluorescence Cell for HPLC

Compound	Solvent 1 ^a		Solvent 2 ^a		Solvent 3 ^a		Solvent 4 ^a		Solvent 5 ^a
	t_R^b	LOD ^c							
o-Bromobenzoic acid	4.5(-) ^d	5.8	4.2(1)	30.	4.5(-)	76.	2.3(-)	40.	--
2,4-Dinitrophenol	2.0(-)	5.5	2.0(-)	13.	2.0(-)	8.	2.0(-)	5.6	1.8(-)
	4.6(-)	8.1	4.1(-)	42.					5.
Carbazole	14(+)	0.05	13.3(+)	0.02	16.3(+)	5.6	3.7(+)	0.02	5.2(+)
Indole	5.6(+)	0.4	5.5(+)	0.06			3.2(+)	0.11	3.8(+)
Tegretol	--	--	7.2(-)	63.			3.4(-)	ND	3.6(-)
Dianabol	--	--	--	--			5.1(-)	ND	--
								ND	ND

a. Solvent 1 = 10 μ g/ml aniline in 60% methanol/40% water.Solvent 2 = 1 μ g/ml aniline in 60% methanol/40% water.Solvent 3 = 1000 μ g/ml aniline in 60% methanol/40% water.Solvent 4 = 9.8 μ g/ml aniline in 80% acetonitrile/20% water.Solvent 5 = 5.0 μ g/ml aniline in 70% acetonitrile/30% water.b. t_R = retention time, in min.c. LOD = limit of detection, in μ g/ml, defined as concentration resulting in signal-to-noise ratio of 3.

d. (-) = negative peak (decrease in fluorescence); (+) = positive peak (increase in fluorescence).

e. ND = not detectable at levels \geq 100 μ g/ml.

and 15, such as the inability to detect *o*-bromobenzoic acid in solvent 5, the rather poor limit of detection of indole in solvent 1, and the two peaks for 2,4-dinitrophenol in solvents 1 and 2, the choice of solvent for the separation is critical for good detection power.

In Table 15, analytical results are given for methanol and ethanol in solvent 1 and ethanol only in solvents 2 and 5. For both ethanol and methanol, 3 peaks were obtained. The identification of these peaks have not been made. The chromatogram of a synthetic mixture of 2,4-dinitrophenol (40 $\mu\text{g}/\text{ml}$), *o*-bromobenzoic acid (40 $\mu\text{g}/\text{ml}$), and carbazole (0.60 $\mu\text{g}/\text{ml}$) is shown in Figure 25.

Table 15. Detection Characteristics of New Fluorescence Cell for HPLC Separation of Ethanol and Methanol

Compound	Solvent 1 ^a		Solvent 2 ^a		Solvent 5 ^a	
	t_R^a	LOD ^b	t_R^a	LOD ^b	t_R^a	LOD ^b
Ethanol	2.6 (+)	2.0	2.6 (+)	4.8	2.1 (+)	1.1
	3.0 (+)	1.4	3.0 (+)	4.2	2.8 (-)	2.1
	4.5 (-)	1.4	4.6 (-)	4.3	3.5 (-)	1.6
Methanol	---	---	---	---	2.1 (+)	0.9
	---	---	---	---	2.8 (-)	1.0
	---	---	---	---	3.5 (-)	2.3

a. See footnotes in Table 14.

b. LOD = Limit of detection in V/V % for S/N = 3.

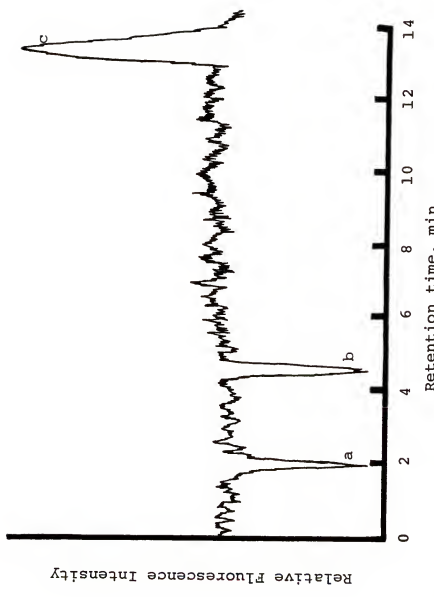


Figure 25. HPLC chromatogram of a 3 component mixture

Peaks identified as: a. 2,4 dinitrophenol; b. o-bromobenzoic acid; c. carbazole

HPLC conditions: column- 4.6 mm x 25 cm length, and 10 μ m Spherisorb ODS; solvent- 10 μ g/ml aniline in 40% water/60%

methanol ; flow rate- 1.0 mL/min

Fluorimeter wavelengths: λ_{ex} = 290 nm and λ_{em} = 340 nm

Experimental IIInstrumentation

The HPLC was the same one as the one used before, but with an Altex ultrasphere 5 μm dp ODS column of 4.6 mm x 25 cm dimension. A 5 $\mu\text{g}/\text{ml}$ aniline spiked 70% acetonitrile, 30% water mobile phase was used with a flow rate of 1.0 ml/min for this study. The Aminco-Bowman spectrophotofluorimeter with excitation and emission bandpass of 12 nm was connected after the Altex UV detector (model 153) with approximately 1 meter of teflon tube (1/64 in i.d.) which was the shortest length of tubing which could be used to connect the two detectors (the HPLC was on a cart and the fluorimeter was on a laboratory bench); the same bakelite holder and quartz sample cell assembly used previously were used in the present work. A Fisher Recordall series 5000 was used with a chart speed of 0.5 in/min throughout the experiment. An Altex model 420 microprocessor was used to control solvent programming. All PAH solutions were prepared in ethanol. A laboratory-constructed fluorimeter, which consisted of an Eimac xenon-arc high-intensity lamp (300 W) (Varian/Eimac Division, San Carlos, CA), two Heath monochromators (GCA/McPherson Co., Acton, MA) and a GCA/McPherson EU-701-30 photomultiplier tube operated at -800 V, was employed in the study of the "solvent effect" for acridine and 7,8-benzoflavone, in which excitation and emission bandpasses of 4 nm were used.

Chemicals

The ethanol was U.S.I. absolute pure reagent grade. The water was demineralized (12 MΩ-cm) via a Nanopure Barnstead exchanger. The acetonitrile was Mallinckrodt chromatographic grade. The PAHs were from-- Eastman Organic Chemicals-- 7,8-benzoflavone and acenaphthalene, Aldrich Chemical Company, Inc.-- acridine, n-ethylcarbazole and 9,10-dimethylanthracene, K & K Laboratories Inc.-- o-quaterphenol, Eastman Kodak-- naphthalene. The aniline was Mallinckrodt analytical reagent grade. The mobile phase for HPLC was 5 µg/ml aniline spiked 70% acetonitrile/30% water.

Results and Discussion IINegative Peaks

As reported in the fluorescence study of PAHs in heptane by Jurgensen et al. (101) there were four PAHs which either did not fluoresce (7,8-benzoflavone) or fluoresced weakly (acridine) or fluoresced due to an impurity and/or a photodecomposition product in the solution (acenaphthalene and 2,3:6,7-dimethylbenzanthracene). When analyzed by the HPLC-spiked mobile phase fluorescence system, three of these four PAHs gave negative peaks as shown in Table 16, except for 2,3:6,7-dimethylbenzanthracene which could not be dissolved in ethanol or water. The acenaphthalene gave two peaks, a negative peak at 9.8 min and a positive peak at 12.9 min. The presence of two peaks confirms the previous conclusion (101) that the fluorescence of

Table 16. Detection Characteristics of Several PAHs by the Spiked Phase Fluorescence Detector

<u>Compound</u>	<u>t_R (min)^a</u>	<u>LOD ($\mu\text{g}/\text{ml}$)^b</u>	<u>Slope of $\log I$ vs. \log concentration</u>
Acenaphthalene	9.8 (-) ^c 12.9 (+)	16. 2.6	---- 0.98
Acridine	5.6 (-) 5.6 (+)	16. 0.37 ^d	0.90 1.14
7,8-Benzoflavone	9.1 (-) 9.1 (+)	8.2 0.15 ^d	0.92 0.97
9,10-Dimethyl-anthracene	23.9 (+)	0.004 ^e	1.10
N-Ethylcarbazole	12.1 (+)	0.19	0.94
Naphthalene	8.0 (+) 8.0 (+)	0.60 0.50 ^e	0.82 ----
<i>o</i> -Quaterphenyl	37.5 (+)	18. ^e	0.88

a. 1 mm i.d. quartz tube and 5 μl aniline/70% acetonitrile, 30% water used.

t_R = retention time (min).

b. LOD = limit of detection ($\mu\text{g}/\text{ml}$), defined as concentration resulting in signal-to-noise ratio of 3. $\lambda_{\text{ex}} = 290$ nm, $\lambda_{\text{em}} = 340$ nm were used except for those labelled with "d" for "e".

c. (-) = negative peak (decrease in fluorescence).
(+) = positive peak (increase in fluorescence).

d. acridine: $\lambda_{\text{ex}} = 352$ nm, $\lambda_{\text{em}} = 412$ nm;
7,8-benzoflavone: $\lambda_{\text{ex}} = 350$ nm, $\lambda_{\text{em}} = 415$ nm.

e. Characteristic wavelengths used to measure LOD (see text).

acenaphthalene was contributed by a photodecomposition product and/or an impurity. Acridine and 7,8-benzoflavone in a latter study were found to fluoresce in a polar HPLC solvent but at different wavelengths than those of aniline. The LOD's for the two positive peaks together with the wavelengths used to obtain the LOD's are shown in Table 16.

Solvent Effect

Acridine has been reported to show weak fluorescence only in nonpolar solvents like heptane (101). In polar solvents, the π, π^* state becomes the lowest excited singlet state and more intense fluorescence occurs (102,103). A solution of acridine in a polar solvent mixture of 70% acetonitrile and 30% water was found to give moderately intense luminescence excitation maxima at 264 nm, 351 nm, 368 nm, and 381 nm and emission maxima at 397 nm and 413 nm (with a spectral bandpass of 4 nm and an uncertainty of ± 3 nm for every excitation and emission wavelength). When acridine was placed in the same solvent but also containing 5 $\mu\text{g}/\text{ml}$ aniline (the spiked mobile phase used in the study), the excitation spectrum profile changed somewhat and showed maxima at 267 nm, 332 nm, 349 nm, and 381 nm (± 3 nm) while the emission profile stayed almost the same. If the aniline-spiked solution sat for approximately 40 hr, the luminescence excitation profile changed again to give maxima at 260 nm, 356 nm, and 380 nm; however, the emission spectrum was the same as before. Interaction between acridine and aniline, probably in the form of conjugation through the nitrogens

in the two molecules, was thought to have been taking place at a slow rate. In order to determine whether the excitation and emission maxima for peak 4 (in Figure 28) were attributable to acridine at the time of elution and detection, the mobile phase flow was momentarily stopped in a chromatographic run at the tip of peak 4, and the excitation and emission spectra were rapidly scanned. Excitation and emission maxima were observed at 352 nm and 412 nm, respectively, hence these wavelengths were employed in the determination of the standard calibration curve for acridine for the case of a positive peak.

Analyte 7,8-benzoflavone apparently did not interact with aniline. In the polar solution in 70% acetonitrile and 30% water with and without aniline spiking, 7,8-benzoflavone showed moderately intense fluorescence at an emission maximum of 415 nm, with the excitation maximum being at 350 nm. These wavelengths were used for the analysis of 7,8-benzoflavone. Because the interaction with aniline differs from compound to compound, one should consider such interactions in the choice of spiking agent to be used in the mobile phase for HPLC.

Positive Peaks

Four model PAH's with positive peaks were chosen for study. N-ethylcarbazole (293 nm and 346 nm) was used because of the similarity of excitation and emission wavelengths with aniline. The 9,10-dimethylanthracene (260 nm and 400 nm) was chosen because of its excellent limit of

detection (LOD) and because its excitation and emission wavelengths deviated largely from those of aniline (290 nm and 340 nm). Naphthalene (280 nm and 323 nm) and o-querterphenyl (248 nm and 396 nm) were chosen as PAHs with poor LODs in heptane and with either similar or dissimilar excitation and emission wavelengths compared to aniline. As can be seen in Table 16, the LOD of n-ethyl-carbazole is affected slightly by the aniline background. However, 9,10-dimethylanthracene is free from the interference of aniline since it was excited and detected at wavelengths far from optimal for aniline. o-Quaterphenyl gave poor LOD in this study even at its peak excitation and emission wavelengths. The poor LOD may be caused by the "solvent effect" mentioned above.

Quartz Sample Cell

In Table 17, LODs and slopes of analytical calibration curves (log I vs. log C) for acenaphthalene and acridine are given when using 1 mm and 3mm inside diameter quartz sample cell. The LODs for the 1 mm i.d. quartz tube for both PAHs are about 2x lower than those for the 3 mm quartz tube. This may indicate the use of even smaller i.d. quartz tubes which enable an irradiated flow cell volume smaller than 1 μ l (as compared to 4 μ l for 1 mm i.d. and 36 μ l for 3 mm i.d. tubes) would result in even lower LODs than the present values.

Table 17. Comparison of Detection Characteristics of 1 mm and 3 mm i.d. Quartz Tubes Used as Flow Cells in Spiked Mobile Phase Fluorescence Detector

<u>Compound</u>	<u>LOD (µg/ml)</u>		<u>Slope of log I vs. log concentration</u>	
	<u>1 mm</u>	<u>3 mm</u>	<u>1 mm</u>	<u>3 mm</u>
Acenaphthalene	16 (-) ^a	32 (-)	--	0.95
	2.6 (+)	4.5 (+)	0.98	0.98
Acridine	16 (-)	28 (-)	0.90	0.95

a. + = positive peak.

b. - = negative peak.

Synthetic Mixtures

A mixture of acridine (110 µg/ml), 7,8-benzoflavone (67 µg/ml), n-ethylcarbazole (1.79 µg/ml), naphthalene (24.4 µg/ml), 9,10-dimethylanthracene (0.41 µg/ml), and o-quaterphenyl (120 µg/ml) was prepared by using ethanol as solvent. A second mixture was also prepared without o-quaterphenyl. The chromatograms for both mixtures are shown in Figures 26 and 27 which used 290 nm and 340 nm excitation and emission wavelengths of aniline to monitor the samples. Peak #4 (peak follows the ethanol solvent peak in the six-component mixture) in Figure 27 may be from a decomposition product of o-quaterphenyl. However, when the six-compound mixture was separated and fluorescence excited and measured at 248 nm and 396 nm (peak wavelengths

Figure 26. HPLC chromatogram of a 5 component mixture

Characteristics: $\lambda_{\text{ex}} = 290 \text{ nm}$, $\lambda_{\text{em}} = 340 \text{ nm}$, sensitivity of fluorimeter = 1, recorder full scale = 100 mV (from 0 to 17 min); $\lambda_{\text{ex}} = 260 \text{ nm}$, $\lambda_{\text{em}} = 400 \text{ nm}$, sensitivity = 1, full scale = 100 mV (from 18.3 min to the end); Altex ultrasphere 5 μm dp ODS 4.6 mm x 25 cm column was used with a flow rate of 1.0 ml/min. Mobile phase was 5 $\mu\text{g}/\text{ml}$ aniline spiked 70% acetonitrile/30% water. Compounds identified as: 1., 2., and 3. ethanol; 4. acridine; 5. naphthalene; 6. 7,8-benzoflavone; 7. n-ethylcarbazole; 8. 9,10-dimethylanthracene. A baseline shift is observed at 3 min position

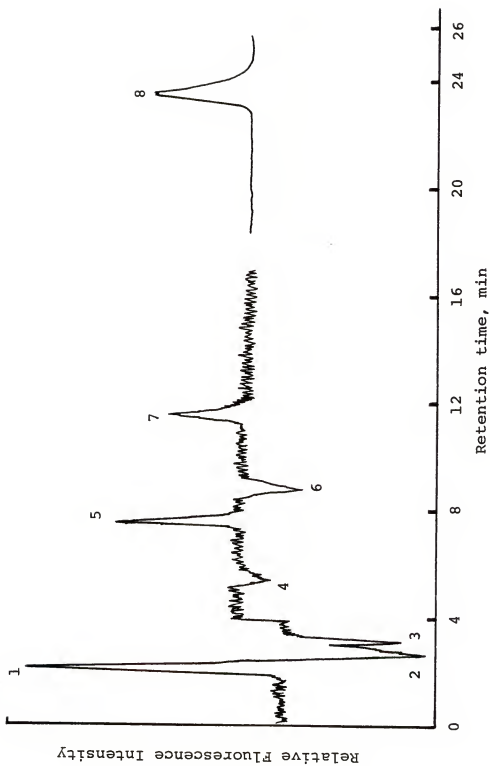
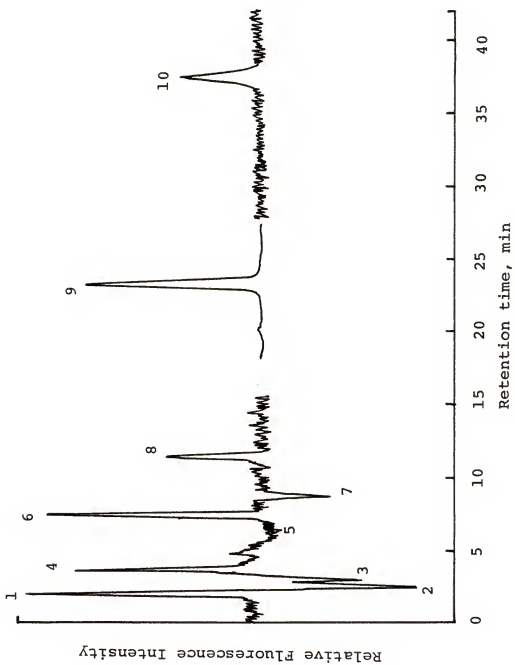


Figure 27. HPLC chromatogram of a 6 component mixture

Characteristics: $\lambda_{ex} = 290$ nm, $\lambda_{em} = 340$ nm, sensitivity = 1, full scale = 100 mV (from 0 min to 15.5 min); $\lambda_{ex} = 260$ nm, $\lambda_{em} = 400$ nm, sensitivity = 1, full scale = 100 mV (from 18 min to 27 min); $\lambda_{ex} = 248$ nm, $\lambda_{em} = 396$ nm, sensitivity = 0.3, full scale = 100 mV (from 27.6 min to the end). Column and mobile phase used were the same as for Figure 26. Compounds identified as: 1., 2., and 3. ethanol; 4. unknown (probably from o-quaterphenol); 5. acridine; 6. naphthalene; 7. 7,8-benzoflavone; 8. n-ethylcarbazole; 9. 9,10-dimethylanthracene; 10. o-quaterphenol



of o-quaterphenyl), the negative peaks disappeared; acridine and 7,8-benzoflavone now showed positive peaks but the peak of naphthalene (Figure 28) disappeared entirely. Acenaphthalene was not included in either mixture studied due to the possibility of interferences in the retention time of its peaks with the peaks 7,8-benzoflavone and n-ethylcarbazole.

Calibration Curve

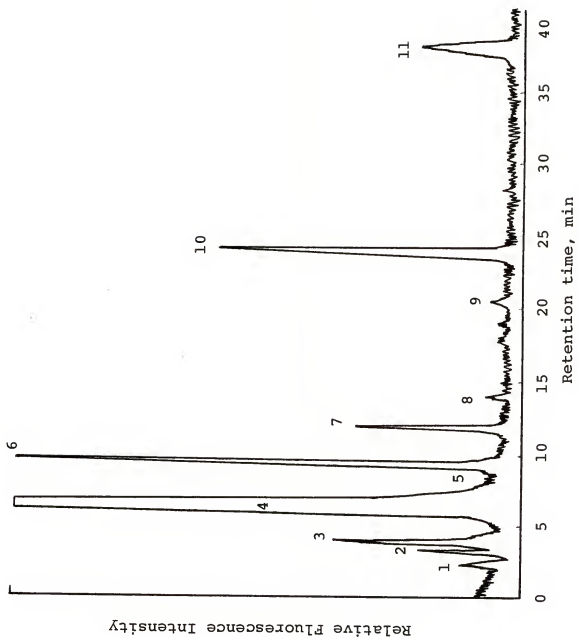
From the log I vs. log C plots given in Figure 29, the linear dynamic ranges (LDRs) are determined for the PAHs measured by the present system. It should be noted that the negative peaks of all compounds studied have the same slopes as the positive peaks. The positive peaks have LDRs of 3-5 orders of magnitude. However, the LDRs of negative peaks have only 1.5-2 orders of magnitude. This may be improved by use of a smaller flow cell volume to further minimize the dead volume of detector.

Solvent Programming

The power of solvent programming or gradient elution of HPLC results in shorter analysis time of sample and sharper (later) eluted peaks. In Figures 30 and 31, the capability of solvent programming with the spiked mobile phase fluorescence detector is shown. The sample was loaded into the sample loop and was injected into the column at 0 min. Solvent programming saved approximately 16 min of analysis time, but it could have been much shorter if needed.

Figure 28. HPLC chromatogram of a 6 component mixture monitored at $\lambda_{ex} = 248$ nm and $\lambda_{em} = 396$ nm

Characteristics: sensitivity = 0.3, recorder full scale = 100 mV. Column and mobile phase used were the same as for Figure 26 and 27. Peaks identified as: 1. ethanol; 2. and 3. unknown (probably from acridine); 4. acridine; 5. naphthalene; 6. 7,8-benzoflavone; 7. n-ethylcarbazole; 8. and 9. unknown; 10. 9,10-dimethylantracene; 11. o-quaterphenol



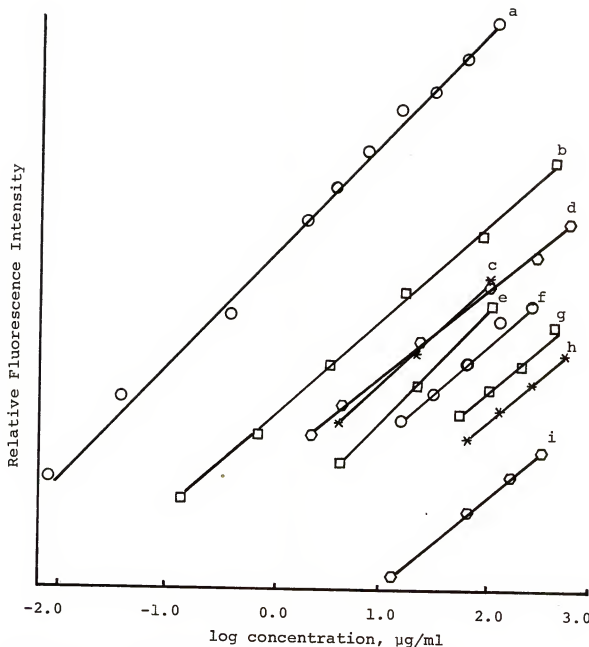


Figure 29. Calibration curves for several PAHs measured by HPLC-spiked mobile phase fluorescence detector

Curves identified as: a. 9,10-dimethylanthracene (+); b. n-ethylcarbazole (+); c. 7,8-benzoflavone (+); d. naphthalene (+); e. acridine (+); f. acenaphthalene (+); g. 7,8-benzoflavone (-); h. acridine (-); i. o-querterphenol (+)

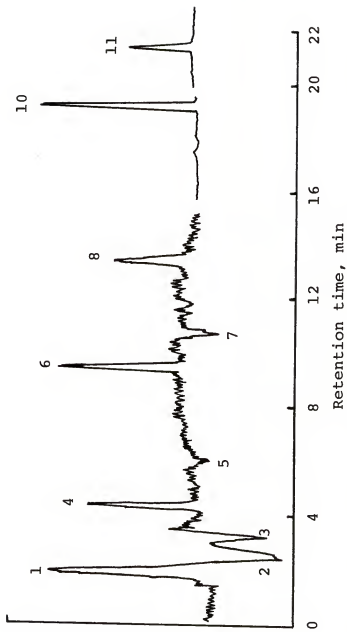


Figure 30. HPLC chromatogram of 6 component mixture with solvent programming
 Characteristics: $\lambda_{\text{ex}} = 290 \text{ nm}$, $\lambda_{\text{em}} = 340 \text{ nm}$ (from 0 min to 15 min);
 $\lambda_{\text{ex}} = 360 \text{ nm}$, $\lambda_{\text{em}} = 400 \text{ nm}$ (from 15.5 min to 19.5 min); $\lambda_{\text{ex}} = 248 \text{ nm}$,
 $\lambda_{\text{em}} = 396 \text{ nm}$ (from 20 min to the end). The sensitivity = 1,
 full scale = 100 mv for all the analysis. Column used was the
 same as for Figure 26, 27, and 28. Peaks identified as Figure 27

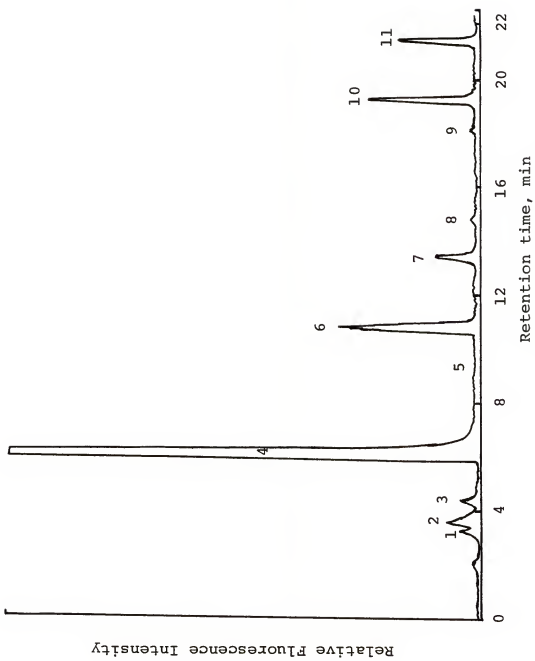


Figure 31. HPLC chromatogram of 6 component mixture with solvent programming monitored at $\lambda_{\text{ex}} = 248$ nm and $\lambda_{\text{em}} = 396$ nm (details same as Figure 28)

In addition, peak #10 (Figure 30) of solvent programming is much sharper than that in Figure 27 and also peaks #10 and #11 in Figure 31 compared to those in Figure 28.

Instrumentation

The 1 m teflon tube, which connects the UV detector and the flow cell in the fluorimeter may result in broadening of the peak resulting in poorer LODs than those in the first work which had the flow cell directly following the column. However, it offers the advantage of monitoring the UV absorption of samples eluted from the column if these samples are not swamped by the spiked solvent (aniline in our case) absorption background. If this does happen, another "spiking" fluorophor could be used to minimize absorption at the UV detector absorption wavelength. In addition, the simple means of connection of the HPLC system with the flow cell makes the HPLC system and fluorimeter readily available for other uses.

Conclusions and Future Work

The spiked mobile phase fluorescence detector-HPLC system shows promise as a general purpose detector. The sensitivity is excellent for fluorescent (positive peak) species (ng/ml or lower levels) and fairly good for non- or weak fluorescent (negative peak) species (μ g/ml levels). There are several outstanding advantages of this detection system: promising general detection mode; solvent programming ability; small detector cell volume (4 μ l or smaller); no analyte derivatization; large LDR for positive peak

species (four or more orders of magnitude); and simple sample preparation. For analysis of PAHs, since all of them fluoresce to a certain degree, use of the normal HPLC solvent (without spiking fluorophor) is suggested. The future works on this detection system should emphasize on establishing a complete theoretical background for negative peak formation; improving the LOD of the negative peak mode by use of different cell design and/or suitable spiking fluorophor; developing systematically the best spiking fluorophor for each group of compounds; studying the possibility of applying this system to the detection of effluents of normal-phase HPLC (sugar, amino acid analyses), ion exchange HPLC (metallic ion analysis), and flow injection analysis; and setting up the data bases for measurement of varieties of compounds, and applications to real sample analyses.

Chapter 7 SUMMARY AND FUTURE WORK

The two techniques discussed in this dissertation, i.e., RTP and spiked mobile phase fluorescence detector-HPLC system (SMPF-HPLC), both possess the same advantages of low cost, simplicity of construction and operation, ease of automation, and fair to excellent sensitivity and detection power. In addition, RTP has merits of excellent selectivity and very small sample volume; SMPF-HPLC enables universal detection of species.

It is rather clear that these two techniques are complement to each other; supposedly any analyte should be able to be measured by use of either one of them, since the analyte should either exhibit phosphorescence, fluorescence, or nonfluorescence. The main problems which may impede the progress and full application of current RTP are insufficient detection power; insufficient generality; and insufficient reproducibility.

To overcome these defects, a better substrate should be developed to improve the detection power; derivatization of more phosphorescent compounds could be carried out either on substrates or off substrate to enable the analysis of most species; and a fully automated RTP system including sample introduction, light source drift compensation, and data handling could improve the reproducibility.

The main disadvantages of the SMPF-HPLC system are: insufficient detection power and relatively small LDR. The disadvantages could be minimized by means of a better cell design with a suitable spiking fluorophor and an optimization of the signal-to-noise ratio.

At the present time, it is still too early to fully appreciate the power of the RTP and SMPF-HPLC systems for routine analysis of real samples. However, if the improvements mentioned above are achieved in the near future, these simple but useful techniques may become two of the major analytical techniques for the routine analysis of complicated real samples.

REFERENCES

1. R.M.A. Von Wandruszka and R.J. Hurtubise, Anal. Chem., 48, 1784 (1976).
2. R.P. Bateh and J.D. Winefordner, Anal. Lett., 15(B4), 373 (1982).
3. F.A.F. Mohamed, Thesis, Rijksuniversiteit Gent-Belgie.
4. T. vo-Dinh, R.B. Gammage, and P.R. Martinez, Anal. Chim. Acta, 118, 131 (1980).
5. T. Hirschfeld, Anal. Chem., 52, 297A-312A (1980).
6. S.Y. Su, A. Jurgensen, D.L. Bolton, and J.D. Winefordner, Anal. Lett., 14(A1), 1 (1981).
7. S.Y. Su, E.P.C. Lai, and J.D. Winefordner, Anal. Lett., 15(A5), 439 (1982).
8. H.E. Millson, "The Phosphorescence of Textile Fibers and Other Substances," Calco Tech. Bull. 753, American Cyanamid Co. (1944) (quoted in Ref. 10).
9. J.B.F. Lloyd and J.N. Miller, Talanta, 26, 180 (1979).
10. H.R. Mauersberger, in H.R. Mauersberger (Ed.), "Matthew's Textile Fibers," 6th Ed., Wiley, N.Y., 1979, p. 38.
11. D.J. Brown, J. Chem. Soc., 1974 (1958).
12. M. Roth, J. Chromatog., 30, 276 (1967).
13. Chemical Abstracts, 67, 104942h (1967).
14. E.M. Schulman and C. Walling, Science, 178, 53 (1972).
15. R.M.A. von Wandruszka and R.J. Hurtubise, Anal. Chem., 49, 2164 (1977).
16. E.M. Schulman and C. Walling, J. Phys. Chem., 77, 902 (1973).
17. R.A. Paynter, S.L. Wellons, and J.D. Winefordner, Anal. Chem., 46, 736 (1974).

18. J.L. Ward, E.L. Yen-Bower, and J.D. Winefordner, Talanta, 28, 119 (1981).
19. S.Y. Su and J.D. Winefordner, Microchem. J., 27, 151 (1982).
20. R.P. Bateh and J.D. Winefordner, Talanta, submitted for publication.
21. S.Y. Su and J.D. Winefordner, Canad. J. Spectrosc., submitted for publication.
22. T. vo-Dinh, E.L. Yen, and J.D. Winefordner, Anal. Chem., 48, 1186 (1976).
23. E.L. Yen-Bower and J.D. Winefordner, Anal. Chim. Acta, 101, 319 (1978).
24. S.L. Wellons, R.A. Paynter, and J.D. Winefordner, Spectrochim. Acta A, 30A, 2133 (1974).
25. J.J. Aaron, E.M. Kaleel, and J.D. Winefordner, Agric. Food Chem., 27, 1233 (1979).
26. J.J. Aaron and J.D. Winefordner, Analysis, 7, 168 (1979).
27. T. vo-Dinh, E.L. Yen, and J.D. Winefordner, Talanta, 24, 146 (1977).
28. E.L. Yen-Bower and J.D. Winefordner, Anal. Chim. Acta, 102, 1 (1978).
29. T. vo-Dinh, G.L. Walden, and J.D. Winefordner, Anal. Chem., 49, 1126 (1977).
30. G.L. Walden and J.D. Winefordner, Appl. Spectrosc., 33, 166 (1979).
31. E.L. Yen-Bower and J.D. Winefordner, Appl. Spectrosc., 33, 9 (1979).
32. S.Y. Su, D.L. Bolton, and J.D. Winefordner, Chem. Biomed. and Environ. Instrumentation J., 12(1), 55 (1982).
33. J.L. Ward, R.P. Bateh, and J.D. Winefordner, The Analyst, 107, 335 (1982).
34. R.P. Bateh and J.D. Winefordner, J. Pharmaceut. Sci., submitted for publication.

35. T. vo-Dinh and J.D. Winefordner, Appl. Spectrosc. Rev., 13, 261 (1977).
36. E.L. Yen-Bower, J.L. Ward, G.L. Walden, and J.D. Winefordner, Talanta, 27, 380 (1980).
37. J.L. Ward, G.L. Walden, and J.D. Winefordner, Talanta, 28, 201 (1981).
38. P.G. Seybold and W. White, Anal. Chem., 47, 1199 (1975).
39. W. White and P.G. Seybold, J. Phys. Chem., 81, 2035, (1977).
40. M.L. Meyers and P.G. Seybold, Anal. Chem., 51, 1609 (1979).
41. G.J. Niday and P.G. Seybold, Anal. Chem., 50, 1577 (1978).
42. C.D. Ford and R.J. Hurtubise, Anal. Chem., 50, 610 (1978).
43. R.J. Hurtubise, Talanta, 28, 145 (1981).
44. R.A. Dalterio and R.J. Hurtubise, Anal. Chem., 54, 224 (1982).
45. C.D. Ford and R.J. Hurtubise, Anal. Chem., 51, 659 (1979).
46. R.M.A. von Wandruszka and R.J. Hurtubise, Anal. Chim. Acta, 93, 331 (1977).
47. C.D. Ford and R.J. Hurtubise, Anal. Lett., 13(A6), 485 (1980).
48. R.J. Hurtubise and R.A. Dalterio, Amer. Lab., Nov. 58 (1981).
49. R.J. Hurtubise, "Solid Surface Luminescence Analysis: Theory, Instrumentation, Applications," Marcel Dekker, Inc., New York, 1981.
50. E.M. Schulman, J. Chem. Educ., 53, 522 (1976).
51. E.M. Schulman and R.T. Parker, J. Phys. Chem., 81, 1932 (1977).

52. R.T. Parker, R.S. Freedlander, E.M. Schulman, and R.B. Dunlap, in R.L. Kisliak and G.M. Brown (Eds.), "Chemistry and Biology of Pteridines," Elsevier-North Holland, New York, 1979, p. 61.
53. R.T. Parker, R.S. Freedlander, E.M. Schulman, and R.B. Dunlap, Anal. Chem., 51, 1921 (1979).
54. R.T. Parker, R.S. Freedlander, and R.B. Dunlap, Anal. Chim. Acta, 119, 189 (1980).
55. R.T. Parker, R.S. Freedlander, and R.B. Dunlap, Anal. Chim. Acta, 120, 1 (1980).
56. T. vo-Dinh and R.B. Gammage, Anal. Chem., 50, 2054 (1978).
57. T. vo-Dinh, R.B. Gammage, A.R. Hawthorne, and J.H. Throngate, Environ. Sci. Technol., 12, 1297 (1978).
58. T. vo-Dinh, R.B. Gammage, and P.R. Martinez, Anal. Chem., 58, 253 (1981).
59. T. vo-Dinh and P.R. Martinez, Anal. Chim. Acta, 125, 13 (1981).
60. T. vo-Dinh and R.B. Gammage, Anal. Chim. Acta, 107, 261 (1979).
61. T. vo-Dinh and J.R. Hooyman, Anal. Chem., 51, 1915 (1979).
62. I.M. Jakovljevic, Anal. Chem., 49, 2048 (1977).
63. J.B.F. Lloyd, Analyst, 103, 775 (1978).
64. J.N. Miller, Trends in Anal. Chem., 1, 31 (1981).
65. C.G. de Lima and E.M. de M Nicola, Anal. Chem., 50, 1658 (1978).
66. J.D. Winefordner, S.G. Schulman, and T.C. O'Haver, "Luminescence Spectroscopy in Analytical Chemistry," J. Wiley, New York, 1972.
67. P. Seybold and M. Gouterman, Chem. Rev., 65, 413 (1965).
68. C.A. Parker and G.G. Hatchard, Trans. Faraday Soc., 57, 1894 (1961).

69. E. Becquerel, Mémoire sur l'analyse de la lumière émise par les composés d'uranium phosphorescents, Ann. de Chim. et Phys., 27, 539 (1871).
70. R.J. Keirs, R.D. Britt, Jr., and W.E. Wentworth, Anal. Chem., 29, 202 (1957).
71. R. Zweidinger and J.D. Winefordner, Anal. Chem., 42, 639 (1970).
72. P. Kubelka and F. Munk, Z. Tech. Phys., 12, 593 (1931).
73. P. Kubelka, J. Opt. Soc. Am., 38, 448 (1948).
74. G.N. Lewis and M.J. Kasha, J. Chem. Soc., 66, 2100 (1949).
75. S. Freed and W. Salmre, Science, 128, 1341 (1958).
76. C.A. Parker and C.G. Hatchard, Analyst, 87, 664 (1962).
77. J.D. Winefordner and H.W. Latz, Anal. Chem., 35, 1517 (1963).
78. L.J. Cline-Love, M. Skrilec, and J.G. Habarta, Anal. Chem., 52, 754 (1980).
79. M. Skrilec and L.J. Cline-Love, Anal. Chem., 52, 1559 (1980).
80. L.J. Cline-Love, J.G. Habarta, and M. Skrilec, Anal. Chem., 53, 437 (1981).
81. L.J. Cline-Love and M. Skrilec, Anal. Chem., 53, 1872 (1981).
82. P. Yarmchuk, R. Weinberger, R.F. Hirsch, and L.J. Cline-Love, Pittsburgh Conference, March 8-13, 1982, Atlantic City, N.J.
83. R. Weinberger, P. Yarmchuk, and L.J. Cline-Love, Pittsburgh Conference, March 8-13, 1982, Atlantic City, N.J.
84. R. Woods and L.J. Cline-Love, Pittsburgh Conference, March 8-13, 1982, Atlantic City, N.J.
85. L.J. Cline-Love and M. Skrilec, Amer. Lab., April, 103 (1981).
86. J.J. Donkerbroek, J.J. Elzas, C. Gooijer, R.W. Frei, and N.H. Velthorst, Talanta, 28, 717 (1981).

87. J.J. Donkerbroek, N.J.R. Van Eikema Homes, C. Gooijer, N.H. Velthorst, and R.W. Frei, Chromatographia, 15, 218 (1982).
88. J.J. Donkerbroek, C. Gooijer, N.H. Velthorst, and R.W. Frei, Anal. Chem., 54, 891 (1982).
89. G.D. Boutilier and J.D. Winefordner, Anal. Chem., 51, 1391 (1979).
90. S.G. Schulman, "Fluorescence and Phosphorescence Spectroscopy, Physicochemical Principles and Practice," Pergamon Press, Elmsford, N.Y., 1977.
91. S. Udenfriend, "Fluorescence Assay in Biology and Medicine," Vol. 2, Academic Press, N.Y., 1969.
92. S.K. Lower and M.A. El-sayed, Chem. Rev., 66, 199 (1966).
93. T-7 Clay and corn starch were generously given by Weber Costello Co.
94. J.L. Kropp and W.R. Dawson, J. Phys. Chem., 71(13), 4499 (1967).
95. J. Najbar, J.B. Birks, and T.D.S. Hamilton, Chem. Phys., 23, 281 (1977).
96. G.D. Boutilier and J.D. Winefordner, Anal. Chem., 51, 1384 (1979).
97. S.P. McGlynn, T. Azami, and M. Kinoshita, "Molecular Spectroscopy of the Triplet State," Prentice-Hall, Englewood Cliffs, N.J., 1969.
98. L.R. Snyder and J.J. Kirkland, "Introduction to Modern Liquid Chromatography," 2nd Ed., J. Wiley & Sons, Inc., N.Y., 1979.
99. J.C. Sternberg, in J.G. Giddings and R.A. Kelly (Eds.), "Advances in Chromatography," Vol. 2, Dekker, N.Y., 1971.
100. S.A. Borman, Anal. Chem., 54, 327A (1982).
101. A. Jurgensen, E.L. Inman, Jr., and J.D. Winefordner, Anal. Chim. Acta, 131, 187 (1981).
102. N. Mataga, Y. Kaifu, and M. Koizami, Bull. Chem. Soc. Japan, 29, 373 (1956).
103. S. Ladner and R.S. Becker, J. Phys. Chem., 67, 2481 (1963).

APPENDIX A
ROOM TEMPERATURE PHOSPHORESCENCE SPECTRA OF
COMPOUNDS NOT SHOWN IN TEXT

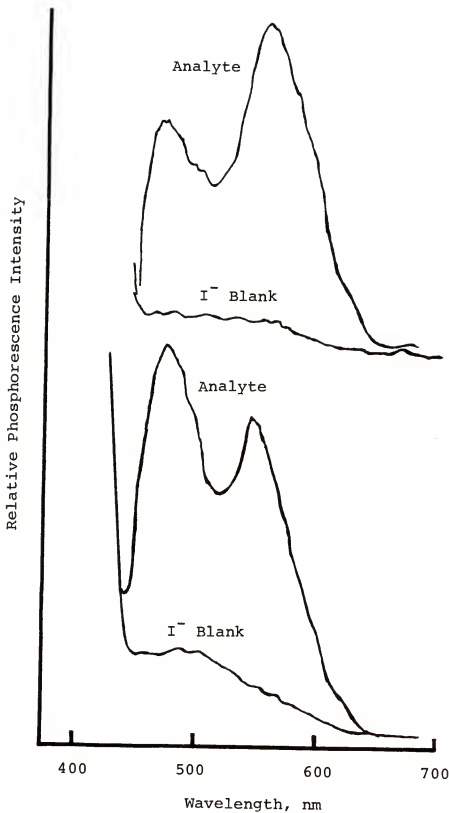


Figure 32. Oxythioquinox (113 $\mu\text{g}/\text{ml}$) in 1 M NaI and on DE-81 (top) and S & S 903 (bottom) filter papers ($\lambda_{\text{ex}} = 396 \text{ nm}$)

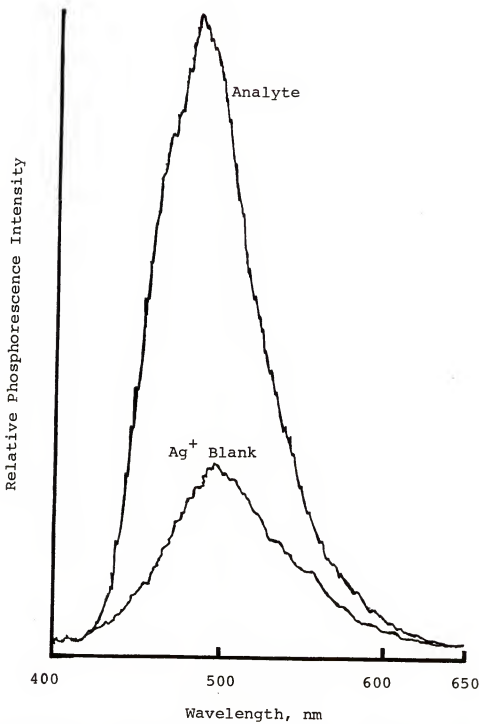


Figure 33. Biphenyl (72 $\mu\text{g}/\text{ml}$) in 1 M AgNO_3 and on S & S 903 filter paper ($\lambda_{\text{ex}} = 266 \text{ nm}$)

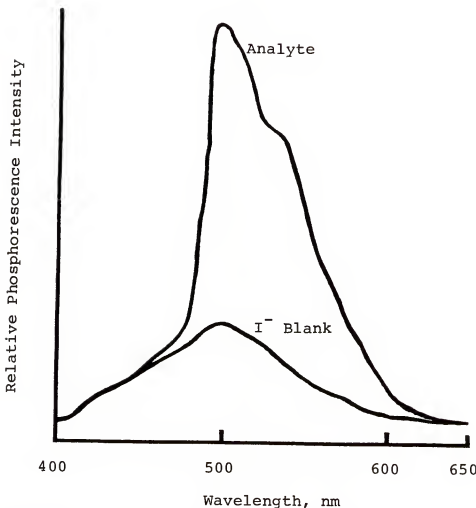


Figure 34. Naphthalene acetic acid (27 $\mu\text{g}/\text{ml}$) in 1 M NaI and on S & S 903 filter paper ($\lambda_{\text{ex}} = 290 \text{ nm}$)

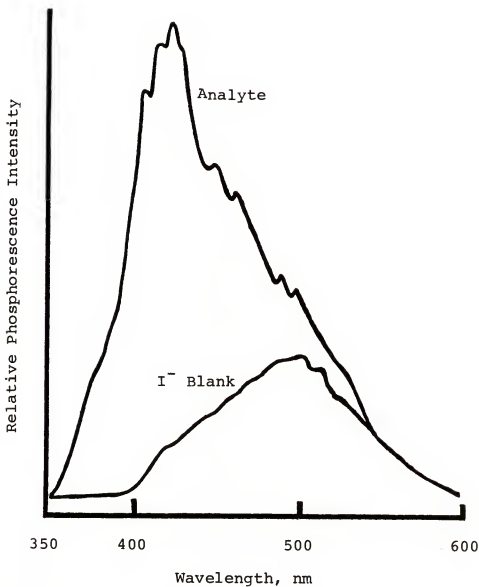


Figure 35. 2-Aminobenzimidazole (55 µg/ml) in NaI and on DE-81 filter paper ($\lambda_{ex} = 280$ nm)

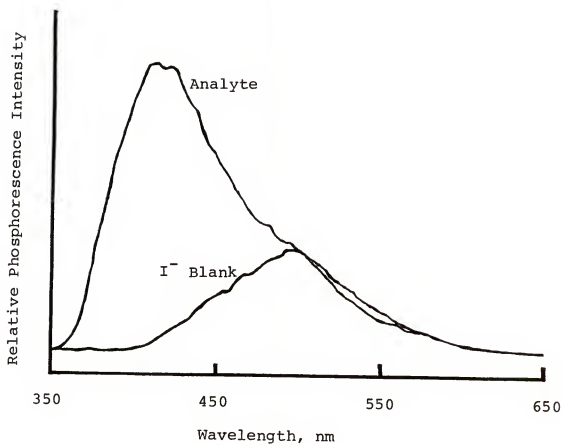


Figure 36. Benomyl (144 μ g/ml) in 1 M NaI on S & S 903 filter paper ($\lambda_{ex} = 280$ nm)

APPENDIX B
BASIC PROGRAM AND CIRCUITRY OF LOW PASS FILTER
USED IN THE STUDY OF RTP BACKGROUND
LUMINESCENCE CORRECTION BY
COMPUTER APPROACH

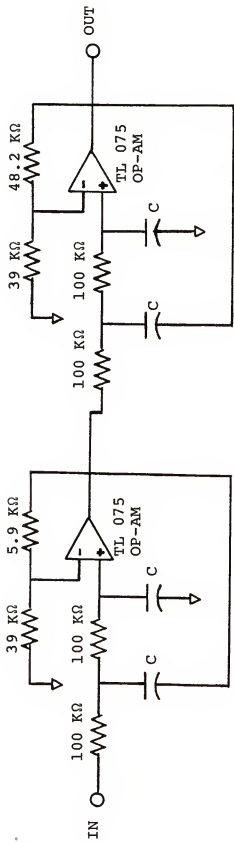


Figure 37. Circuitry of low pass Sallen-Key active filter used in RTP study
 C is the capacitor used in the circuitry, and all four capacitors have the same value of $0.016 \mu F$. The value of resistor $5.9 k\Omega$ is determined by use of equation $(2-d)$. $39 k\Omega$ and $d = 1.848$ in this case; and $d = 0.765$ for the case of $48.2 k\Omega$.

```

]LOAD AMINCO
]LIST

5 REM THIS PROGRAM WILL KEEP SP
   ECT AND CORRCT THE GAIN TO T
   HE BASE OF 0.1 (AMINCO) AND
10 100 (SCALER)
15 DIM SIG(1500)
20 DIM M(300)
25 GOSUB 1000
30 PRINT "RUN 16 BLANK READINGS
35 "
40
106 INPUT Z$
107 IF Z$ = "N" GOTO 110
108 GOTO 7000
110 GOSUB 2000
120 GOSUB 3000
130 IF X > 1.580 GOTO 160
140 GOSUB 4000
150 GOTO 120
160 GOSUB 5000
165 PRINT "# OF DATA =";I
170 PRINT "SAVE SPECTRUM"
180 INPUT A$
190 IF A$ = "Y" GOTO 250
200 PRINT "GET ANOTHER SPECTRUM"
210 INPUT A$
220 IF A$ = "N" GOTO 260
230 GOTO 100
240 GOSUB 6000
250 PRINT D$;"PR#0"
255 TEXT
260 END
270
1000 REM SUBROUTINE TO DO INITI
   ALIZATION
1005 I = 0
1006 MN = 1000:MX = - 1000
1007 D$ = "": REM D$ IS CTRL-D
1010 PRINT "SENSITIVITY OF AMINC
   O"
1015 INPUT G1
1020 PRINT "ELECTROMETER GAIN OF
   SCALER"
1025 INPUT G2
1030 RETURN
2000 REM SUBROUTINE TO DETECT B
   EGINNING OF SCAN
2010 GOSUB 3000
2020 IF X > 0.0190 THEN RETURN
2025 PRINT "WAITING..."
2030 GOTO 2010
3000 REM GET X AND Y SIGNAL FRO
   M AMINCO
3010 REM GET X SIGNAL ( VOLTS )
3020 CH = 0
3030 GOSUB 3500
3040 X = V * 10 / 4095
3050 REM GET Y SIGNAL ( PHOTOCU
   RRENT )
3060 CH = 1
3070 GOSUB 3500
3080 Y = V * 10 / 4095
3090 RETURN
3500 REM SUBROUTINE TO GET ONE
   VALUE FROM A/D CONVERTER
3520 PRT = 49368: REM PIA #2 IN
   SLOT #5 TO A/D BOX

```

```

3530 REM INIT PIA
3540 POKE PRT,0
3550 POKE PRT + 2,255
3560 POKE PRT,4
3565 POKE PRT + 2,0
3570 POKE PRT + 1,0
3580 POKE PRT + 3,255
3590 POKE PRT + 1,52
3595 POKE PRT + 3,0
3600 REM GATE CONTROL INFO INTO
A/D
3610 POKE PRT + 2,160 + (CH * 2)
3620 POKE PRT + 3,1
3630 POKE PRT + 3,0
3640 REM TRIGGER A/D CONVERSION
3650 POKE PRT + 2,161 + (CH * 2)
3660 POKE PRT + 3,1
3670 POKE PRT + 3,0
3680 POKE PRT + 2,160 + (CH * 2)

3690 POKE PRT + 3,1
3700 POKE PRT + 3,0
3710 REM READ CONVERTED DATA
3720 POKE PRT,0
3730 POKE PRT + 2,0
3740 POKE PRT,4
3750 POKE PRT + 3,8
3760 A = PEEK (PRT + 2)
3770 POKE PRT + 3,4
3780 B = PEEK (PRT + 2)
3790 POKE PRT + 3,0
3805 V = A * 16 + B / 16
3810 POKE PRT,0
3820 POKE PRT + 2,255
3830 POKE PRT,4
3850 RETURN
4000 REM SUBROUTINE TO PUT Y SI
GNAL IN MEMORY
4010 I = I + 1
4020 SIG(I) = Y * G1 * G2 / (0.1 *
100)
4030 RETURN
5000 REM SUBROUTINE TO PLOT S
PECTRUM ON SCREEN
5010 HGR
5020 HCOLOR= 3
5050 REM SCAN THE DATA FOR MAXI
MUM AND MINIMUM
5060 FOR K = 1 TO I
5070 IF SIG(K) < MN THEN MN = SI
G(K)
5080 IF SIG(K) > MX THEN MX = SI
G(K)
5090 NEXT K
5095 PRINT "MN=";MN
5096 PRINT "MX=";MX
5100 FOR K = 1 TO I - 1
5110 HPLOT 279 * K / I,159 - (SI
G(K) - MN) / (MX - MN) * 159
TO 279 * (K + 1) / I,159 -
(SIG(K + 1) - MN) / (MX - MN
) * 159
5115 NEXT K
5120 RETURN
6000 REM SUBROUTINE TO SAVE DAT
A IN A DISK FILE
6005 PRINT "ENTER NAME OF FILE"
6010 INPUT F$
6015 PRINT "NAME OF SAMPLE"
6020 INPUT T$

```

```

6021 PRINT "FIRST WAVELENGTH"
6022 INPUT FW
6023 PRINT "LAST WAVELENGTH"
6024 INPUT LW
6025 PRINT "CONCENTRATION OF SAM
PLE"
6026 INPUT CN
6027 PRINT "PEAK WAVELENGTH"
6028 INPUT PW
6030 PRINT D$;"OPEN ";F$
6035 PRINT D$;"WRITE";F$
6040 PRINT FW: REM FIRST WAVELE
NGTH SCANE
6050 PRINT LW: REM LAST WAVELEN
GTH SCANE
6060 PRINT I: REM NUMBER OF DAT
A
6065 PRINT CN: REM CONCENTRATIO
N OF SAMPLE
6070 PRINT PW: REM PEAK WAVELEN
GTH OF EITHER EXCITATION OR
EMISSION
6080 PRINT G1: REM SENSITIVITY
OF AMINCO
6081 PRINT G2: REM ELECTROMETER
GAIN OF SCALER
6090 PRINT MN: REM MINIMUM SIGN
AL
6100 PRINT MX: REM MAXIMUM SIGN
AL
6110 PRINT T$: REM SAMPLE NAME
6120 FOR K = 1 TO I
6130 PRINT SIG(K): REM SPECTRAL
DATA
6140 NEXT K
6150 PRINT D$;"CLOSE ";F$
6160 RETURN
7000 REM TO OBTAIN 16 BLANK REA
DINGS
7035 L = 0
7040 PRINT "HOW MANY READINGS"
7050 INPUT S
7080 L = L + 1
7085 GOSUB 3000
7087 M(L) = Y * G1 * G2 / (0.1 *
100)
7088 PRINT "L=";L
7089 PRINT M(L)
7090 IF L < S GOTO 7080
7120 PRINT "ENTER NAME OF FILE"
7130 INPUT F$
7140 PRINT "BLANK NAME"
7150 INPUT S$
7160 PRINT "RUN FOR WHICH SAMPLE
7170 INPUT T$
7200 PRINT D$;"OPEN ";F$
7210 PRINT D$;"WRITE";F$
7220 PRINT L: REM TOTAL READI
NGS
7230 PRINT T$: REM SAMPLE NAME
7240 PRINT S$: REM BLANK NAME
7250 FOR K = 1 TO L
7280 PRINT M(K): REM BLANK READ
INGS
7270 NEXT K
7280 PRINT D$;"CLOSE ";F$
7290 PRINT "RUN ANOTHER BLANK"
7300 INPUT X$
7310 IF X$ = "Y" GOTO 7035
7350 GOTO 260

```

```

10 REM THIS PROGRAM IS TO CORRE
CT THE SPECTRA FROM BLANK OR
SPECTRA FROM OTHER COMPOUND
S IN THE MIXTURE
20 DIM S(350),T(350),U(350)
100 GOSUB 1000
110 GOSUB 2000
120 GOSUB 3000
130 PRINT "I1=";I1
140 PRINT "I2=";I2
150 PRINT "QUIT THE CORRECTION"
160 INPUT A$
170 IF A$ = "Y" GOTO 300
180 PRINT "NUMBER OF DATA POINTS
TO BE CORRECTED"
190 INPUT I
200 FOR K = 1 TO I
210 U(K) = S(K) - T(K); REM ONE-
TO-ONE SIGNAL CORRECTION
220 IF U(K) < MN THEN MN = U(K)
230 IF U(K) > MX THEN MX = U(K)
240 NEXT K
250 GOTO 400
300 PRINT "GET ANOTHER FILES TO
BE CORRECTED"
310 INPUT B$
320 IF B$ = "N" GOTO 680
330 GOTO 110
400 PRINT "SAVE SPECTRUM"
410 INPUT H$
420 IF H$ = "Y" GOTO 440
430 GOTO 300
440 GOSUB 4000
450 PRINT "PLOT ANY SPECTRUM"
460 INPUT J$
470 IF J$ = "N" GOTO 680
500 PRINT "SELECT SPECTRUM - S(T
BE CORRECTED), T(TO CORREC
T WITH), U(CORRECTED), N(EXT
T)"
510 INPUT K$
520 IF K$ = "S" GOTO 555
530 IF K$ = "T" GOTO 595
540 IF K$ = "U" GOTO 635
550 IF K$ = "N" GOTO 680
555 HGR
556 HCOLOR= 3
560 FOR K = 1 TO I1 - 1
570 HPLOT 279 * K / I1,159 - (S(
K) - N1) / (X1 - N1) * 159 TO
279 * (K + 1) / I1,159 - (S(
K + 1) - N1) / (X1 - N1) * 1
59
580 NEXT K
590 GOTO 500
595 HGR
596 HCOLOR= 3
600 FOR K = 1 TO I2 - 1
610 HPLOT 279 * K / I2,159 - (T(
K) - M1) / (X1 - N1) * 159 TO
279 * (K + 1) / I2,159 - (T(
K + 1) - M1) / (X1 - N1) * 1
59
620 NEXT K

```

```

630 GOTO 800
635 HGR
636 HCOLOR= 3
640 FOR K = 1 TO I - 1
650 HPLOT 279 * K / I,159 - (S(K)
/ - T(K) - MN) / (X1 - N1) *
159 TO 279 * (K + 1) / I,159
- (S(K + 1) - T(K + 1) - MN
) / (X1 - N1) * 159
660 NEXT K
670 GOTO 500
680 PRINT D$;"PR#0"
685 TEXT
690 END
695 PRINT "KEEP THE DATA"
700 INPUT Y$
710 IF Y$ = "N" GOTO 500
720 PRINT "FILE NAME"
730 INPUT Z$
740 PRINT D$;"OPEN";Z$
750 PRINT D$;"WRITE";Z$
760 PRINT FW
770 PRINT LW
780 PRINT I2
790 PRINT N1
800 PRINT X1
810 PRINT M1
820 PRINT C1
824 PRINT G3
825 PRINT M2
826 PRINT T$
830 FOR K = 1 TO I2
840 PRINT T(K): REM DATA OF BLA
NK
850 NEXT K
860 PRINT D$;"CLOSE";Z$
870 GOTO 500
880 REM SUBROUTINE TO DO INITI
ALIZATION
890 MN = 0:MX = 0
900 D$ = "": REM D$ IS CTRL-D
910 RETURN
920 REM SUBROUTINE TO READ SPE
CTRUM TO BE CORRECTED
930 PRINT "NAME OF FILE TO BE C
ORRECTED"
940 INPUT F$
950 PRINT D$;"OPEN";F$
960 PRINT D$;"READ";F$
970 INPUT FW,LW,I1,CN,PW,G1,G2,
N1,X1,T$
980 FOR K = 1 TO I1
990 INPUT S(K): REM SPECT TO B
E CORRECTED
1000 NEXT K
1010 PRINT D$;"CLOSE";F$
1020 RETURN
1030 REM SUBROUTINE TO READ SPE
CTRUM TO CORRECT WITH
1040 PRINT "NAME OF FILE TO CORR
ECT WITH"
1050 INPUT F$
1060 PRINT D$;"OPEN";F$
1070 PRINT D$;"READ";F$
1080 INPUT FW,LW,I2,C1,P1,G3,G4,
M1,M2,S$
1090 FOR K = 1 TO I2
1100 INPUT T(K): REM SPECT TO C
ORRECT WITH

```

```
3080  NEXT
3090  PRINT I$;"CLOSE";F$
3100  RETURN
4000  REM SUBROUTINE TO SAVE COR-
      RECTED SPECTRUM
4010  PRINT "ENTER NAME OF FILE"
4020  INPUT F$
4030  PRINT "NAME OF SAMPLE"
4040  INPUT T$
4050  PRINT I$;"OPEN";F$
4060  PRINT I$;"WRITE";F$
4070  PRINT FW
4080  PRINT LW
4090  PRINT I
4100  PRINT N1
4110  PRINT X1
4120  PRINT MN
4130  PRINT CN
4140  PRINT G1
4150  PRINT MX
4160  PRINT T$
4170  FOR K = 1 TO I
4180  PRINT U(K)
4190  NEXT K
4200  PRINT I$;"CLOSE";F$
4210  RETURN
```

```

10 REM THIS PROGRAM WILL CALCUL
11 ATE LDR AND LIR
20 DIM U(220),V(220),M(50),Y(2),
21 B(2)
30 GOSUB 1000
40 PRINT "SKIP MAIN PROGRAM TO L
50 ODLDR FILE"
50 INPUT A$
60 IF A$ = "Y" GOTO 6000
110 PRINT "ENTER NUMBER OF DATA
PAIR FOR LDR CALCN"
120 INPUT L
130 FOR K = 1 TO L
140 GOSUB 2000
150 U(K) = LOG (MX)
160 IF U(K) < U1 THEN U1 = U(K)
170 IF U(K) > U2 THEN U2 = U(K)
180 V(K) = LOG (N)
190 IF V(K) < V1 THEN V1 = V(K)
200 IF V(K) > V2 THEN V2 = V(K)
210 NEXT K
220 GOSUB 3000
230 PRINT "ORDERS OF MAGNITUDE O
F LDR"
240 INPUT J
250 PRINT "LOW CONCN POINT IN LI
NEAR RANGE"
260 INPUT P
270 PRINT " HI CONCN PT IN LINEA
R RANGE"
280 INPUT Q
285 GOSUB 3500
290 FOR K = P TO Q
300 MX = EXP (U(K))
310 N = EXP (V(K))
320 MSUM = MSUM + MX * N
330 YSUM = YSUM + MX
340 XSUM = XSUM + N
350 QSUM = QSUM + N * N
360 NEXT K
370 R = Q - P + 1
380 SLP = ((R * MSUM) - (YSUM * X
SUM)) / ((R * QSUM) - (XSUM *
XSUM))
390 INCPT = ((MSUM * XSUM) - (YSU
M * QSUM)) / ((XSUM * XSUM) -
R * (QSUM))
400 PRINT "SLP=";SLP
410 PRINT "INCPT=";INCPT
450 GOSUB 4000
455 PRINT "SAVE FILE"
456 INPUT H$
457 IF H$ = "N" GOTO 465
460 GOSUB 5000
465 PRINT "ANOTHER SET OF BLANK
READING"
466 INPUT B$
467 IF B$ = "N" GOTO 470
468 SX = 0:SY = 0:XY = 0:QX = 0:X
SUM = 0:YSUM = 0:MSUM = 0:QS
UM = 0:BSUM = 0:DEV = 0
469 GOTO 220
470 PRINT "OUTPUT OF ANAL FIG OF
MERIT"
480 INPUT G$
490 IF G$ = "N" GOTO 510
500 GOSUB 6000
510 PRINT D$;"PR#0"
520 END

```

```

1000 REM SUBROUTINE TO DO INITI
ALIZATION
1010 D$ = ""; REM D$ IS CTRL-D
1020 U1 = 10:U2 = -10:V1 = 10:V
2 = -10:BSUM = 0:DEV = 0:M
SUM = 0:YSUM = 0:XSUM = 0:QS
UM = 0
1021 SY = 0:SX = 0:QX = 0:XY = 0
1030 RETURN
2000 REM SUBROUTINE TO READ DAT
A
2010 PRINT "ENTER FILE NAME OF C
ORRECTED SPECT"
2020 INPUT F$
2030 PRINT D$;"OPEN";F$
2040 PRINT D$;"READ";F$
2050 INPUT FW,LW,I,N1,X1,MN,N,G1
,MX,T$
2060 PRINT D$;"CLOSE";F$
2070 RETURN
3000 REM SUBROUTINE TO PLOT THE
LDR (LN-LN)
3004 TEXT
3010 HGR
3020 HCOLOR= 3
3030 FOR K = 1 TO L
3040 HPLOT 279 * (V(K) - V1) / (
V2 - V1),159 - (U(K) - U1) /
(U2 - U1) * 159
3041 NEXT K
3060 RETURN
3500 REM SUBROUTINE TO CHOOSE T
HE RIGHT LINEAR RANGE
3505 FOR K = P TO Q
3510 SY = SY + U(K)
3520 QX = QX + V(K) * V(K)
3530 SX = SX + V(K)
3540 XY = XY + U(K) * V(K)
3550 NEXT K
3555 LZ = Q - P + 1
3560 SPN = ((LZ * XY) - (SY * SX)
) / ((LZ * QX) - (SX * SX))
3570 CPT = ((XY * SX) - (SY * QX)
) / ((SX * SX) - (LZ * QX))
3580 PRINT "SLOPE OF LN-LN PLOT=
";SPN
3590 PRINT "INTERCEPTION OF LN-L
N=";CPT
3600 PRINT "WANT TO TRY ANOTHER
SET OF POINTS"
3610 INPUT C$
3620 IF C$ = "N" GOTO 3630
3625 SX = 0:SY = 0:XY = 0:QX = 0
3626 GOTO 220
3630 RETURN
4000 REM SUBROUTINE TO CALAULAT
E LOD
4010 PRINT "FILE NAME OF BLANK "
4020 INPUT F$
4030 PRINT D$;"OPEN";F$
4040 PRINT D$;"READ";F$
4050 INPUT R,T$;S$
4060 FOR K = 1 TO R
4070 INPUT MK$): REM BLANK READ
INGS
4080 BSUM = BSUM + MK$)
4090 NEXT K
4100 PRINT D$;"CLOSE";F$
4110 AVG = BSUM / R

```

```

4120 FOR K = 1 TO R
4130 DEV = DEV + (M(K) - AVG) * (
M(K) - AVG)
4140 NEXT K
4150 SD = SQR (DEV / (R - 1))
4160 LOD = SD * 3 / SLP
4170 PRINT "LOD=";LOD
4180 RETURN
5000 REM SUBROUTINE TO KEEP THE
DATA
5010 PRINT "ENTER FILE NAME"
5020 INPUT F$
5030 PRINT "NAME OF SAMPLE"
5040 INPUT T$
5050 PRINT "NAME OF BLANK"
5060 INPUT S$
5070 PRINT D$;"OPEN";F$
5080 PRINT D$;"WRITE";F$
5090 PRINT T$; REM SAMPLE NAME
5100 PRINT S$; REM BLANK NAME
5110 PRINT SLP; REM SLOPE OF LD
R
5115 PRINT SPN; REM LN-LN SLOPE
5120 PRINT J; REM ORDERS OF MAG
NITUDE
5130 PRINT INCPT; REM INTERCEPT
OF LDR
5135 PRINT CPT; REM LN-LN INTER
CEPT
5140 PRINT LOD; REM DETECTION L
IMIT
5150 PRINT V1; REM MINIMUM LN O
F CONCN
5160 PRINT V2; REM MAXIMUM LN O
F CONCN
5170 PRINT U1; REM MINIMUM LN O
F SIG
5180 PRINT U2; REM MAXIMUM LN O
F SIG
5185 PRINT L; REM # OF DATA PAI
R USED
5186 PRINT P; REM LOW CONCN PT
5187 PRINT Q; REM HI CONCN PT
5190 FOR K = 1 TO L
5200 PRINT U(K); REM SIGNAL IN
LN VALUE
5210 PRINT V(K); REM LN CONCN
5220 NEXT K
5230 PRINT D$;"CLOSE";F$
5240 RETURN
6000 REM SUBROUTINE TO RETRIEVE
AND PLOT LDR AND LOD
6010 PRINT "FILE NAME OF LOD/LDR"

```

```
      "
6020  INPUT F$
6030  PRINT D$;"OPEN";F$
6040  PRINT D$;"READ";F$
6050  INPUT T$,S$,SLP,SPN,J,INCPT
      ,CPT,LOD,V1,V2,U1,U2,L,P,Q
6060  FOR K = 1 TO L
6070  INPUT U(K)
6080  INPUT V(K)
6090  NEXT K
6095  PRINT "SAMPLE NAME=";T$
6100  PRINT "LOD=";LOD
6110  PRINT "SLOPE OF SIG VS COCN
      =";SLP
6115  PRINT "SLOPE OF LN(SIG) VS
      LN(COCN)";SP
6120  PRINT "ORDER OF MAGNITUDE="
      ;J
6130  PRINT "INCPT=";INCPT
6135  PRINT "INTERCEPT OF LN-LN =
      ";CPT
6140  GOSUB 3000
6150  Y1 = CPT + SPN * 0
6160  Y2 = CPT + SPN * 279
6180  HPLOT 0,159 TO 279,159 - (Y
      2 / (Y2 - Y1) * 159)
6200  PRINT D$;"CLOSE";F$"
6210  RETURN
```

```

1PR#0
1SAVE PLOT AMINCO.1
1LOAD LPLOT AMINCO.2
1LIST

5 REM TO PLOT SPECTRUM FROM 200 TO
700 NM
10 REM PROGRAM TO PLOT SPECTRAL
DATA ACQUIRED FROM AMINCO S
PECTROPHOTOFUORIMETER ON HI
PLOT BMP-4 DIGITAL PLOTTER
15 DIM SIG(2500)
20 GOSUB 1000: REM INITIALIZE P
LOTTER
30 GOSUB 2000: REM DRAW BORDER
AROUND DATA
40 GOSUB 3000: REM GET DATA & P
LOT IT
50 GOSUB 4000: REM DRAW HASHMAR
NS
52 GOSUB 5000: REM DRAW LABELS
60 GOSUB 1000: REM MOVE PEN BACK
A TO LOWER LEFT CORNER
68 PRINT D$;"PR#0"
70 END
1000 REM SUBROUTINE TO INITIALI
ZE HIPLUT BMP-4 PLOTTER
1010 D$ = ":"; REM D$ = CTRL-D
1020 PRINT D$;"PR#2"
1030 PRINT ":";I 21 100 AUH"
1050 RETURN
2000 REM SUBROUTINE TO DRAW BO
RDER AROUND DATA AREA OF PLO
T
2020 PRINT "284,236 "
2030 PRINT "D"
2040 PRINT "1874,236 "
2050 PRINT "1874,1205 "
2060 PRINT "284,1205 "
2070 PRINT "284,236 "
2080 PRINT "U"
2085 PRINT "B"
2090 PRINT D$;"PR#0"
2100 RETURN
3000 REM SUBROUTINE TO RETRIEVE
DATA & PLOT IT
3010 REM FIRST RETRIEVE DATA
3020 PRINT "ENTER NAME OF FILE";
3030 INPUT F$;
3040 PRINT D$;"OPEN ";F$;
3050 PRINT D$;"READ ";F$;
3060 INPUT FW: REM FIRST WAVELE
NGTH
3070 INPUT LW: REM LAST WAVELEN
GTH
3080 INPUT N: REM NUMBER OF DA
TA
3090 INPUT CN: REM CONCENTRATIO
N OF SAMPLE
3100 INPUT PW: REM PEAK WAVELEN
GTH OF EITHER EXCITATION OR
EMISSION
3110 INPUT G1: REM GAIN OF AMIN
CO
3120 INPUT G2: REM GAIN OF SCAL
ER
3130 INPUT MN: REM MINIMUM SIGN
AL
3140 INPUT MX: REM MAXIMUM SIGN
AL

```

```

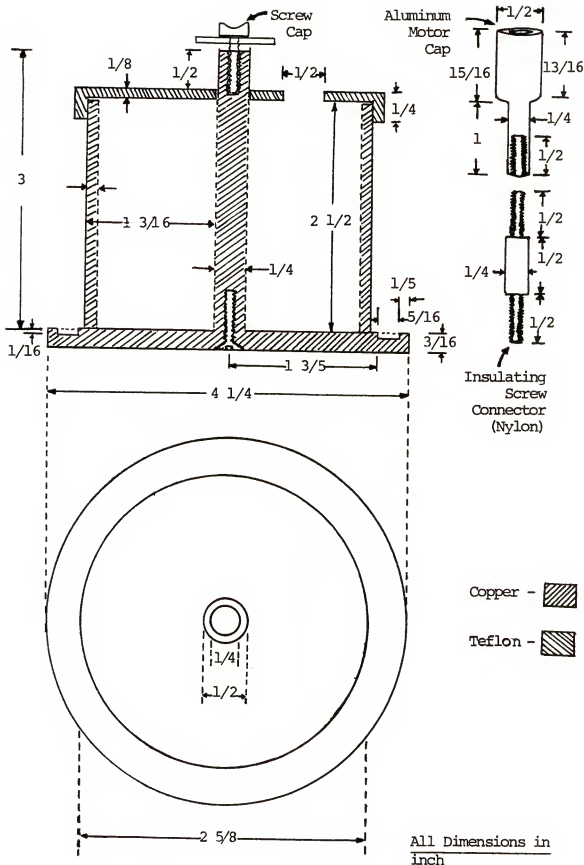
3150 INPUT T$: REM NAME OF SAMP
3160 FOR I = 1 TO N
3170 INPUT SIG(I)
3180 NEXT I
3190 PRINT D$;"CLOSE ";F$
3200 REM NOW PLOT THE DATA
3210 PRINT D$;PR#2"
3215 PRINT ":";
3220 PRINT INT (284 + (FW - 200
) * (1874 - 284) / ((800 - 2
00)));"; INT (256 + (1185 -
256) * (SIG(1) - MN) / (MX -
MN));";"
3230 PRINT "D"
3240 FOR I = 2 TO N
3250 PRINT INT (284 + (1874 - 2
84) * ((FW - 200) / (800 - 2
00) + I * (LW - FW) / ((800 -
200) * N));"; INT (256 +
(1185 - 256) * (SIG(I) - MN)
/ (MX - MN));"
3260 NEXT I
3270 PRINT "U"
3290 RETURN
4000 REM SUBROUTINE TO DRAW HAS
HMARKS
4005 NH = 0
4010 FOR I = 1 TO NH
4020 PRINT 284 + (I - 1) * 318,2
36
4022 PRINT "D"
4024 PRINT 284 + (I - 1) * 318,2
11
4026 PRINT "U"
4030 NEXT I
4040 RETURN
4142 PRINT (1874 + 284) / 2 - 15
* 12";100 "
4144 PRINT "S12 WAVELENGTH (NM)"
; CHR$(95)
5000 REM SUBROUTINE TO DRAW LAB
ELS ON PLOT
5010 PRINT "248,150 "
5020 PRINT "S12 200"; CHR$(95)
5030 PRINT "513,150 "
5040 PRINT "S12 300"; CHR$(95)
5050 PRINT "778,150 "
5060 PRINT "S12 400"; CHR$(95)
5070 PRINT "1043,150 "
5080 PRINT "S12 500"; CHR$(95)
5090 PRINT "1308,150 "
5100 PRINT "S12 600"; CHR$(95)
5110 PRINT "1573,150 "
5120 PRINT "S12 700"; CHR$(95)
5142 PRINT (1874 + 284) / 2 - 15
* 12";100 "
5144 PRINT "S12 WAVELENGTH (NM)"
; CHR$(95)
5150 PRINT "200,";236 + (1205 -
236) / 2 + 144
5160 PRINT "S22 PHOTOCURRENT"; CHR$(95)
5170 PRINT D$;PR#0"
5180 PRINT "ENTER PLOT LABEL (TO
P):"
5190 INPUT P$
5200 PRINT D$;PR#2"
5210 PRINT (284 + 1874) / 2 - LEN
(P$) * 24 / 2,";1225"
5220 PRINT "S12 "#P$; CHR$(95)
5230 RETURN

```

APPENDIX C
MECHANICAL DRAWINGS OF VERSATILE LUMINESCENCE
SAMPLING DEVICE

Figure 38. Diagram of 20-spot circular versatile luminescence sampling device

Twenty equally spaced 5/16 in diameter circular depressions around the edge of the circular plate to contain the solid substrate or liquid sample or small cups which can contain samples in any phase (all of these not shown in the diagram)



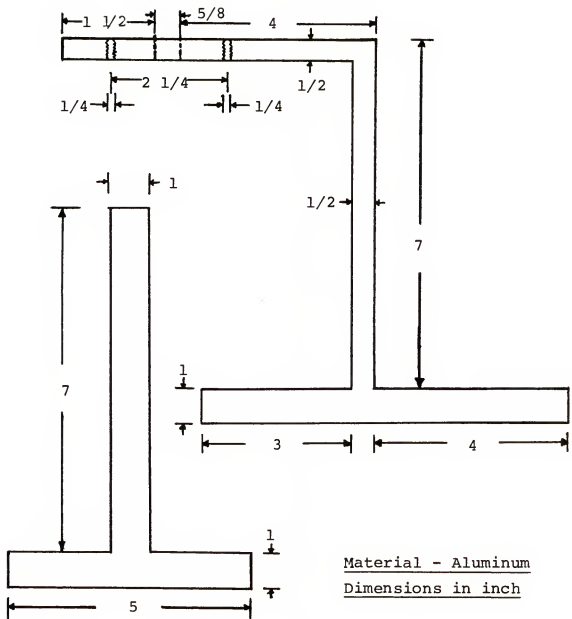
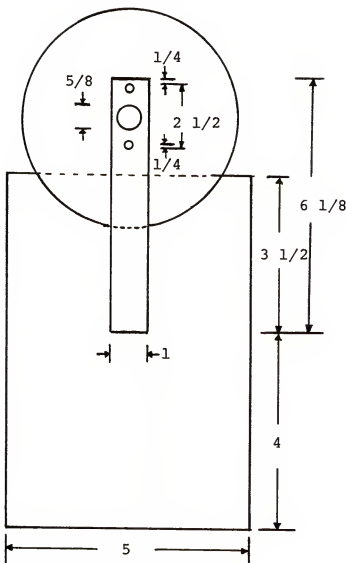


Figure 39. Diagram of stand of versatile luminescence sampling device for use on Aminco-Bowman spectrophotofluorimeter system



All Dimensions in inch

Figure 40. The top view of the versatile luminescence sampling device with the stand

APPENDIX D
HISTOGRAMS OF SEVERAL MODEL COMPOUNDS

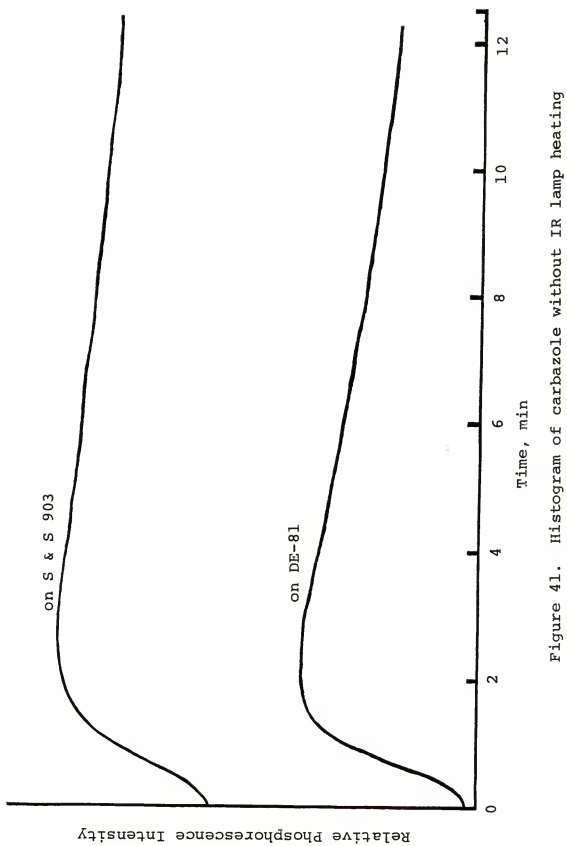


Figure 41. Histogram of carbazole without IR lamp heating

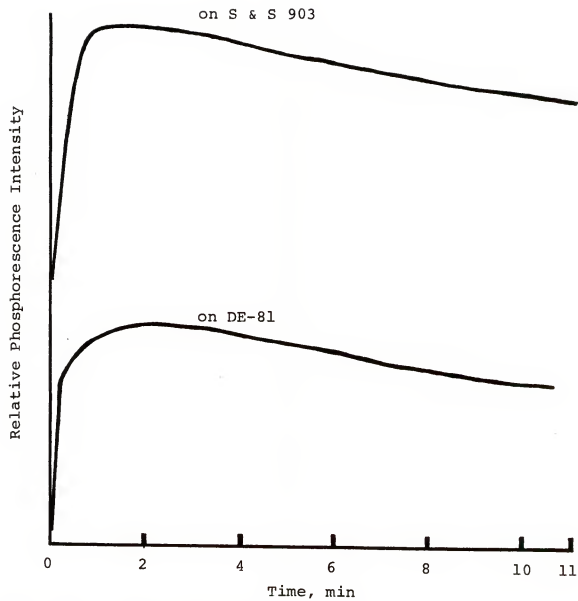


Figure 42. Histogram of carbazole with IR lamp heating

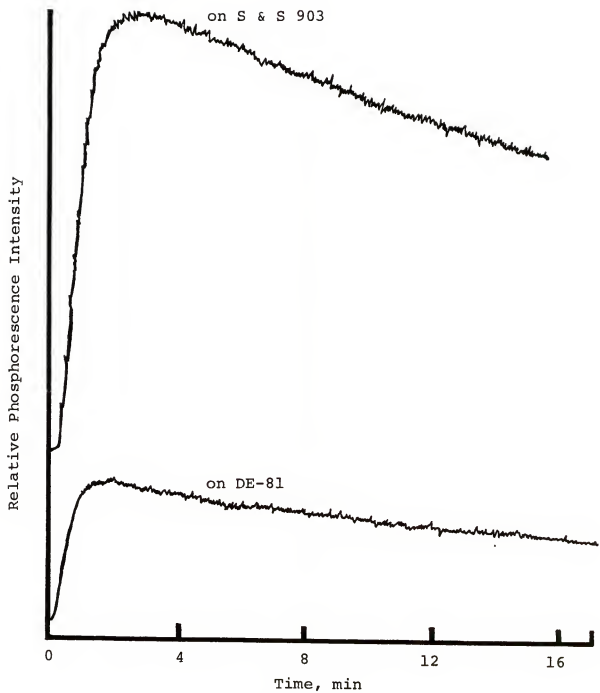


Figure 43. Histogram of phenanthrene without IR lamp heating

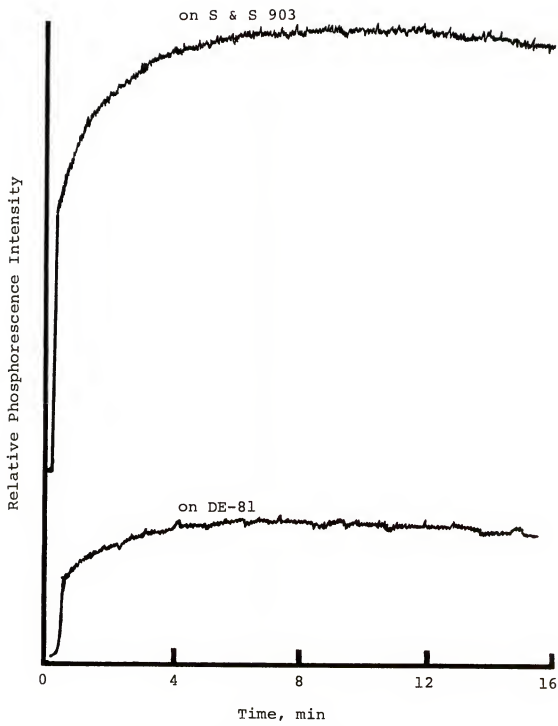


Figure 44. Histogram of phenanthrene with IR lamp heating

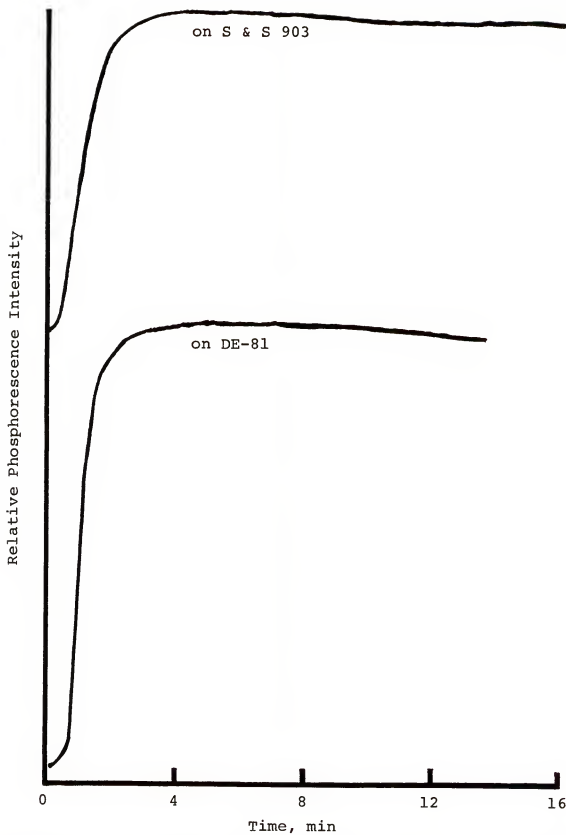


Figure 45. Histogram of privine HCl without IR lamp heating

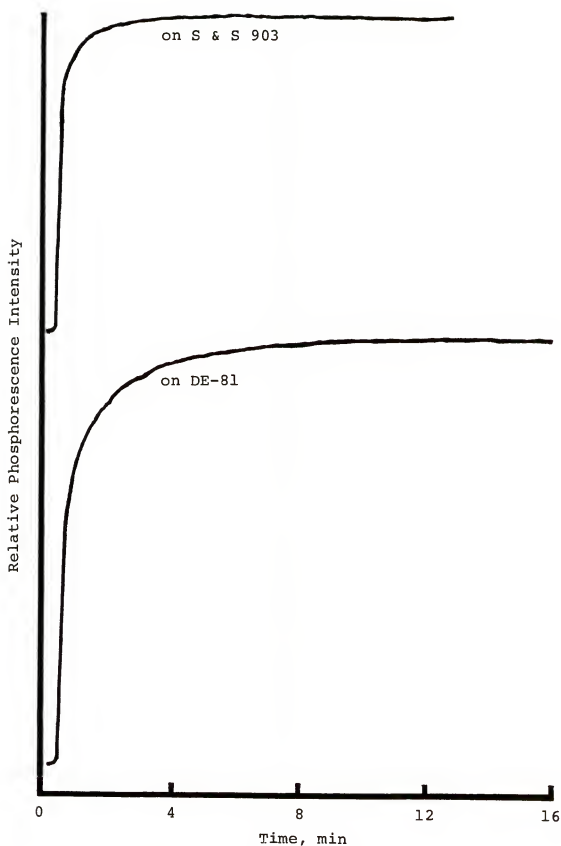


Figure 46. Histogram of privine HCl with IR lamp heating

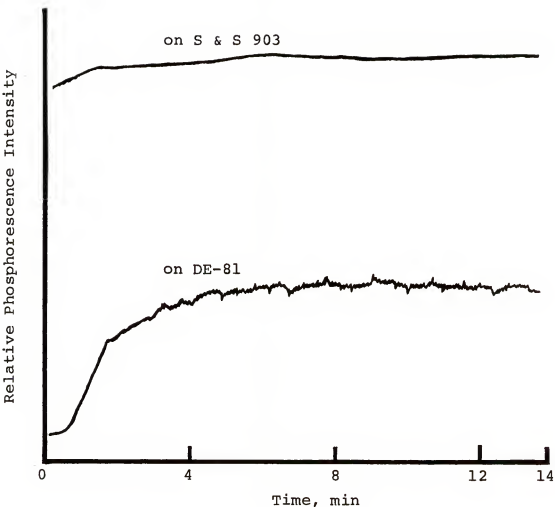


Figure 47. Histogram of 2-aminobenzimidazole without IR lamp heating

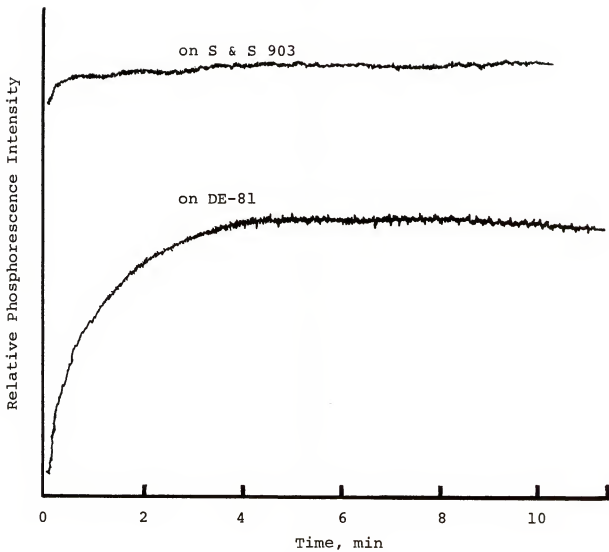


Figure 48. Histogram of 2-aminobenzimidazole with IR lamp heating

APPENDIX E
RESPONSE AND CALIBRATION CURVES OF COMPOUNDS
NOT SHOWN IN TEXT

Figure 49. RTP response (left) and calibration (right) curves of PABA on DE-81

Curves identified as:

(left) a. 100 $\mu\text{g/ml}$; b. 50 $\mu\text{g/ml}$; c. 20 $\mu\text{g/ml}$;
d. 4 $\mu\text{g/ml}$; e. 0.8 $\mu\text{g/ml}$; f. 0.16 $\mu\text{g/ml}$
of PABA

(right) a. 2 M, 1.4 M, and 1 M; b. 0.5 M;
c. 0.1 M and 0.05 M; d. 0.01 M and
0.002 M of I^-

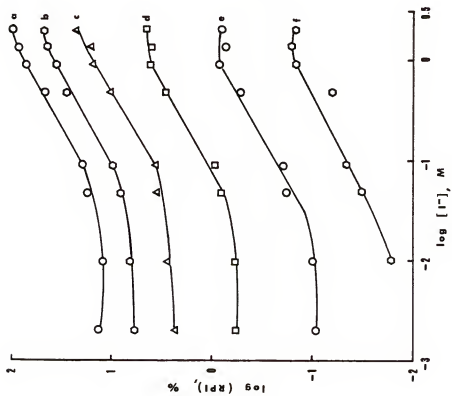
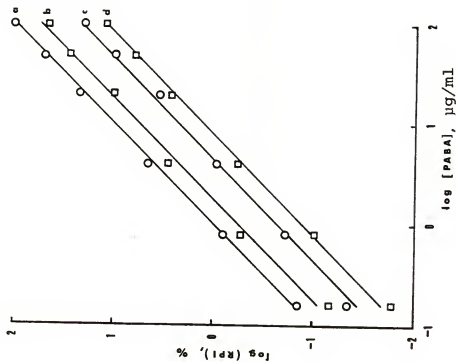


Figure 50. RTP response (left) and calibration (right) curves of PABA on S & S 903

Curves identified as:
(left) same as Figure 49(a)
(right)a. 2 M and 1 M; b. 0.5 M; c. 0.1 M;
d. 0.01 M of I^-

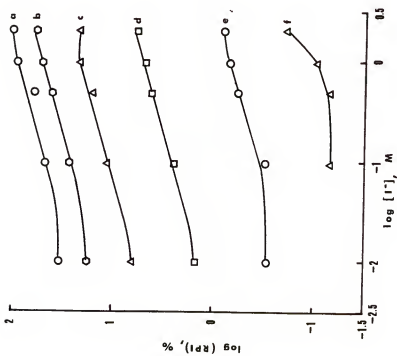
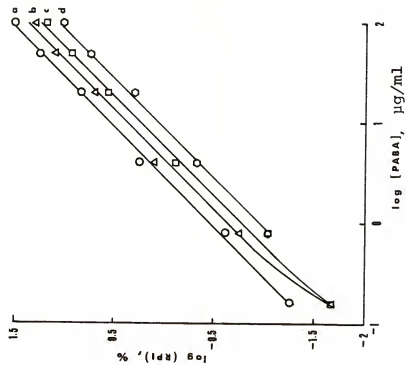


Figure 51. RTP response (left) and calibration (right) curves of NAA on DE-81

Curves identified as:

(left) a. 105 $\mu\text{g/ml}$; b. .53 $\mu\text{g/ml}$; c. 27 $\mu\text{g/ml}$;
d. 14 $\mu\text{g/ml}$; e. 7 $\mu\text{g/ml}$ of NAA
(right)a. 2 M and 1 M; b. 0.097 M; c. 0.01 M
of I^-

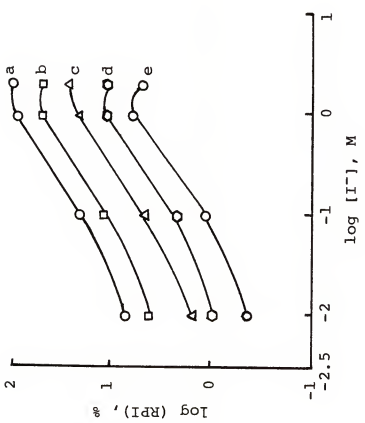
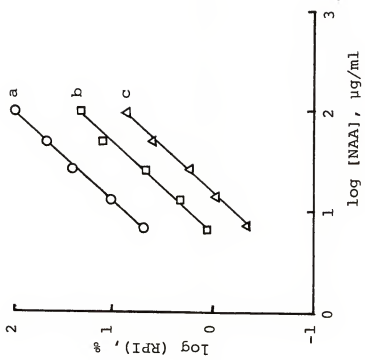
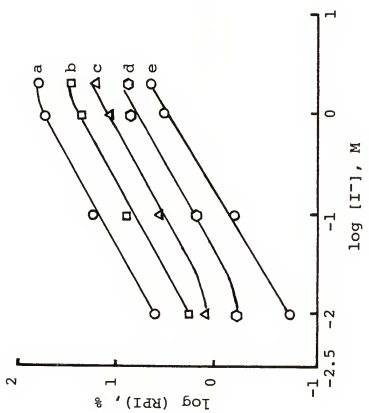
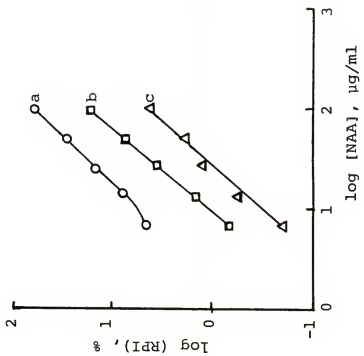


Figure 52. RTP response (left) and calibration (right)
curves of NAA on S & S 903

Curves identified as:
(left) same as Figure 51(a)
(right) same as Figure 52(b)



BIOGRAPHICAL SKETCH

Syang Yang Su was born in Kaohsiung, Taiwan, Republic of China (R.O.C.), on February 12, 1951. In the summer of 1969 he graduated from Kaohsiung Senior High School, Kaohsiung, Taiwan. He received his B.S. degree in chemistry from National Chung-Hsing University, Taichung, Taiwan, in 1974. After two years' military service and one year's work as researcher and teaching assistant, Syang enrolled in the University of Washington, Seattle, WA, where he received the M.S. degree in analytical chemistry (chromatography) in 1979. Since that time he has worked toward the Ph.D. degree at the University of Florida. He is a member of the American Chemical Society and the Society for Applied Spectroscopy.

I certify that I have read this study and that in my opinion it conforms to acceptable standards of scholarly presentation and is fully adequate, in scope and quality, as a dissertation for the degree of Doctor of Philosophy.

James D. Winefordner
James D. Winefordner, Chairman
Graduate Research Professor of
Chemistry

I certify that I have read this study and that in my opinion it conforms to acceptable standards of scholarly presentation and is fully adequate, in scope and quality, as a dissertation for the degree of Doctor of Philosophy.

John G. Dorsey
John G. Dorsey
Assistant Professor of
Chemistry

I certify that I have read this study and that in my opinion it conforms to acceptable standards of scholarly presentation and is fully adequate, in scope and quality, as a dissertation for the degree of Doctor of Philosophy.

Richard A. Yost
Richard A. Yost
Assistant Professor of
Chemistry

I certify that I have read this study and that in my opinion it conforms to acceptable standards of scholarly presentation and is fully adequate, in scope and quality, as a dissertation for the degree of Doctor of Philosophy.



Marvin L. Muga
Professor of Chemistry

I certify that I have read this study and that in my opinion it conforms to acceptable standards of scholarly presentation and is fully adequate, in scope and quality, as a dissertation for the degree of Doctor of Philosophy.



Stephen G. Schulman
Professor of Pharmacy

This dissertation was submitted to the Graduate Faculty of the Department of Chemistry in the College of Liberal Arts and Sciences and to the Graduate Council, and was accepted as partial fulfillment of the requirements for the degree of Doctor of Philosophy.

August 1982

Francis G. Stehli
Dean for Graduate Studies and
Research